PHYSICAL STUDIES OF SUGAR-BASED SURFACTANTS

SEYED MOHAMMAD MIRZADEH HOSSEINI

FACULTY OF SIENCE
UNIVERSITY OF MALAYA
KUALA LUMPUR

2017

PHYSICAL STUDIES OF SUGAR-BASED SURFACTANTS

SEYED MOHAMMAD MIRZADEH HOSSEINI

THESIS SUBMITTED IN FULFILMENT OF THE REQUIREMENTS FOR THE DEGREE OF DOCTOR OF PHILOSOPHY

FACULTY OF SIENCE
UNIVERSITY OF MALAYA
KUALA LUMPUR

2017

UNIVERSITI MALAYA

ORIGINAL LITERARY WORK DECLARATION

Name of Candidate: **SEYED MOHAMMAD MIRZADEH HOSSEINI**

Registration /Matric No: **SHC070006**

Name of Degree: **Doctor of Philosophy**

Title of Thesis ("this Work"):

PHYSICAL STUDIES OF SUGAR-BASED SURFACTANTS

Field of Study:**Physical Chemistry**

I do solemnly and sincerely declare that:

(1) I am the sole author/writer of this Work;
(2) This Work is original;
(3) Any use of any work in which copyright exists was done by way of fair dealing and for permitted purposes and any excerpt or extract from, or reference to or reproduction of any copyright work has been disclosed expressly and sufficiently and the title of the Work and its authorship have been acknowledged in this Work;
(4) I do not have any actual knowledge nor do I ought reasonably to know that the making of this work constitutes an infringement of any copyright work;
(5) I hereby assign all and every rights in the copyright to this Work to the University of Malaya ("UM"), who henceforth shall be owner of the copyright in this Work and that any reproduction or use in any form or by any means whatsoever is prohibited without the written consent of UM having been first had and obtained;
(6) I am fully aware that if in the course of making this Work I have infringed any copyright whether intentionally or otherwise, I may be subject to legal action or any other action as may be determined by UM.

Candidate's Signature Date

Subscribed and solemnly declared before,

Witness's Signature Date

Name:

Designation:

ABSTRACT

Phospholipids are widely used to produce delivery systems for the entrapment and release of drugs from vesicles, also called liposomes, especially for chemotherapy. The replacement of ionic phospholipids with non-ionic glycolipids may help to improve the stability of drug carriers due to stronger molecular interactions. However, the synthetic challenge for highly pure glycolipids in combination with the vast structural diversity of carbohydrates makes a random testing of sugar head-groups for the optimization of vesicle stability highly inefficient. On the other hand, computational methods may be used to predict detailed interactions of the surfactants. However, this method requires experimental validation. Of particular interest is hydrogen bonding within the hydrophilic sugar head-group region. Unfortunately the intermolecular hydrogen bonding between surfactants is difficult to measure. Instead, the validation of computational results can focus on the interaction of the surfactants with water. This study aims to determine the bound water content of glycolipids in the lamellar phase, which is a good approximation for vesicular assemblies. In this regard, several glycolipid molecules were synthesised and investigated. The bound water content was examined by deuterium NMR (^{2}H-NMR) and differential scanning calorimetry (DSC). In the latter the melting enthalpy of free water was measured to indirectly determine the bound water content. These experimental results are compared with computational studies, which model the slightly curved vesicle bilayer as a multilayer analogue of the lamellar phase. The complexity of carbohydrate stereochemistry and their hydrogen bonding is very intriguing, and minor changes in orientation can cause significant effects on the self-assembly. With respect to this, the stereo chemical effect of anomers and epimers on the self-assembly of Guerbet glycosides was investigated. The comparison of phase transition temperatures revealed a cis-trans correlation of anomeric-epimeric pairs based on glucose and galactose, which can be explained by the direction of hydrogen bonding of the hydroxyl group at the epimeric C-4 carbon.

ABSTRAK

Fosfolipid digunakan secara meluas dalam menghasilkan sistem penghantaran untuk pemerangkapan dan pelepasanubat dari vesikel, juga dikenali sebagai liposom, terutamanya untuk kemoterapi. Penggantian fosfolipid ionik dengan glikolipidtak ionik boleh membantu dalam meningkatkan kestabilan pembawa ubat kerana interaksi molekul yang lebih kuat. Namun, cabaran menyediakanglikolipid dengan ketulinan yang tinggiberserta kombinasi kepelbagaian struktur karbohidrat membuat ujian rawak keataskumpulan karbohidratpada bahagian berkutubdalam mengoptimumkan kestabilan vesicle adalah sangat tidak cekap. Sebaliknya, kaedah pengkomputan boleh digunakan untuk meramalkan interaksi terperinci surfaktan. Walau bagaimanapun, kaedah ini memerlukan pengesahan secara empirikal. Perkara yang penting adalah ikatan hidrogen diantara bahagian hidrofilik pada kumpulan karbohidrat. Malangnya ikatan hidrogen di antara molekul surfaktan adalah sukar untuk diukur. Sebaliknya, pengesahan keputusan pengkomputanmembenarkanpenumpuan kepada interaksi surfaktan dengan air. Kajian ini bertujuan untuk menentukan kandungan air terikat bagi glikolipid dalam fasa lamela, yang merupakan penghampiran yang kena bagi perhimpunan vesikel. Dalam hal ini, beberapa molekul glycolipid telah disintesis dan dikaji. kandungan air yang terikat dikajimenggunakan NMR deuterium (^{2}H-NMR) dan pengimbasan pembezaan kalorimeter (DSC). Dengan DSC entalpi peleburan bagi air bebastelah diukur secara tidak langsung dalam menentukan kandungan air terikat. Keputusan ujikaji ini dibandingkan dengan kajian pengkomputan, yang prototaipsedikit melengkung dwilapisan vesikel sebagai analog berbilang lapis fasa lamela.Kerumitan stereokimia karbohidrat dan ikatan hidrogen mereka adalah sangat menarik, dan perubahan kecil dalam orientasi boleh menyebabkan kesan yang besar ke atas penghimpunan-sendiri. Berkenaan dengan ini, kesan stereokimia daripada anomer dan epimerke atas penghimpunan-sendiriglikosida Guerbet dikaji. Perbandingan suhu peralihan fasamenunjukkan korelasi cis-trans daripada pasangan anomerik-epimerik berdasarkan glukosa dan galaktosa, yang dapat dijelaskan oleh arah ikatan hidrogen kumpulan hidroksil pada karbonepimer C-4.

ACKNOWLEDGEMENTS

First and foremost, I would like to thank the Great God who gave me the wisdom and strength to accomplish this important task in my life; God who communicated with me and my family through the Holy Quran and gave us the courage to tolerate the difficulties.

I am incredibly grateful to all individuals who helped me in doing this dissertation, especially to the head of the group of "Glycolipid and Science Technology", **Professor Dr. Rauzah Hashim**; without her invaluable supervision, assistance, and support in all stages of my PhD studies this study could not be completed. I am also deeply indebted to **Associate Professor Dr. Thorsten Heidelberg** for his knowledgeable perfect assistance during laboratory experimental and drafting of the present thesis. I am highly grateful to **University of Malaya** for providing me with the excellent academic and laboratory facilities to complete this research project.

I never forget to appreciate the help of people who assisted me in laboratory work and in the writing of my thesis including **Dr. Sara Ahmadi, Dr. Rusnah Syahila, Dr. Vijayan Manickam Achari, Dr. Noraini Ahmad, Dr. Noor Idayu Binti Mat Zahid and Dr. Zahrabatoul Mosapour.**

I dedicate this thesis to **my loving wife** who always supported me with her kind understanding of my PhD life.

TABLE OF CONTENTS

LIST OF FIGURES

LIST OF TABLES

ABBREVIATIONS

2-D	2-dimensional (NMR)
Ac	Acetyl
Ac2O	Acetic anhydride
APG	Alkyl polyglucoside
Ar	Aryl
ATG	Alkyl triazole glycoside
B.W.	Bound Water
BF3.Et2O	Boron trifluoride diethyl etherate
br	(NMR) broad signal
CD3OD	Methanol-d4
CDCl3	Chloroform-d
CH2	Methylene
CH3	Methyl group
CMC	Critical micelle concentration
Col	Columnar
Cr	Crystals
Cub, Q	Cubic
d	(NMR) doublet
D2O	Deuterium oxide
DCM	Dichloromethane
dd	(NMR) doublet of a doublet (double doublet)
ddd	(NMR) double of doublet of doublet
DEPT	Distortionless Enhancement by Polarization Transfer
DFT	Density Functional Theory
DMF	N, N-Dimethylformamide
DMSO	Dimethyl Sulfoxide
DMSO-d6	Dimethyl sulfoxide-d6
DSC	Differential scanning calorimetry
e.g.	for example
EDTA	Ethylenediaminetetraacetic acid
et al.	and others
etc.	and the others
EtOAc	Ethyl acetate
EtOH	Ethanol
Glc	Glucose
h	hour(s)
H1	Normal hexagonal
HMQC	C-H Correlation Spectroscopy
HPLC	high performance liquid chromatography
H.B.	Hydrogen bond
I	Isotropic
IR	Infra-Red spectroscopy
IUPAC	International Union Pure and Applied Chemistry
J	coupling constant

LAS	linear alkyl benzene sulfonates
LC	Liquid crystal
LCLC	Lyotropic chromonic liquid crystal
L_α	Lamellar phase
M	(NMR) multiplet
m_c	Multiplet centre
Me	Methyl
MeOH	Methanol
Min	Minute(s)
N_2	Nitrogen gas
NaOAc	Sodium acetate
NaOMe	Sodium methoxide
NMR	Nuclear Magnetic Resonance
Nu	Nucleophile
OPM	Optical Polarizing Microscope
POE	Polyethoxy Ethylene
p-TsOH	para-toluenesulfonic acid
Py	Pyridine
Ref	Refrence
ROH	Alcohol
S	singlet
SC	smectic C
SA	smectic A
$SnCl_4$	Tin tetrachloride
T	(NMR) triplet
THF	Tetrahydrofuran
T_K	Krafft temperature
TLC	thin layer chromatography
TP	Triphenylene core
Ts	Toluenesulfonyl
Γ	Surface tension

CHAPTER 1: INTRODUCTION

1.1 Bound water and its importance to membrane

Bound water is formed by adsorption of water to hydrophilic compounds based on hydrogen bonding. Possible compounds for bound water include surfactant absorbents, like certain polymers, phospholipids and glycolipids. The surfactant absorbents are amphiphilic and compounds, which means that they are both hydrophilic and hydrophobic. When in contact with water they usually form various phases, including the lamellar phase. The lamellar phase, both in single and multilayers, may be used to form vesicles which may be used as delivery systems based on their ability to encapsulate both hydrophilic and hydrophobic compounds (Smirnova et al., 2004). Bound water is attached to the hydrophilic head of phospholipids or glycolipids by hydrogen bonding. Of course, this aspect is examined in lamellar or the vesicle phases. The measurements of bound water have been undertaken by a broad range of research methods (Garti et al., 2000; Kerch et al., 2012a, 2012b; Matsumoto et al., 1986). There are two general methods to obtain bound water. The first one is by the computational methods with software (Manickam Achari et al., 2011 (unpublished)) and the other one is the experimental methods which are conducted in the laboratory. Two experimental methods which have been widely used are the deuterium NMR technique and the measurement of enthalpy by using differential scanning calorimetery (DSC). In this study, both measurement methods are investigated and reported. Recently, the computational methods have been widely used by researchers, and numerous articles are

published in this field each year (Ahmadi et al., 2014; Manickam Achari et al., 2012; ManickamAchari et al., 2014; Misran et al., 2013). In this method, the number of hydrogen bonds was calculated and reported by the computational methods and different softwares (Manickam Achari et al., 2012).

In fact, there are two types of hydrogen bonding examined in these calculations. The first hydrogen bonding is intermolecular hydrogen bonding between two hydrophilic heads of surfactant molecules which are adjacent in lamellar or vesicle phase. The second hydrogen bonding is between water molecules and the hydrophilic head of surfactant molecule. The second type is the subject of this research. Although the number of bondings between the hydrophilic head of surfactant molecules with each other and also with water have been reported according by the computational methods (Manickam Achari et al., 2012), comparing of these results with the experimental results will confirm the computational data. This constitutes to the validation of computational results and reliability of model used in the simulation. In the meantime, although the computational method refers to the bonding between the two adjacent hydrophilic molecules, confirming this via experimental methodology is extremely difficult in the laboratory and rarely reported. Since the experimental methods and apparatus may measure the number of bonding between the hydrophilic surfactant molecules and water molecules, it will create a comparative view with the computational data. Accordingly, the base and aim of study is to measure the bound water by experimental technique.

The vesicles are used in medical science, so they have a broad application in the construction of chemotherapy serums nowadays with the aim of carrying the drug in the body which is considered as the main subject of this study. The task of vesicles is drug

delivery for example to destroy a cancer cell. Unfortunately, other molecules are affected by this type of treatment. To choose a correct vesicle formulation which deals with only cancer cells effectively and cubic phases for topical creams and implants can be used for slow release of actives, is the aim of many researches. There are many previous studies and researches, which have used phospholipid molecules in manufacturing the drug carrier vesicles. But in the recent years, researches have been conducted using glycolipid in the construction of the vesicles. Our present work aims to complement such effort. In particular, we develop the lamellar self-assemblies from a range of disaccharides glycolipids, namely maltoside, cellobioside and lactoside. Three different chains were considered namely the monoalkylated octyl- and dodecyl and the branched chain octyl butyl. We then measure the bound water using deuterium NMR and DSC of these selected systems.

Membrane structure, which is constructed from a lipid bilayer is strongly determined by water or other solvents. In phospholipids for example, the structure and dynamics of the headgroup and the acyl chain are highly dependent by the degree of hydration (Ho et al., 1995; Holte & Gawrisch, 1996; Ulrich & Watts, 1994). The reduced reorientational mobility of water in phospholipid head-groups environment provides name evidence for this(Sciortino et al., 1992). However, more research are needed to study the restricted motions (Konig et al., 1994). For example, the technique of ^{1}H-NMR with pulsed field gradient spin-echo (PFGSE) may be used to measure the diffusion of water in the lamellar phase of phosphatidylcholine-water. In addition DSC can also be used to study the water association to the phospholipid bilayers (Chapman et al., 1967).

In a lipid solution there are three types of water. The water molecule, which is attached to the headgroup (bound water) is limited to move due to its strong bond with the headgroup. The second type is the free water molecule, which is close to the headgroup and this water can exchange with the free bulk water molecule in the aqueous solution. The motion of bound water is naturally anisotropic; this is provide by the D-NMR spectrum for PC-D_2O in the lamellar phase (Finer, 1973). The quadrupolar splitting is formed when there is an angle θ between the deuterium bond and the magnetic field. This splitting is related to the order parameter defined by $\langle P_2(\cos\theta)\rangle$ see Section 2.6 (Pope & Cornell, 1979). Although there are numerous models for bound water, the details are still to be discussed (Finer, 1973; Gawrisch et al., 1978; Wassall, 1996). Dehydration of a wet substance comprises two stages: taking moisture from the surface of the substance and removing the water from the surrounding (Lee et al., 2013).

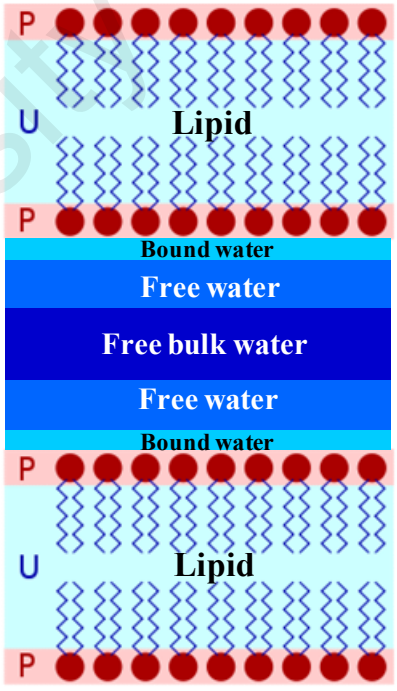

Figure 1-1 Three types of water in lipid bilayers.

1.1.1 Theory of bound water in lipid

Bound water plays important role in lipid self-assembly from both aspects of fundamental understanding and application. In general, when a solute dissolved in water a chemical equilibrium is established between bound and free water governed by an equilibrium constant (Carvell et al., 1986; Davey et al., 2002; Funari et al., 1994; Tiddy, 1980). For simple solutes in water, a single binding site may be defined. But in complex glycolipid systems, several binding sites, each has its own binding constant. Water can bind (via H-bonds) either through the oxygen or through hydrogen. The amount of bound water varies with the water/solute concentrations – strictly dependent on the water chemical potential (μ_{water}). Therefore, a study on bound water involves the knowledge of the various binding sites, the strength of binding, the structure of bound water (which H-bonds are involved) and, of course, the amount of bound water (Carvell et al., 1986). These information may be extracted from both thermodynamic and spectroscopic (molecular) measurements (Bonicelli et al., 1998; Morley & Tiddy, 1993; Rendall & Tiddy, 1984).

1.1.1.1 ^{2}H-NMR technique using heavy water as probe

Owing to their orientational order, liquid crystalline phases can be investigated by deuterium NMR, provided that the molecules are specifically deuterated (Burnell & de Lange, 2005; Hamasuna et al., 2011; Sandström et al., 1996). High costs and challenging synthesis for these compounds, however, limit such studies. A more practical approach applies a deuterated probe instead; heavy water (D_2O) is an easy accessible and economic probe. It is particularly suitable for systems containing water, like bio-related surfactant formulations (Meier & Seelig, 2010; Rendall & Tiddy, 1984).

The interaction between the electric field gradient of the bond involving the deuterium and the electric quadrupole moment of the deuterium atom (S=1) causes a splitting of the resonance signal in anisotropic samples, like lamellar or hexagonal phases. This is called the 'quadrupole slitting'. On the other hand, isotropic phases, like normal liquids and cubic liquid crystal phases, only show singlet signals in the ^{2}H-NMR. Uniaxial phases, accounting for the great majority of lyotropic liquid crystalline states, exhibit so-called powder spectra if they are not macroscopically aligned, These are characterised by the presence of two doublets; an inner set of high intensity, reflecting an orientation perpendicular to the magnetic field, and an outer shoulder of half intensity, resulting from parallel orientation of the phase director and the magnetic field. The (sharp) inner peak set defines the quadrupole splitting Δ, given in Equation 1.1 (Halle & Wennerstrom, 1981).

Equation 1.1 $$\Delta = \frac{3}{4} Q_{OD} S_{OD}$$

Equation 1.1 indicates a linear dependency of the quadrupole splitting and the order parameter S_{OD}, where Q_{OD} is the linking quadrupole coupling constant of the OD bond; for deuterium oxide this is 220 kHz. The order parameter for D_2O, S, is related to the time average, or ensemble, of the angle between the director of the phase and the symmetry axis of the water molecule, θ. Equation 1.2 describes this relation, in which the time average is indicated as ⟨⟩.

Equation 1.2 $$\mathbf{S} = \frac{1}{2}\langle 3cos^2\theta - 1\rangle,$$

Due to the intermolecular hydrogen bonding network in an aqueous glycolipid formulation, hydrogen atoms, referring to both H and D, are quickly (based on the NMR scale) exchanged both between water molecules at different sites as well as between

water and the hydroxyl groups of the glycolipid. Therefore, the observed quadrupole splitting, Δ, will be an average (Halle & Wennerstrom, 1981; Morley & Tiddy, 1993), and Equation 1.1 leads to the following:

Equation 1.3 $$\Delta = \sum \boldsymbol{P_i}\,\Delta_i = \frac{3}{4}\boldsymbol{Q_{OD}} \sum \boldsymbol{P_i}\,\boldsymbol{S_{iOD}} = \frac{3}{4}\boldsymbol{Q_{OD}}\langle \boldsymbol{S_{OD}}\rangle$$

In **Equation 1.3** the fraction of the population at site $i$is indicated by P_i, where as the corresponding splitting and the order parameter for the OD-bond are termed as Δ_i and S_{iOD}, respectively. Instead of averaging the time average of OD bonds over different sites, both, time and site averaging may be combined in an average OD-bond order parameter $\langle S_{OD}\rangle$. The angular dependency of S_{iOD}enables both positive and negative values (Halle & Wennerstrom, 1981).As a result, Δ may turn to zero, if different S_{iOD}cancel out each other. Moreover, a powder pattern may collapse into a single peak, if the liquid crystalline domains are too small and diffusion between them become too rapid to be observed by NMR. This particularly can happen in for dilute lyotropic samples that have been exposed to excessive sheer forces, e.g. intense shaking (Halle & Wennerstrom, 1981).

The importance of deuterium nuclear magnetic resonance (^{2}H-NMR) technique has been demonstrated for research on the properties of liquid crystals (Domenici et al., 2007; Luckhurst, 1988). The strong dependence of the quadrupolar splitting on the angle between the molecular orientation and direction of the magnetic field means that ^{2}H-NMR spectroscopy can be used to examine the dynamic and static molecular orientation (director) in a thin layer of nematic phase, in the presence or absence of an electric field (Luckhurst et al., 2001; Luckhurst et al., 2002). The static and dynamic orientational behaviour in the lamellar phase has been studied by deuterium NMR technique (Hamasuna et al., 2011; Misran et al., 2013).

The deuterium NMR technique has been successfully used to measure the amount of bound water in lyotropic phases (Rendall & Tiddy, 1984). Within the interfacial region, there are two distinct types of water, which can be described as "free" and "bound". Between them a fast exchange may apply. In consideration of the different water types **Equation Equation 1.3** can be written as follows:

Equation 1.4 $$\Delta = P_f \Delta_f + P_b \Delta_b$$

In **Equation 1.4** P_f and P_b indicate the mole fractions of the "free" and "bound" water, while the corresponding splittings are termed as Δ_f and Δ_b. Free water is expected to reflect the properties of pure water, which is isotropic and, hence, does not show any quadrupole splitting. Therefore Δ_f is assumed to be zero and **Equation 1.4** reduces to:

Equation 1.5 $$\Delta = P_b \Delta_b = \frac{3}{4} Q_{OD} P_b S_b$$

Equation 1.5 indicates linear dependencies of the quadrupole splitting with both the order parameter and the concentration of the D_2O-probe, which is commonly provided as mole fraction. The order parameter of water in lyotropic systems is typically assumed to be more or less constant; hence the quadrupole splitting is expected to change linearly with the ratio of surfactant to water molecules.

Equation 1.6 $$P_b = N(N_S/N_W)$$

In **Equation 1.6 N** represents the number of bound water molecules per head-group, while the term N_S/N_W denotes the molar ratio of surfactant (N_S) and water molecules (N_W). The bond water content can be determined from the slope of a plot of the experimental quadrupole splittingagainst the molar ratio of surfactant and water molecules (Blackmore & Tiddy, 1990; Carvell et al., 1986). For the lamellar phase a

linear rise of Δ with increasing N_S/N_W is expected. However, the plot approaches a maximum at higher surfactant to water ratio, and subsequently can even decrease. This behaviour can be explained based on a refined model that assumes constant equilibrium of bound and free water, according to following chemical reaction, where n represents the bound water content **N** (Rendall & Tiddy, 1984).

Equation 1.7 $$\mathbf{Surfactant + nH_2O \rightleftharpoons [Surfactant(H_2O)_n]}$$

Rendall and Tiddy have shown that the equilibrium due to **Equation 1.7** prevents water to only occupy bond states that this subsequently causes the observed deviation from the expected linear relation of the quadrupole splitting and the surfactant-water ratio at low water (hence high surfactant) concentration (Rendall & Tiddy, 1984). For all $N > 1$, the maximum of the quadrupole splitting occurs at the following ratio:

Equation 1.8 $$\mathbf{[(water/surfactant)molar\ ratio] = (N - 1)}$$

Based on **Equation 1.8** the bound water content can be determined from the surfactant-water ratio at the maximum (or levelling-off) of the plot of Δ against N_S/N_W. This is the basis of the ^{2}H-NMR technique for the determination of bound water contents.

1.1.1.2 Differential scanning calorimetry (DSC)

For some hydrophilic polymers, bound water can also be measured by thermal technique such as differential thermal analysis (DTA) and differential scanning

calorimetry (DSC) and thermogravimetry (TG). From the enthalpy of melting or freezing temperature of water, the amount of bound water was calculated by

Equation 1.9. In this equation $\mathbf{W_t}$ is the total water content in the sample, $\mathbf{W_f}$ is free water content, and $\mathbf{W_b}$ is for the measurement of bound water content. In most of hydrophilic polymers, $\mathbf{W_b}$ is the total of non-freezing bound water given by $\mathbf{W_{nf}}$, while the freezing bound water is given as $\mathbf{W_{fb}}$. In DTA and DSC curve, $\mathbf{W_b}$ content can be measured. At the same time, we can estimate $\mathbf{W_b}$ in TG. As a result, by mixing DSC, DTA, and TG, it is possible to compare the exact amount of bound water (Hatakeyama et al., 1988).

Equation 1.9 $$W_t = W_f + W_b$$

The use of free Gibbs free energy (ΔG) for the measurement of bound water has been reported in accordance with **Equation 1.10** (Michel et al., 2009).

Equation 1.10 $$\Delta G_b(water) = G_{water}^{site} - G_{water}^{bulk} = -kTln\frac{Q_{water}^{site}}{Q_{water}^{bulk}}$$

Measuring the ratio of water to lipid is done and reported by DSC and the number of free water molecules have been calculated with the ice-melting point (Kodama et al., 2004). Measuring the melting and freezing point of free water and related study has been reported for many materials, such as cotton, rayon, linen, kapok, hemp, and wood cellulose by differential scanning calorimeter (DSC). For cellulose, two peaks of water were observed. One was a broad peak, and the other was a sharp. These indicate that there are two kinds of water, and the melting point of one of them is not specified. Therefore, the absorbed water on the cellulose is categorised into three kinds: free water (Peak I), freezing bound water (Peak II), and nonfreezing bound water.

The amounts of estimated bound water are reported from 1.0 to 2.1 moles per one glucose unit of cellulose (Nakamura et al., 1981).

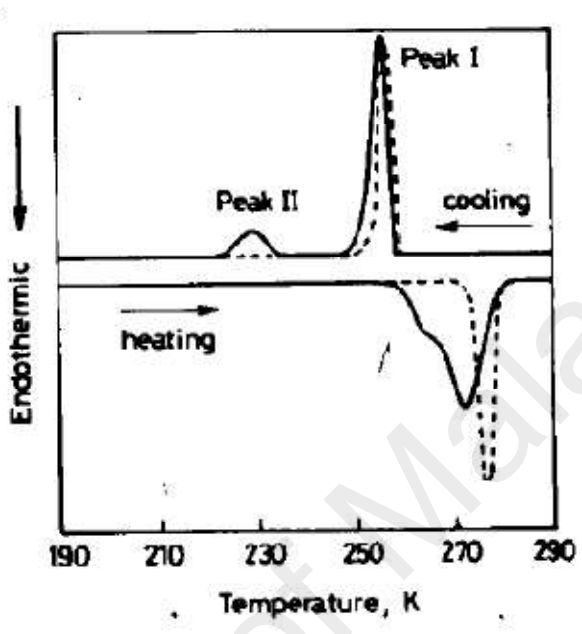

Figure 1-2 Schematic DSC curves of water adsorbed (bound water). on different cellulose samples. Heating and cooling rate is 8 K/min. Figure from (Nakamura et al., 1981).

However, the DSC technique is one of the most used methods to calculate free and bound water contents (Hatakeyama et al., 1980).

1.1.2 Hydration of glycolipids

Glycolipids are conjugates of sugars (carbohydrates) and lipids. They are amphiphilic compounds; this means that they possess both hydrophilic and hydrophobic properties due to two molecular regions: a water-attracting (hydrophilic) sugar and a water-resistant (hydrophobic) alkyl chain. They are surface active agents, or in short surfactants. When glycolipids are dispersed in water they form assemblies; a particularly interesting assembly is the vesicle. Vesicles can be used for medical

applications. A drug can be trapped inside the vesicle and the vesicle moves in the blood until it binds to e.g. a cancer cell. The general behaviour of medicine is to kill cancer or infected cells. Unfortunately healthy cells are also destroyed by the drug. Ideally the drug should selectively kill the cancer cells but not others. For this a target delivery system (vesicles) must combine three tasks.

Initially the vesicle is isolating the drug. The vesicle must be stable to avoid breaking and release of the drug. As long as the vesicle is covering the drug, the drug cannot do any damage, which is important to avoid killing of non-target cells. The second requirement is interaction of the vesicle with cancer cells only, but not with other cells. Cancer cells have different cell receptors. In order to direct a vesicle, the latter requires something that is interacting with a cancer cell receptor. Finally, the vesicle must be able to release the drug into the cancer cell. In short the requirements of a drug delivery system (DDS) are; stability under physiological condition; target and timely release of the drug. The aim of this work is for cused on the first point, i.e. the stability of vesicles.

The membrane structure of a vesicle is more or less similar to the bilayer in the lamellar phase. Therefore, the stability of the lamellar phase reflects the stability of a vesicle, which is interesting for our scope of study. The more stable a lamellar phase is, the more stable is the corresponding vesicle. Contributing factors to the stability of the lamellar phase are: interactions between polar surfactant domains; interactions of alkyl chains and geometry of the surfactant.

The first component (inter-head-group interaction) is relevant in order to optimise the sugar of the glycolipid for best bilayer stability. As long as the hydrophobic tail remains the same, the interactions between tails remain constant and

differences in the lamellar stability between glycolipids reflect only different interactions between sugars inside the lamellar phase. These interactions are based on hydrogen bonding (H–bonding). More H–bonding between sugar head-groups implies more stability of the Bilayer (Hashim et al., 2011). Computer simulations enable the comparison of different surfactants with respect to the extent of H–bonding. However, these data require experimental validation from the simulation studies which can provide: number of H–bonding between sugars; detailed geometry of simulation (bilayer spacing) and number of H–bonding between sugar and water.

The H–bonding between sugars cannot be measured directly. However, computational results on inter sugar H-bonding can be validated indirectly by comparing computer results for the H–bonding between sugar and water with experimental bound water contents. Bound water correlates with H–bonding between sugar head and water.

1.2 Sugar stereochemistry: epimers and anomers

Carbohydrates, also termed as sugars are poly-hydroxyl compounds. They can be divided into categories according to the number of sugar units that are involved. Monosaccharides, or simple sugars, comprise of a single ring, whereas in disaccharides two monosaccharides are covalently. The cyclic shape of carbohydrates originates from the intramolecular reaction of one of the hydroxyl groups with an aldehyde function, resulting in a cyclic hemiacetal. The ring-size is typically determined by the size of the carbon chain of the carbohydrate. For the naturally most abundant hexoses, which comprise of a linear 6-carbon skeleton, typically six-membered rings, or pyranoses, are formed. The stereochemistry at the acetalic carbon gives rise to diastereomers, which

are called anomers. A cis-orientation of the anomeric hydroxyl group and C-6 typically indicates the α-anomer, whereas the groups adopt a trans-relation in the β-anomer. **Figure 1-3** shows the anomers of glucose, the most abundant monosaccharide in nature.

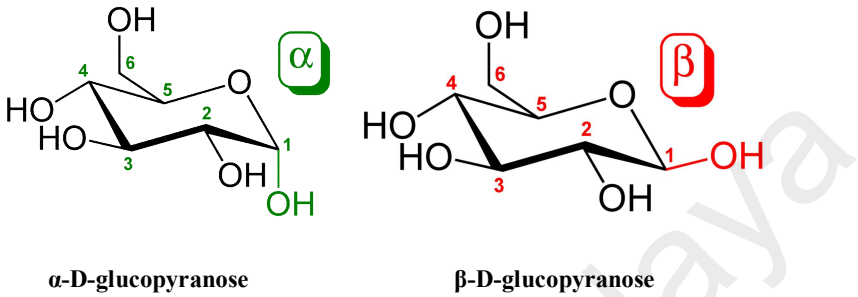

α-D-glucopyranose **β-D-glucopyranose**

Figure 1-3 Structure of α-anomer and β-anomer of D-glucopyranose.

The presence of several asymmetric carbons in monosaccharides provides a wide range of stereoisomers. While diastereomers differing solely at the acetalic carbon (C-1) are called anomers, the term epimer is used to indicate diastereomers differing in a single stereo-centre other than the anomeric carbon; examples are glucose and galactose as well as glucose and mannose, whereas galactose and mannose differ in two stereo-centres and are, hence, no epimers (Bertozzi & Rabuka, 2009). The stereochemical relations are visualised in **Figure 1-4**.

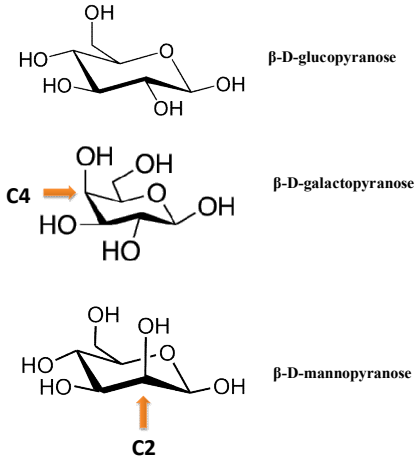

Figure 1-4 Structure of glucose, galactose & mannose.
Galactose is C4-epimer and mannose is C2-epimer.

The tetrahedral geometry of sp^3-hybridised carbon causes a non-planar shape for pyranoses. They can adopt chair or boat conformations, as sketched in **Figure 1.5.** Typically chairs are energetically favoured. The position of substituents, for carbohydrates mostly hydroxyl groups, can be either in an axial or in an equatorial position. Due to steric hindrance an equatorial position for the substituent is more favourable. The position (axial or equatorial) of a hydroxyl group affects the interaction (hydrogen bonding) of the carbohydrate with other molecules, which in this investigation refers to either another carbohydrate molecule or water. Because of this, stereochemical differences can affect the assembly behaviour of glycolipids very much.

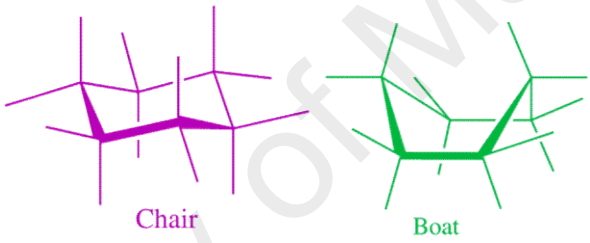

Figure 1-5 Possible sugar conformational isomers.

1.3 Objectives and overview of thesis

One of the principle components in a cell membrane is glycolipids and these are held together in the cellular matrix by the network of hydrogen bonds. Thus the focus in this thesis is to evaluate the hydration effect of glycolipids with water in a lamellar phase which is related to a model for cell membrane. The outline of the thesis is as follows:

Chapter 1:This chapter describes bound water and its importance in liquid crystal phases and also the hydration of glycolipid. Since glycolipids are very complex

molecules and their properties are very dependent on the stereochemistry. A summary on sugar stereochemistry is also given especially on the epimers and anomers.

Chapter 2: The background of liquid crystals and the molecules forming the liquid crystal phase is described in Chapter 2. Detailed behaviours of liquid crystalline phases that include the thermotropic and lyotropic kinds are explained. In addition, brief descriptions of glycolipids as liquid crystal materials are given. We have also commented on their importance especially in relation to the cell membrane. This chapter also gives the background of the measurement of bound water by ^{2}H-NMR and DSC.

Chapter 3: This chapter contains, the raw materials used in this thesis as well as the synthesis of glycolipids. Different analytical methods for the characterization of the liquid crystal phases, including optical polarizing microscope (OPM), differential scanning calorimeter (DSC) and nuclear magnetic resonance spectroscopy (NMR), both for ^{1}H & ^{2}H are described. We also give in detail different methods of sample preparation in lamellar phase and compare them with each other.

Chapter 4: It describes the results and discussion in two parts. Chapter 4.1 describes the disaccharide investigation and results of ^{2}H-NMR and DSC measurements and discussion and also the comparison of ^{2}H-NMR and DSC results. In Chapter 4.2 we have considered of α/β-octyl-galactosides (α/β- C_8Gal) and α/β-octyl-glucosides (α/β-C_8Glc) and studied their liquid crystal properties especially their phase transitions. This work was complemented by the simulation of the anhydrous bilayer where we expected to gain knowledge on the molecular interactions within the hydrophilic region of bilayer, without any solvent. We examine in detail the anomeric and epimeric linkages and hope to find the molecular explaination to justify their observed phase transitions.

Chapter 5: Finally, Chapter 5 presents suggestions for future work.

CHAPTER 2: LITERATURE REVIEW

2.1 Liquid crystals

1850 Willhelm Heintz observed a strange behaviour near the melting point of stearin, or glyceryl tristearate; a cloudy liquid formed below the complete melting point, which formed to a clear liquid only at higher temperature. Liquid crystalline behaviour was also observed by Rudolf Ludwig Carl Virchowin 1853 with nerve myelin (Sluckin et al., 2004; Virchow, 1860). However, the discovery of liquid crystals is commonly associated with a study of cholesteryl benzoate by an Austrian botanist named Friedrich Reinitzer and Otto Lehmann, a German physicist and an optics expert. They were the first to provide an explanation for the unique melting behaviour. Due to the special nature of the material both liquid and crystalline properties are observed parallel. To reflect this, they created the term “fliessende Kristalle”, meaning flowing crystals, which is now known as liquid crystal (Sluckin et al., 2004). From its discovery until today liquid crystal science remains an interdisciplinary research field. It relates function and macroscopic behaviour with molecular structure, dynamics and energy.

2.2 Liquid crystal molecular structure

Generally, material exists in three main states; solid, liquid and gas. In addition, intermediate states may exist between the isotropic liquid and the solid crystal phase. These states, also called “mesophases”, include liquid crystals and plastic crystals, **Figure 2-1** Molecules forming a liquid crystalline phase are phrased as ‘mesogens”.

Typical shapes are rods and plates. The anisotropic shapes promote a molecular alignment with a preferred orientation, which is called the director (n).

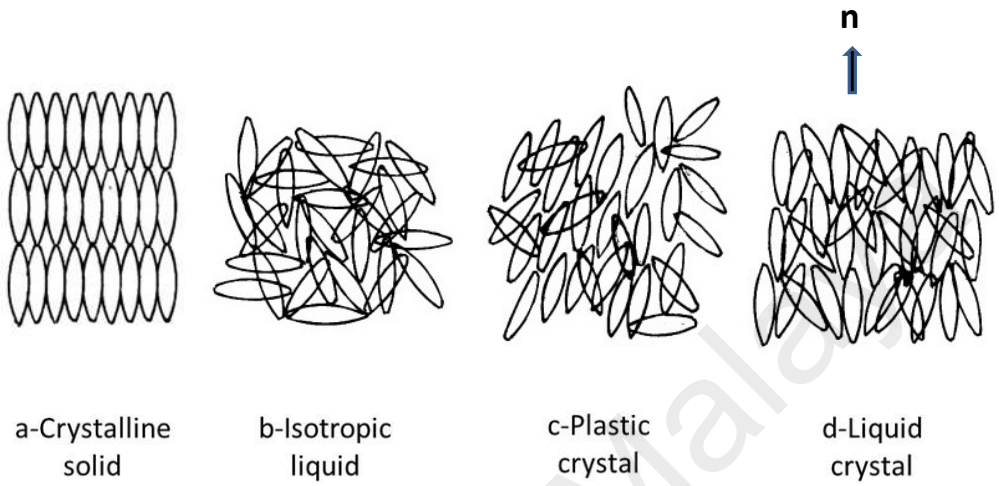

Figure 2-1 Sketch of the arrangement of molecules in various phases. *n* is the director. Figure from (Singh, 2000).

To form a liquid crystal phase, molecules need to be anisotropic, which means that they cannot adopt a spherical shape orientation. A preferred orientation of molecules causes different physical behaviour along the director and perpendicular to it. This feature forms the basis for most liquid crystal applications. Particularly interesting are those, where the director can be influenced by electric or magnetic fields, leading to induced changes of properties. Liquid crystalline phases can develop and disappear with temperature changes. Purely temperature sensitive, or thermotropic, liquid crystals are typically materials comprising of a single molecule only. Common examples include the cyanobiphenyls found in many of the early liquid crystal display (LCD) applications (some examples **Figure 2-2**).

Liquid crystal is a phase and it is sometimes called a mesophase or the middle phase. It can be obtained from material in a pure state or a mixture of them. Unlike ordinary materials, mesomorphic materials have different mechanical, optical and

structural properties. For example, these have crystalline properties but mechanically these flow like a liquid. The liquid crystalline phases can be derived in numerous ways for example by thermal process (thermotropic), by solvent effects (lyotropic)(Kumar, 2001; Neto & Salinas, 2005). It can be said that many organic molecules and mixtures (for example micellar solution) surfactants, and branched-chain polymer and large range of biological systems are some known examples of liquid crystal material. These days, organometallic liquid crystals have also been reported **Figure 2-2** (Halls et al., 2012).

About two decades ago, it was realised that in addition to rod-shaped and discotic molecules, bent-core (banana-shape) or the V-shape molecules can also form liquid crystals (Ito et al., 1974). Actually, the synthesis of bent-shaped liquid crystal molecules was reported some 80 years ago by (Vorländer & Apel, 1932), and was synthesised by Matsunaga & Simionescu (Matsunaga et al., 2003; Simionescu et al., 1977) in the early 1990s. Banana-shaped molecules with the smectic phase and their property have been discussed in detail by Ramamoorthy (Ramamoorthy, 2007). In **Figure 2-2**, an example of a liquid crystal molecule is observable that is capable of forming thermotropic disc and the columnar phases (Memmer, 2001).

Molecules that are both hydrophilic and hydrophobic (amphiphiles), can dissolve in solvents like water to form liquid crystals. Ordering, or self-assembly, of these amphiphiles is based on the interaction of their molecular antipodes with the solvent (attraction / repulsion). Unlike for thermotropic liquid crystals, the phase behaviour for so called amphitropic material is affected not only by the temperature, but also by the composition, or concentrations of solvent and solute (Barón, 2001) .Liquid crystalline with a solvent dependence are called lyotropic.

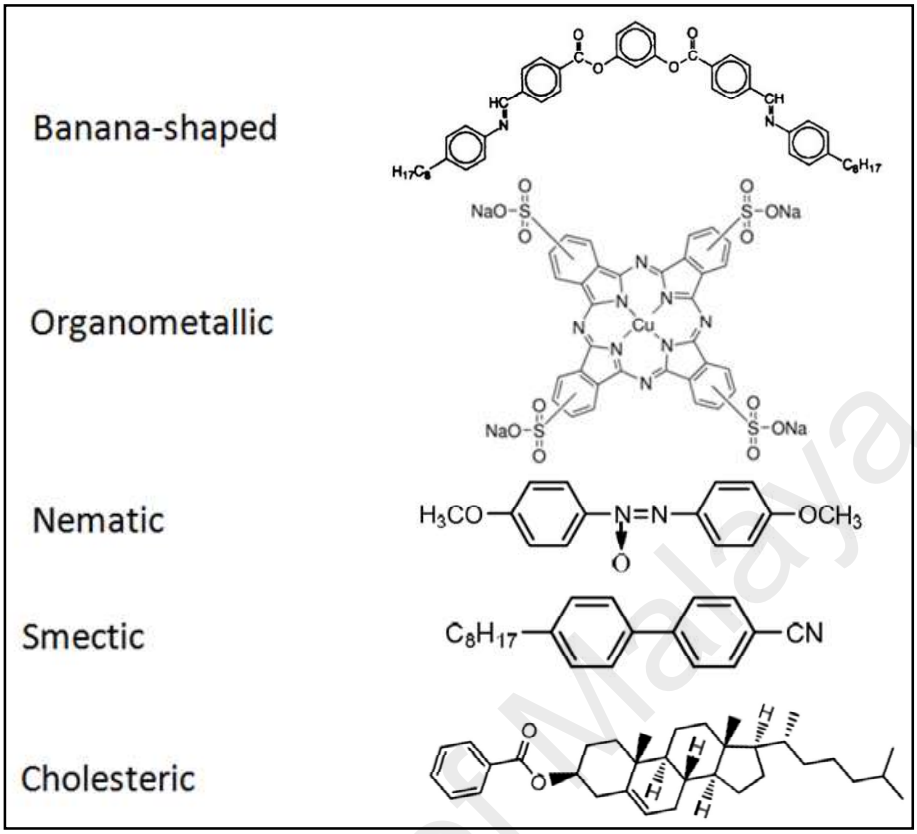

Figure 2-2 Sketch of some mesogens, and some common liquid crystal phases. Banana-shaped (Memmer, 2002), organometallic (Halls et al., 2012), nematic (Jákli & Saupe, 2006), cholesteric phase (Singh & Dunmur, 2002), smetic (Chandrasekhar, 1992).

Therefore in general liquid crystal phases are divided to thermotropic phases, lyotropic phases and metallotropic phases. Lyotropic and thermotropic phases usually include organic molecules. Thermotropic studies are related to the phase change caused by heat. Lyotropic studies are related to the concentration of liquid crystal in a solvent (usually water) and simultaneously by heat. But metallotropics are made up of organic and inorganic substances. In addition to heat and the concentration changes, metallotropic phases will also change with the proportion of organic and inorganic material in a vast range (Martin et al., 2006).

In liquid crystals, unlike crystals which have a base unit and are repeated throughout the crystal lattice, the orientational order is the major alignment for the

overall direction, i.e. the direction to which most of molecules (not all molecules) are aligned to. This direction is referred to as the director. In ordinary crystals, such as plastics, the basic unit is globular molecules in which no orientational order is present. Liquid crystals have optical properties like normal crystals but visually they flow similar to normal liquid (Vicari, 2003).

A phase transition can occur from one phase to the other. The phase is classified into two categories, based on physical and chemical parameters, namely lyotropics and thermotropics. The phase change in thermotropic liquid crystals takes place because of changes in temperature and pressure. An isotropy in thermotropic liquid crystals is also dependent on shape an isometry in molecules. The rods, disc and bananas are the common shapes for thermotropic materials. Both pure substances and mixtures of these can show thermotropic property. Due to the properties of liquid crystals between crystals' properties and normal liquid, as a result, they show unique optical, magnetic and electrical properties. Combining these special properties and the fact that thermotropic materials often require less energy to change phase, they can be manipulated easily for electropical devices such as liquid crystal display devices (LCD) and sensitive sensors (forehead thermometer). Although liquid crystals were known a century ago, their application in electro-optic devices emerged only from 1960 onwards (Vicari, 2003).

The electrical property of a certain molecule may be understood from the nature of the molecular alignment (with respect to the electric field electrical susceptibility) (Vicari, 2003). When one end of the molecule is positively charge and the other is negative charge, a permanent dipole is formed. In the absence of the permanent dipole moment, molecules can still be aligned in the direction of the external electric field due

to the formation of induced dipole arising from molecular polarizibility. The effect of magnetic fields on liquid crystals is similar to the electric field (Demus et al., 2011). Since magnetic field is formed by the movement of electrons around the nucleus of an atom, the magnetic field is also created from the movement of the existing electrons in the molecules of liquid crystals. When an external magnetic field is applied, the liquid crystal molecules are aligned in the direction or perpendicular to direction of the field. The special optical properties of liquid crystals will be described in section 2.4.

2.3 Phase behaviour

Mesophases can be classified by the general orientation of the majority of the molecules. In fact, two factors differentiate the phases from each other; the first is the positional order (whether molecules are placed in any kind of ordered frame) and the second is the orientational order (whether molecules are mostly placed in the same direction). Furthermore, the nature of an ordering in a liquid crystal can be either short-range (the position of a molecule to itself or at a microscope dimension) or long-range (the position of a molecule to other molecules on a macroscopic dimension). At a high enough temperature, a thermotropic liquid crystal exists as a thermotropic isotropic phase. This temperature is called the clearing temperature (T_C), when a cloudy appearance of a liquid crystal phase becomes clear. In fact, beyond this clearing temperature, it behaves like a normal liquid (Prost, 1995; Raynes, 1993). Nematic (N) and smectic (Sm) are the two main types of mesophases (liquid crystal phases). In the nematic phase molecules are solely orientated along the director, whereas the smectic phase adds a clustering of molecules in layers on top. Nematic and smectic liquid crystalline phases can be observed for both thermotropic and lyotropic systems. However, in lyotropic systems, a different terminology is more common, which *e.g.*

addresses the smectric phase as lamellar. **Table 2.1** gives the corresponding terms between the two branches of liquid crystal phase studies.

Table 2.1 Common terminologies for thermotropic mesophases. and their lyotropic counterparts (Barón, 2001).

Terminology in thermotropic mesophases	Synonyms in lyotropic mesophases
Smectic A, SmA	Neat phase or lamellar phase, L_α,
Columnar phase, Colhd	Hexagonal phase, middle phase, H_I, H_{II}
Bicontinous cubic phase Cubbi	Bicontinous cubic phase, Ia3d, Q_I, Q_{II}
Discontinuous cubic phase Cubdis	Discontinuous cubic phase, micellar cubic

2.3.1 Thermotropic liquid crystals

Liquid crystals form different phases with a changing temperature are called thermotropic liquid crystals. In any liquid crystal, when its temperature changes, the molecular motion including molecular orientations may change resulting in the formation of a new phase with different orientational and positional ordering. This change of phase is called a thermotropic phase transition (Ramamoorthy, 2007). When the temperature reaches the clearing point, the liquid crystal phase becomes isotropic liquid. And if the temperature goes down until the glass point, a gel phase may form. In fact, for a particular liquid crystal material, within this temperature range between the glass point to the clearing point, there may exist one or many different liquid crystal phases such as nematic, smectic, cholesteric, cubic etc.

2.3.1.1 Nematic phase

The mechanical properties of the nematic phase reflect an isotropic liquid. However, while the centres of mass for all molecules are randomly arranged, the orientation of the molecules is partially preserved from a crystalline solid, thus leading

to an anisotropic optical behaviour. This property forms the basis for the application of nematic phases in optical switching devices, such as liquid crystal displays. Presence of chirality within a nematic phase can cause a helical twist of the director, leading to a so called cholesteric phase, **Figure 2-3**. Cholesteric liquid crystals have particularly found applications as temperature sensors. Typically a uniaxial symmetry is assumed for the nematic phase. The biaxial geometry of most nematic mesogens, however, has led to the hypothesis of a biaxial nematic phase.

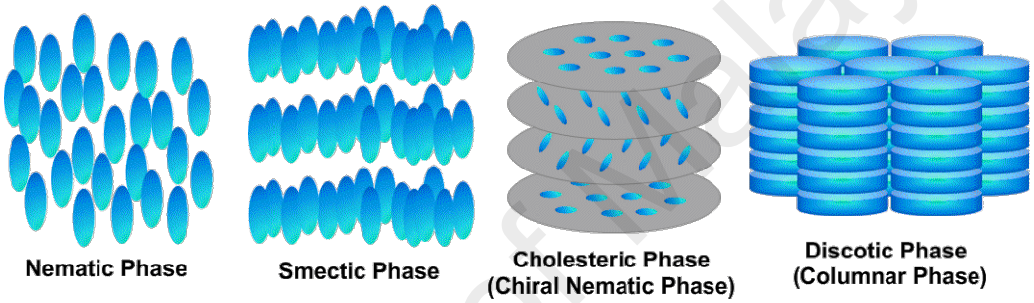

Figure 2-3 Sketch of thermotropic liquid crystal phases.
Figure from (http://www.tcichemicals.com).

A chiral liquid crystal is formed by the presence of chiral centres within the molecule or induced by a chiral dopant (Vicari, 2003). A chiral molecule has one or more stereogenic centres producing the left and right-handed stereoisomers. In addition, the equimolar of the right and left-handed stereoisomers (i.e. the racemic mixture) will produce a non-chiral liquid crystal phase. A chiral phase always possesses a twisting structure with a defined pitch. When the twisted structure of defined pitch is placed in the visible light, the phase rotates the plane of linearly polarised light for two different reasons (Vicari, 2003) **Figure 2-4**. First, the inherent molecular chirality, which appears even in the isotropic phase (such as sugar solution is optically active). And secondly, the formation of the spiral (or twisted) structure of chiral mesogens. Based on the refractive index, the pitch of the helix and the wavelength of light used, the system may rotate polarised light to the right or left and tilt sharply polarised light system (Vicari, 2003).

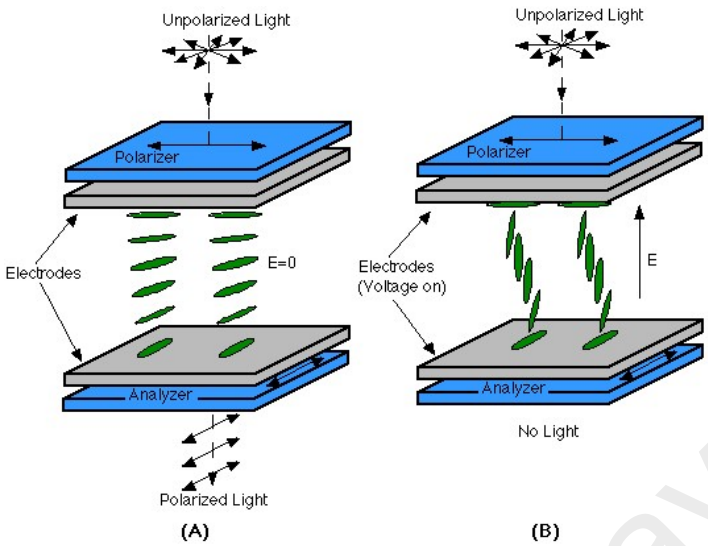

Figure 2-4 Sketch of Liquid crystal in cross polar plates.
(A) Liquid crystal (B) Non liquid crystal material.
Figure from (https://bly.colorado.edu)

Chiral liquid crystal molecules are essentially capable of creating a chiral mesophases. A good example is the linear a chiral complex phase by DNA molecule in a certain range of concentration and molecular weight (Cabuil et al., 2004). Recently an interesting discovery is made that a chiral liquid crystal molecules formed a chiral mesophase. Although its mechanism has not yet been determined, the liquid crystals may be ferroelectric or anti-ferroelectric (Baus & Colot, 1989; Uehara & Hatano, 2002). If a mesophase is not chiral, it can be chiral by adding a small amount of a chiral substance while that substance could not be a liquid crystal material. Often there is a small amount of impurities (dopant) in mixtures of nematic twisted or severely twisted for creating chirality.

2.3.1.2 Smectic phase

The layer structure in smectic and lamellar phases, combines the liquid crystalline feature of orientational order with some positional order. Because of this, smectic phases are more related to a solid phase than to an isotropic liquid. While

molecules are randomly distributed within the layers and can move freely within, the switch between layers is less likely. Within the layers molecules orient along the layer normal, as shown in **Figure 2.3**. In a smectic A phase the resulting director is parallel to the layer normal, while it forms an angle towards the bilayer normal in a smectic C phase. Finally, the smectic B phase is structurally very similar to smectic A. However, a hexagonal positioning of the molecular centres of mass adds additional positional order to the smectic A phase.

2.3.1.3 Some applications of thermotropic phases

In recent decades, the number of the fundamental and application studies of liquid crystals has greatly increased, and the scientific knowledge (physics and chemistry) have grown dramatically, therefore, a large number of technical and specialised articles have been published. Several conferences were held, and numerous books in the field of liquid crystals and their applications were published. Now, hundreds of scientists, especially chemists and physicists are working in the field of liquid crystals with their applications so that several good books can be found for research in every branch of the liquid crystal (Vicari, 2003).

One of the important applications of thermotropic liquid crystals is the display technology. The base of this application is the optical properties of liquid crystals in the presence or absence of an electric field and between two polarizing crossed sheets (Chen, 2011). Usually, a thin layer of liquid crystal of 10 micrometers is placed between two light polarizing sheets which are oriented at 90° to one another. The selected liquid crystal is placed in the absenceof an electric field in a half-twisted director configuration generated by rubbing the surface of the glass plates suitably (Castellano, 2005). As a

result, the light passes through it appears to be clear. But when an electric field is applied to the liquid crystal layer, the long molecular axes tend to align parallel to the electric field thus gradually untwisting the liquid crystal director, so that led to the lack of transmission of light, and that part becomes opaque. The electric field is a switch to turn on or off a liquid crystal cell, and a colour effect is generated by using RGB colour pixels (Castellano, 2005). Other devices of the optical properties of liquid crystals follow the same principles that have been mentioned above (Alkeskjold et al., 2007). Other important applications of liquid crystal are in the manufacture of tunable filters as electro-optical devices e.g., in hyperspectral imaging.

Another interesting application of thermotropic liquid crystals is their use in the manufacture of liquid crystals thermometers. Chiral liquid crystals have twisted structures. The pitch varies with temperature. The pitch is also within the wavelength of visible light. Hence the pitch will change colour with temperature, and this property can be used in the manufacture of thermometers (Witonsky & Scarantino, 2001). These thermometers are used for temperature measurement in most aquariums and pools and for the measurement of an infant's body temperature. Liquid crystals have also been stretched or stressed to change colour or to show hot spots in industry or they are used in the industry for the study of tension pattern and the electrical distribution (Plimpton, 1988).

Liquid crystals have a successful application in the external mirrors on both the reflection of the laser radiation and the radiation passing through the sets will be identified with a single colour wavelength (Dolgaleva et al., 2008; Kopp et al., 1998). A nematic liquid crystal has been used in making smart polymer film sheets of PDLC

(Polymer Dispersed Liquid Crystal) for windows in order to prevent the visibility of inside.

2.3.2 Lyotropic liquid crystals

Two or more materials which exhibit the properties of liquid crystals at different concentrations form a lyotropic liquid crystal. In the lyotropic phases, solvent molecules provide fluidity to the system by filling the space around the compounds (Liang et al., 2005). Like thermotropic liquid crystals, lyotropic liquid crystals also possess degrees of freedom in terms of temperature and pressure. However, in addition to these in the lyotropic phase, another degree of freedom, namely concentration enables the phase to have a variety of mesophases. A molecule that has two immiscible hydrophilic and hydrophobic parts is called an amphiphile. The formation of lyotropic liquid crystalline phase sequence with an amphiphilic molecule depends on the volume which balances between the hydrophobic and hydrophilic parts. These structures are shaped through the micro-phase separation of two mismatched components on a nanometer scale (Neto & Salinas, 2005). Soap and water is a daily example of a lyotropic liquid crystal with amphiphilic molecules.

Self-assembled structure varies with the content of water or the type of solvents. Amphiphilic molecules will disperse without any ordering at very low concentrations. The solution is slightly thicker (but still is low concentration) amphiphilic molecules will spontaneously assemble into micelles or vesicles at slightly higher (but still low) concentration. This concentration is called the critical micelle concentration (CMC) (Ruckenstein & Nagarajan, 1975). To hide the hydrophobic tail of the amphiphiles inside the micelle core, exposing a hydrophilic surface to the aqueous solution. In this

case, these spherical objects do not have any orientation in the solution hence the phase is isotropic and is not considered as a liquid crystal. At a higher concentration, the assemblies will become ordered. A typical hexagonal columnar phase is formed, where the amphiphiles form long cylinders that order themselves into a roughly hexagonal lattice. This is called the middle soap phase (**Figure 2-5**). At a still higher concentration, a lamellar phase (neat soap phase) may be formed. This phase is composed of amphiphilic layers of molecules covered by thin layers of water.

Inverse phases or sometimes also called the reversed phases are observed at high concentrations. That is, an inverse hexagonal columnar phase (columns of water encapsulated by amphiphiles) or an inverse micellar phase (a bulk liquid crystal sample with spherical water cavities) is created due to the low water content and high amount of amphiphilic molecules (**Figure 2-5**). Whether lyotropic phase is a normal (type I) or reverse (type II) depends on the average "shape" of the lipid molecules, which may be cylindrical, wedgelike or conical in a normal (type 1) or a reversed state (type 2) (Kulkarni, 2011). Variations in parameters such as concentration and temperature modify this average shape and may lead to lyotropic phase transitions (e.g., the lamellar phase to other phases such as hexagonal and a whole variety of cubic structures) (Grossmann et al., 2007).

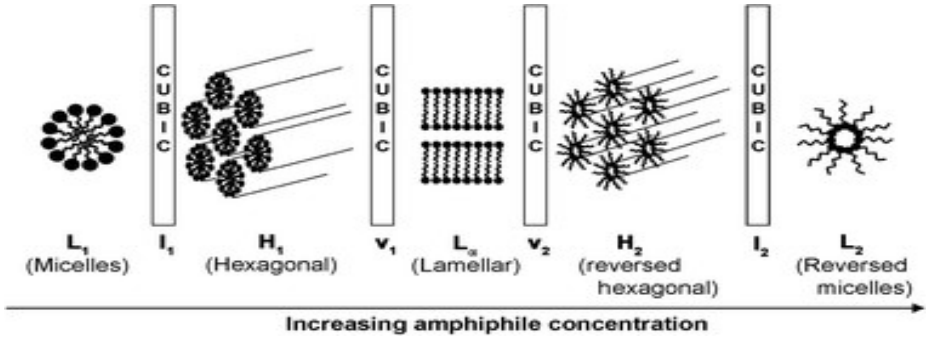

Figure 2-5 Sketch of the sequence of phases of amphiphile concentration. Names and abbreviations for the different mesophases. figure from (Kaasgaard & Drummond, 2006).

For some systems, a cubic phase (also called the viscous isotropic phase) may be formed between the hexagonal and the lamellar phases with increasing concentration. These phase form channels which may also be connected to one another, forming a bicontinuous cubic phase, whose existence is intriguing. It can be traversed in any direction in both the hydrophilic (water-like) and the hydophobic (oil-like) regions. Cubic phases have been observed, usually at relatively low curvatures, on the basis of one of three fundamental triply periodic minimal surfaces (TPMS). The bicontinuous cubic phase of an amphiphilic molecule can be divided into the normal (direct) and inverse (reverse) phases (Garstecki & Hołyst, 2001; Seddon & Templer, 1995). **Figure 2-7**(a) shows the normal phase (denoted as V_I in this thesis (Seddon & Templer, 1995)) in which water film is centred on the TPMS while the surfactant molecules are filling the two disjoint subspaces. The second group is an inverse phase (denoted as V_{II}) (Seddon & Templer, 1995) where the TPMS is occupied by a surfactant bilayer and the two channels are filled with water, see **Figure 2-7**(b) (Garstecki & Holyst, 2002; Garstecki & Hołyst, 2001). The TPMS can be further categorised into three common structures: Schwarz diamond (D), primitive (P) and Schoen gyroid (G) minimal surfaces, with crystallographic space groups of Pn3m (224), Im3m (229) and Ia3d (230) respectively, see **Figure 2-6** (Squires et al., 2005; Tresset, 2009; Zahid et al., 2013). The explanation of **Figure 2-6** is shown in **Table 2.2**.

.

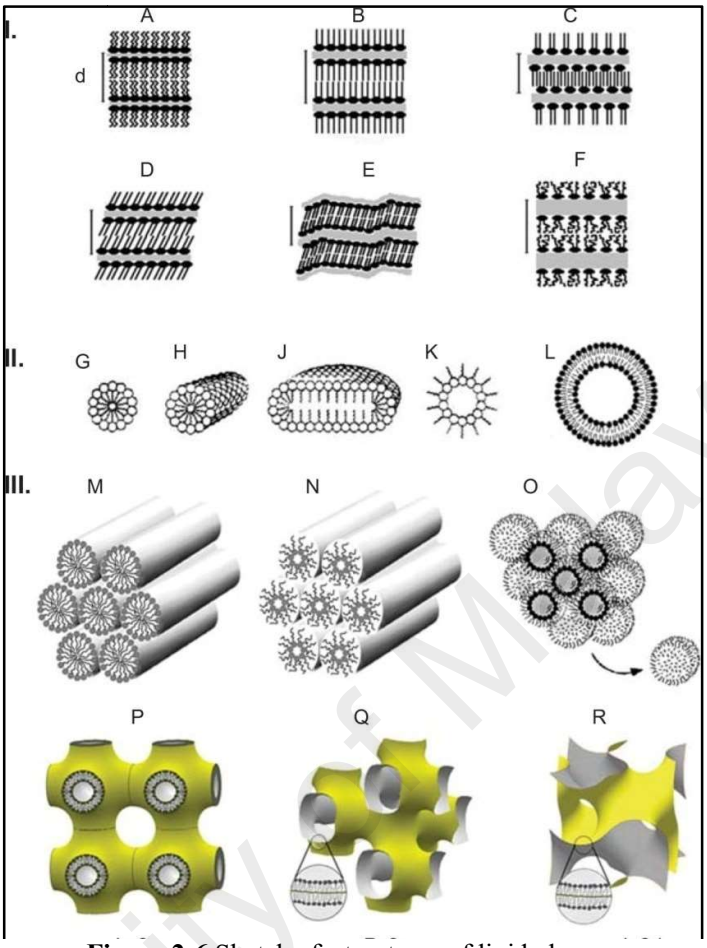

Figure 2-6 Sketch of structures of lipid phases.
Figure for (Koynova & Tenchov, 2013). Refer to **Table 2.2** for the notations A-R.

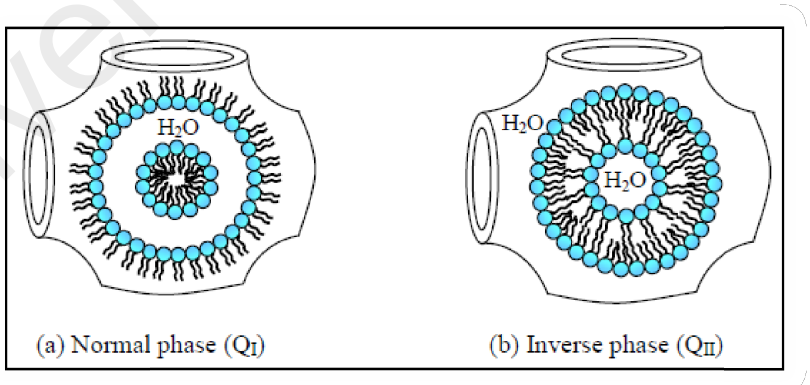

Figure 2-7 The bicontinuous cubic phase of an amphiphilic molecule.
Redrawn from (Garstecki & Holyst, 2002)

Table 2.2 Table of lipid phases.
Refer to **Figure 2-5** for nomenclatures used.

State	Mark in Figure 2-6	Name phase	Symbol
I. Lamellar phases	(A)	subgel	L_c
	(B)	gel	L_β
	(C)	interdigitated gel	$L_{\beta int}$
	(D)	gel, tilted chains	$L_{\beta'}$
	(E)	rippled gel	$P_{\beta'}$
	(F)	liquid crystalline	L_α
II. Micellar aggregates	(G)	spherical micelles	M_I
	(H)	cylindrical micelles	(tubules)
	(J)	disks	------
	(K)	inverted micelles	I_{II}
	(L)	liposome	------
III. Non-lamellar liquid-crystalline phases of various topology	(M)	hexagonal phase	H_I
	(N)	inverted hexagonal phase	H_{II}
	(O)	inverted micellar cubic phase	I_{II}
	(P)	bilayer cubic (V_{II}) phase	Im3m
	(Q)	bilayer cubic (V_{II}) phase	Pn3m
	(R)	bilayer cubic (V_{II}) phase	Ia3d

2.3.2.1 Molecular packing parameter

Molecular structure is related to phase geometry. This knowledge is useful in the design strategy of new materials. A simple packing theory was proposed to predict the phase behaviour from the knowledge of packing geometry parameter by Jacob Israelachvili (Israelachvili, 1991). The packing geometry of a molecule depends on its equilibrium area per molecule at the aggregate interface, $\mathbf{a_o}$, the hydrocarbon chain volume, V and the critical hydrocarbon chain length, L_C. The value of the dimensionless packing parameter **P**, also known as shape factor, $\mathbf{P = V/a_o L_C}$. **P** determines whether they form spherical micelles, non-spherical or cylinder micelles, vesicles or bilayers, or

inverted structures. The preferred phase formed corresponds to the minimum-sized aggregate in minimum free energy. In general, the packing theory emphasises the importance of the surfactant head-group in predicting what phase can be observed. However, the surfactant tail also has a controlling role in some cases (Nagarajan, 2002). Moreover, a few other factors also affect the phase formations and changes such as head-group size, ionic strength, and chain saturation, temperature, and lipid mixtures. **Table 2.3** illustrates the possible structures formed by lipids with different critical packing shapes.

A generalised sequence of thermotropic phase transitions in membrane lipids, such as phospholipids and glycolipids may be as follows (Tenchov, 1991):

$$L_c \leftrightarrow L_\beta \leftrightarrow L_\alpha \leftrightarrow Q^B{}_{II} \leftrightarrow H_{II} \leftrightarrow Q^M{}_{II} \leftrightarrow M_{II} \ ,$$

Also a lot of fluids like water and soap that we use are actually a liquid crystal which produces different liquid crystal mesophases (see **Figure 2-8**) in different water concentrations (Luzzati et al., 1957).

Table 2.3 Preferred geometries for different values of critical packing. parameter. Redrawn from (Israelachvili, 1991).

Lipid	Critical Packing Paramiter(V/a_oL_C)	Critical Packing Shape	Perferred Phase Geometry
Single-chained lipids with large head-group areas	< 1/3	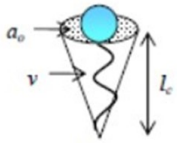 Cone	Spheres
Single-chained lipids with small head-group areas	1/3 – 1/2	 Truncated cone	Cylinders
Double-chained lipids with large head-group	1/2 - 1	 Truncated cone	Flexible bilayers
Single-chained lipids with small head-group	~1	 Cylinder	Planar bilayers
Single-chained lipids with small head-group areas	> 1	 Inverted truncated cone / wedge	Inverse structures

2.4 Physical properties and symmetry

The anisotropic physical properties are the result of the orientational order of liquid crystals combined with their molecular anisotropy. For example, the refractive index of a nematic liquid crystal is different along the average molecular direction (the director). In addition, since the nematic phase has a uniaxial symmetry, it has an equal refractive index in two dimensions but it has a different refractive index in the third dimension), because the optical indicatrix has only isotropic. The system is uniaxial because of the incomplete rotational degeneracy around the main axis. Likewise, the sample is true for the SmA phase. But when the phase is biaxial, such as a SmC phase,

the ellipsoid index does not have a complete rotational symmetry about any axis. This is because of the hindered molecular rotation around the long axis. Thus there are three distinct refractive indices. It should be noted that the symmetry of the phase is not the same as that of the symmetry of the constituent molecules. For example, a uniaxial phase can be formed by biaxial molecules (eg, phase SmA) and also a biaxial phase may be formed by uniaxial molecules (eg, phase SmC_A).

2.5 Identification of liquid crystal phase by texture

The most useful technique for identification of the liquid crystal phase is using the optical polarizing microscope. This qualitative technique depends on the interaction of polarised light, and defects within the phase and gives a unique texture when viewed in polarised light under a microscope. Defects in liquid crystals can be classified as point, line and wall defects. Disclination is an example of a line defect, which is unique to liquid crystals and it is a discontinuity of orientation of the director. This effect gives typical textures such as schlieren texture of a nematic phase, the fingerprint of a cholesteric (chiral nematic) phase, the fan-shaped texture of a smectic A phase and focal conic texture of a smectic A phase (Dierking, 2006) **Figure 2-8**. Typical textures from optical polarizing microscope of common liquid crystal phases are shown in **Figure 2-8**

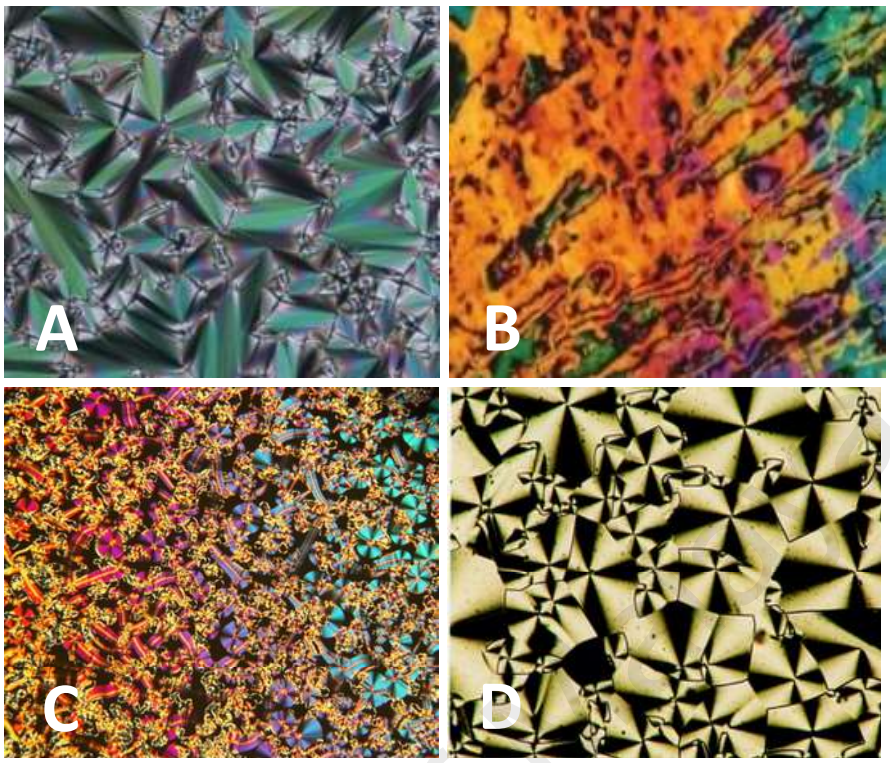

Figure 2-8 Examples liquid crystal textures.
A is Smectic phase (Starkulla et al., 2009); B is Marble texture for Nematic phase (Al-Hamdani, 2011); C is Cholesteric phase (Tantrawong, 2014); D is Columnarphase (Date et al., 2003).

2.6 Order parameter

In general, in a nematic phase (see **Figure 2-9**), the order parameter, S, is the degree of orientational ordering of the molecules defined by the following equation (**Equation 2.1**) (Vicari, 2003).

Equation 2.1 $$\boldsymbol{S = \langle P_2(\cos\theta)\rangle = \langle \frac{3}{2}\cos^2\theta - \frac{1}{2}\rangle}$$

Whereθ is the angle between the orientation of molecules and the orientation of the director, n,and P_2, is the second-order legendre polynomial. This average is taken over an assemble of molecules.

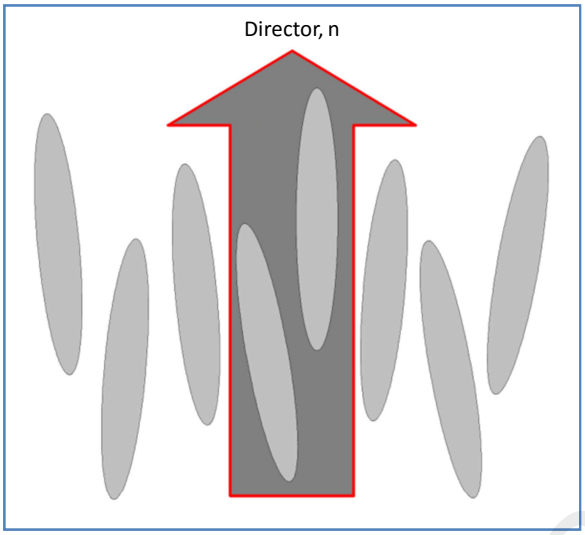

Figure 2-9 A schematic nematic domain and its director. which is also the local optical axis is given by the spatial and temporal average of the long molecular axes over a small element of volume and time.

The smectic phase with the layer structure has two ordering, corresponding to the orientation and position. Like the nematic phase (see **Equation 2.1**), the orientational ordering corresponds to the local orientation of molecules. The positional ordering is related to the density of the centres of mass of the molecules as the linear function of the normal layers, x, follows a sinusoidal variation (**Equation 2.2**), where ρ_0 is the average density and δ is layer distance which is usually a few nanometers. ψ is the positional order parameter of smectic phase.

Equation 2.2 $$\boldsymbol{\rho(x) = \rho_0(1 + \psi \sin(\frac{2\pi x}{\delta}))}$$

2.7 Glycolipids

Glycolipids are a member of a larger family of substances known as glycoconjugates, produced when carbohydrates interact with biomolecules other than carbohydrates (Allen & Kisailus, 1992; William Curatolo, 1987). There are many

natural glycolipids and these can be classified into glycosphingolipids, glycoglycerolipids and glycosyl phosphopolyprenols. For example, glycoglycerolipids are formed by the combination of carbohydrates with 1,2-di-O-acyl glycerols. Two glycoglycerolipids are found in the higher plant chloroplast, monogalactosyl diacylglycerol (MGDG) and digalactosyl diacylglycerol (DGDG) (Ishizuka & Yamakawa, 1985). The chemical structures of these glycoglycerolipid compounds are shown in **Figure 2-10**.

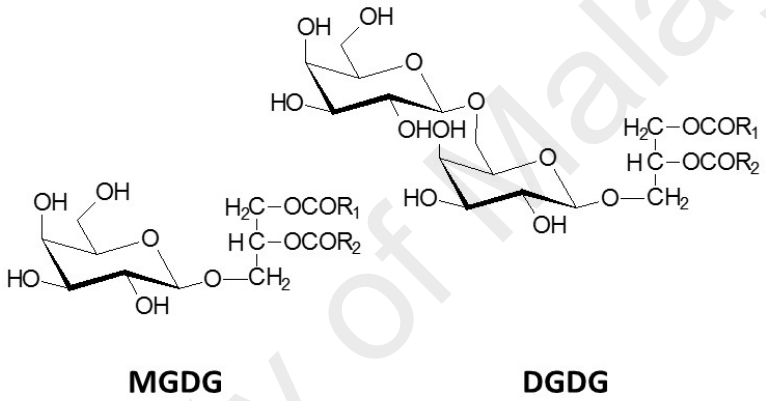

Figure 2-10 General chemical structures of some natural glycoglycerolipids.

Moreover, glycolipids can be synthesised from renewable resources like fatty alcohols oligosaccharides, and they are also produced enzymatically, which have less damage to the environment (von Rybinski, 1996). Thus, glycolipids have importance as a new type of surfactant (Shinoda et al., 1996) for delivering the drug into the body (Lasic, 1993) and are also used in different aspects of biotechnology (Lockhoff, 1991). Despite many researches on glycolipids, their physical and fundamental studies are still limited. This is due to the difficulty of obtaining pure chemical substances extracted from the cell membrane, and the difficulty of synthesizing them. Usually the extract from the cell membrane contains the bulk of the molecules with long chain unsaturated and a complicated isomeric mixture in the carbohydrate part as well (Curatolo, 1987a,

1987b). And such a mixture is difficult to characterise in order to clearly understand their properties. Though reliable methods of preparing glycolipids have been developed (Soderberg et al., 1995), it requires some procedures to obtain stereochemically pure compounds with specific spatial arrangement of molecules. It is vital to know how to control or modify the glycolipid structures at the molecular level in order to predict the self-assembly phase structures. Sugar molecules are strongly hydrophilic, so it can be concluded that the hydrophilicity of a lipid enhances with the increase in size of the oligosaccharide headgroup.

2.7.1 Importance of glycolipids

Glycolipids are amphiphiles (molecules that have a hydrophilic head and hydrophobic end) that bear a mono-, di- or oligosaccharide unit (a molecule that contain a sugar unit) as their hydrophilic head-group. Many technological and biological applications can be derived from glycolipids (Lindhorst, 2000; J. M. Seddon, 1996). For example, they play important role in cell biology and host microbial interactions (Lang, 2002). They are considered as the host sites of cell attachment for a number of pathogenic organisms and bacterial toxins; act as immuno-modulators, recognition markers for targetting drug delivery systems (Lasic, 1993) and they are considered as antiviral agents. On the other hand synthetic glycolipids have many useful surfactant applications such as drug delivery systems, stabilization of hydrocarbon foam, primary solvents for topical medication, simple household soaps and synthesis of nanostructure materials. In biological cell membranes, glycolipids play important roles in different physiological phenomena (Curatolo, 1987a, 1987b) such as the recognition of molecule at cell surfaces (Eggens et al., 1989) and stabilization of the membrane archaebacteria protein which grow under extreme environmental conditions (Kates, 1990).

2.7.2 Cell membranes

Cell membrane contains many natural glycolipids. The concentration and distribution of glycolipids depends on the type of tissue in question, its developmental stage and whether it is normal or diseased. Normally, the weight percent of membrane glycolipids in several types of membranes is given in **Table 2.4** (Alberts et al.).

Table 2.4 Weight percent of membrane glycolipids. in several types of membranes.

Type of Membrane	% By Weight
Liver plasma membrane	7
Erythrocyte plasma membrane	3
Myelin(brain)	28
Mitochondrial (inner and outer)	Trace
Endoplasmic reticulum	Trace

The cell membrane separates the external environment from the internal environment of the cell. It act as a passive barrier for diffusion and permeability (Brown, 2012). It allows the exchange of ions gases selectively in and out of the cell. The cell membrane is described as a bilayer of lipids and proteins, which is composed of various cholesterols, phospholipids, glycolipids and proteins. Cholesterols help to pack phospholipids in the membrane giving the membrane its stable structure. Biological membranes are fluid in nature and depend on its composition and temperature. The membrane fluidity is decreased by lowering the temperature because the molecules of the lipid bilayer tend to form regular, more rigid crystalline structures. The composition of the lipid affects the phase transition temperature of the membrane. **Figure 2-11** shows a schematic model of the cell membrane. A typical cell is full of liquid crystalline structures. The outer plasma membranes and intracellular organelles such as the mitochondrion, nucleus and endoplasmic reticulum are all bounded by the lipid Bilayer (J. M. Seddon, 1996).

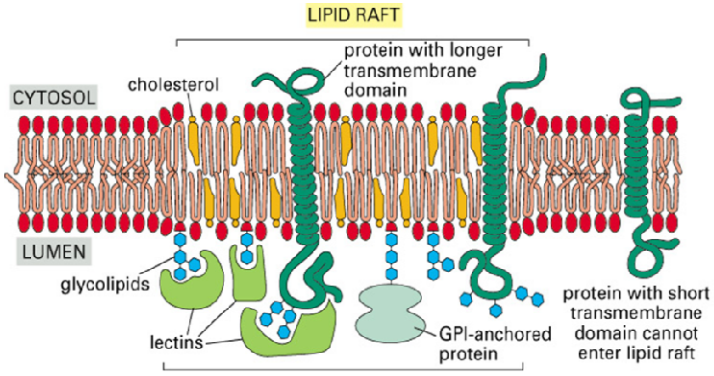

Figure 2-11 Schematic model of the cell membrane.

2.7.3 Lipid bilayer

A thin polarmembrane is composed of two layers of amphiphilic molecules that are called bilayer of lipids. A lipid bilayer is normally taken to be a model for a cell membrane. Though some of them are only a few nanometres in width (Andersen & Koeppe, 2007), they are resistant to the penetration of hydrophilic molecules. A bilayer is formed when amphiphiles are placed in the water, and these arrange themselves into a two-layered sheet (a bilayer) so that all the hydrophobic tails point toward the centre of the sheet. See **Figure 2-12** for a typical construction of bilayer. The central hydrophobic region of this layer does not have any water, and excludes molecules of sugar and salt dissolved in water but not in oil. The formation is similar to the formation of oil droplets in the water, molecules driven by the same force called hydrophobic effect. Bilayers are very challenging to study because the lipid layers are very fragile so thin that cannot be seen under the microscope. The experiments on bilayers need advanced techniques of atomic and electron microscopy.

The bilayer can also form a solid gel phase state at low temperature but changes to a fluid phase state at high temperature and influences the chemical properties of lipid's tails at any temperature. The mechanical properties, of resistance to stretching

and bending are influenced by the packing of lipids between the bilayers. Many of these properties have been investigated by constructing the artificial "model" bilayers in the laboratory. Vesicles which are made by model bilayers have also been used in delivering drugs clinically.

Bilayer lipid is very thin compared to its lateral dimensions. If a mammalian cell with the diameter of almost 10 microns, were enlarged to a watermelon size with the diameter of 30 cm, the plasma membrane's thickness would be as a piece of paper. Although the bilayer is only a few nanometers thick, it includes several different chemical areas across its cross-section. These areas and their interactions with the surrounding water have been explored over the past decades with techniques of x-ray reflectometry, (Lewis & Engelman, 1983), nuclear magnetic resonance (NMR), and neutron scattering (Zaccai et al., 1975).

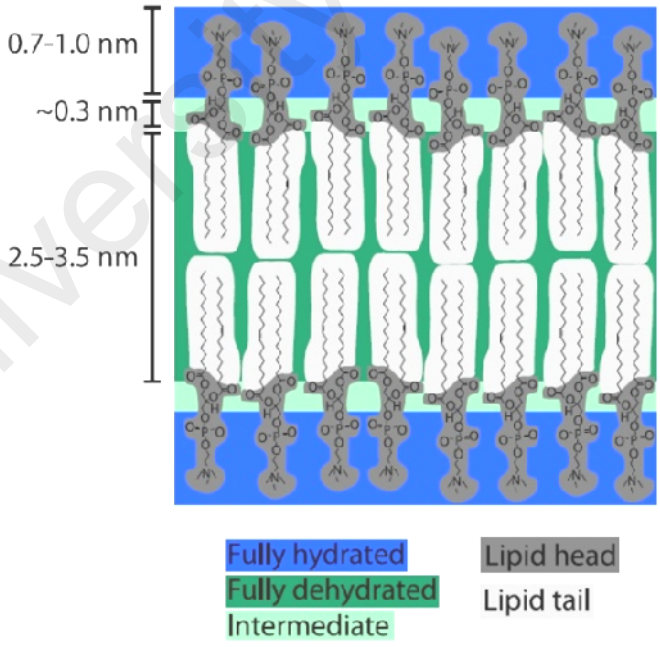

Figure 2-12 Schematic cross sectional profile of a typical lipid bilayer.

There are three distinct regions: the fully hydrated headgroups, the fully dehydrated alkane core and a short intermediate region with partial hydration. Although the head-groups are neutral, they have significant dipole moments that influence the molecular arrangement. Figure from (Mashaghi et al., 2012).

The first area is located on both sides of a layer of the hydrophilic molecules. This part of the membrane is covered with water, and it is about 0.7 to 1.1 nm thick. In bilayer of phospholipid, the phosphates at the end of the area are covered with water and the hydrophobic region is with a thickness of about 0.3 nm (Nagle & Tristram-Nagle, 2000). In some cases, the extension of the hydrated region is due to the large lipid proteins and the long sugar molecules. One example in nature is LPS (lipopolysaccharide) on the outer membrane of bacteria (Michael et al., 2003) that prevents dehydration. In **Figure 2-12**, the next area is the central area covered with a little water and a thickness of about 0.3 nm. In these two areas with low thickness, the water concentration decreases from 2M on the head-group to almost zero on the tail (Marsh, 2001, 2002). Tail hydrophobic molecules are normally 2.5 to 3.5 nm, which varies according to the chain length of the tail and its chemical formation (Lewis & Engelman, 1983; Rawicz et al., 2000). The thickness of this area also differs very much with temperature, mainly near the phase transition (Träuble & Haynes, 1971).

2.8 Bound water content

In the concept of dewatering of material, there are two types of water involved to be removed (Lee et al., 2013). One of them is water at the materials' level and the other is water which is trapped or bound to the material. This trapped water must be freed. This concept leads to the idea of "bound water", as it describes the properties of

bound water and the strength of bond between bound water and the materials' level. Some scientists have reported three types of water next to polymers, especially cellulose, by calorimetery (Magne et al., 1947). They have also reported two types of water that the melting point temperature of them is not zero degrees (Nomura et al., 1977). These two types of water are called bound water.

A number of researchers have reported that bound water in natural polymers have different properties compared to free water. It seems that the mobility of water molecules through the polymer is limited. These waters have been called by different names such as free water, bound water, ordered, and ice-like and non-freezing. There are many literatures which reported that the melting point and crystallization temperatures of water bonded within natural polymers such as cellulose are different from those free water (Magne et al., 1947; Magne & Skau, 1952). And a number of researchers (Andronikashvili et al., 1976; Froix & Nelson, 1975; H. Hatakeyama et al., 1980; Nomura et al., 1977; Preston & Tawde, 1956). Depending on the amount of bound water these transition temperatures can vary considerably.

Water plays a role in determining the membrane structure and is involved in its function. For example, the presence of water is essential in the formation of the phospholipid membrane. The degree of hydration is related to the mobility of the acyl chains of the phospholipid molecule. The water dynamics surrounding the lipid has been described but its characterization is limited, with limited interpretation (Konig et al., 1994). In the lamellar phase, NMR and pulsed field gradient spin-echo method (PFGSE) have been used in measuring bound water. In addition, Chapman also found that the DSC can be used to determine the water content near the membrane of phospholipids (Chapman et al., 1967). For molecules of phosphatidylcholine, the

amount of water that is not frozen at zero degree temperature is calculated to be about 10 molecules per lipid. In addition, the bound water in the phospholipid can be accurately described by ^{2}H-NMR (Hsieh & Wu, 1995). Some water molecules cling tightly to the hydrophilic groups and their movements are severely restricted. But waters between two adjacent layers of the lamellar with the aqueous phase are also moving faster. Abnormal mobility of water molecules in the vicinity of the border phosphatidylcholine has been reported (D_2O) (Finer, 1973; Wassall, 1996).

The chemical structure of glycolipids is related to the bilayer stability. Computer simulations of studies of disaccharide based glycosides have been performed to determine the molecular interactions within the glycolipid bilayer. The results show the different extents of hydrogen bonding between the sugars contribute to the stability of the assembly (Achari et al., 2012; Ahmadi, 2014). The simulation results can be explained by appropriate experimental study on hydrogen bonding. The interaction of surfactants with water can be correlated to the so called bound water content. For its determination several methods have been applied (Giammona et al., 1992; Hauser et al., 1989; Onori & Santucci, 1993; Rosano et al., 1989; Senatra et al., 1984; Senatra et al., 1991). We have selected deuterium NMR (Hauser et al., 1989; Senatra et al., 1991). and differential scanning calorimetry (DSC) based on freezing water (Rosano et al., 1989; Senatra et al., 1984). While the first method investigated the deuterium quadrupole splitting in an anisotropic medium over a concentration range, the latter monitors the melting of ice in formulations of different concentrations, assuming that only non-bound or 'free' water can freeze. The melting enthalpy of water in formulations provides information on the latter; therefore, the bound water content can be determined as the difference between total and freezing water content. (Mirzadeh Hosseini et al., 2012)

CHAPTER 3: MATERIALS, METHODS& SAMPLING

In this chapter, the applied materials and methods for the study will be explained. It is worth mentioning that the used materials include two groups; the first of them was obtained from commercial sources (commercial material), while the latter was chemically synthesised in the laboratory (synthetic material).

3.1 Materials

Owing to unavailability of commercial sources for most disaccharide-based glycolipids and extreme high pricing for even monosaccharide-based analogues, all investigated compounds needed to be chemically synthesised prior to their physical investigation. The glycolipids are listed in **Table 3.1**. The preparation emphasised on economy in costs and time rather than on optimised total yields. Highest priority was given to the achievement of high chemical purity, in particular with respect to the stereo-chemical configuration at the reducing sugar.

Glycolipids with β-configuration were obtained from the peracetylated sugars in a kinetically controlled reaction catalysed by boron trifluoride (Vill, 1989) or applied the Koenigs-Knorr sequence (Koenigs & Knorr, 1901). The preparation of β-glycosides, on the other hand, required longer reaction times and a stronger catalyst, i.e. tin tetrachloride (Hashim et al., 2006; Kwong et al., 2010). In this case, the reaction output is determined by the relative thermodynamic stability of the product anomers. Typically the separation of diastereomeric anomers from thermodynamic determined

glycosylations is more challenging, owing to larger contents of unwanted anomer. All syntheses involve several steps, which are described below.

Table 3.1 Synthesised moleculs.

No.	Compounds	Yield(%)	Catalyst
1	β-CelloC_{12}	30	BF_3
2	β-CelloC_{12}Tech	19	BF_3
3	β-MeliC_{12}	19	BF_3
4	β-CelloC_8	39	BF_3
5	β-LactoC_{12}	20	BF_3
6	β-MaltoC_8C_4	34	BF_3
7	β-Gluco$C_{12}C_8$	21	BF_3
8	α-GlucoC_6C_2	5	$SnCl_4$
9	α-Gluco$C_{10}C_6$	11	$SnCl_4$
10	α-Gluco$C_{14}C_{10}$	8	$SnCl_4$
11	β-GalactoC_6C_2	43	BF_3
12	α-GalactoC_8	7	BF_3

3.1.1 Raw materials

The applied preparation of glycolipids involved four distinct phases. These are peracetylation (protection and activation of the sugar), glycosylation (forming a chemical bond between a hydrophobic alcohol at the sugar), purification, and deacetylation (final deprotection), respectively.

Starting materials and reagents were purchased from reputable suppliers (Merck, Sigma-Aldrich, Acros etc.) in high purity, while solvents of AR grade from various manufacturers were used without prior purification steps. All materials were classified into four groups, according to the stage of their application in the glycolipid preparation. The first group of materials was used in the peracetylation stage (**Table 3.2**); the second group contains compounds for the glycosylation (**Table 3.3**); the third group refers to

material for the chromatographic purification process (**Table 3.4**), and the fourth group lists materials for the final glycolipid deprotection (**Table 3.5**).

3.1.1.1 Acetylation (protection)

Starting materials and reagents used for the acetylation of the sugar are found in **Table 3.2**. The acetylation procedure is described in section 3.1.2.1 below. There are several reasons for the necessity of the acetylation, which are mentioned there as well.

Table 3.2 Materials for acetylation (Protection).

No.	Name	Formula
1a	Monosaccharide	$C_6H_{12}O_6$
1b	Disaccharide	$C_{12}H_{22}O_{11}$
2	Sodium acetate	$CH_3COO\ Na$
3	Acetic anhydride	$(CH_3CO)_2O$
4	Ethanol	C_2H_5OH

3.1.1.2 Glycosylation

Depending on the targeted glycoside (α or β) either kinetic control using BF_3 as catalyst or thermodynamic control with $SnCl_4$ were applied. The materials used for the glycosylation step are shown in **Table 3.3**, while the glycosylation procedure is described in section 3.1.2.2 below.

Table 3.3 Materials for synthesise glycosylation.

No.	Name	Formula
1a	Sugar pentaacetates (monosaccharides)	$(C_6H_{12}O_6)5Ac$
1b	Sugar octaacetates (disaccharides)	$(C_{12}H_{22}O_{11})8Ac$
2	Dichloromethane	CH_2Cl_2
3	Alcohols	R-OH
4	Boron trifluoride Diethyl etherate	$BF_3 \cdot O(C_2H_5)_2$
5	Tin tetrachloride	$SnCl_4$
6	Celite (for α)	SiO_2
7	Sodium bicarbonate	$NaHCO_3$
8	Acetonitrile	CH_3CN
9	Hexane	C_6H_{14}
10	TLC sheets	SiO_2/Al

3.1.1.3 Purification (chromatography)

Column chromatography was used for purification of the glycolipids. The chromatography was performed on silica as stationary phase using a mixture of ethyl acetate and hexane as eluent. The ratio of the solvents was adjusted to achieve an R_f of about 0.2 for the targeted product on TLC. The materials for the column chromatography are shown in **Table 3.4**, while a full description of the process is provided in section 3.1.2.3 below.

Table 3.4 Raw material for choromatography.

No.	Name	Formula
1a	Acetylated Glycolipids(monosaccharides)	$C_{14}H_{19}O_9OC_nH_{2n+1}$
1b	Acetylated glycolipids (Disaccharides)	$C_{26}H_{31}O_{17}OC_nH_{2n+1}$
2	Hexane	C_6H_{14}
3	Ethyl acetate	$CH_3COOCH_2CH_3$
4	Silica gel	SiO_2
5	Dichloromethane	CH_2Cl_2
6	Triethylamine	$N(CH_2CH_3)_3$

3.1.1.4 Deacetylation (deprotection)

The final deprotection stage after the purification is very important and the purity of molecule should be preserved. The materials used are shown in **Table 3.5**, while a description of the process is provided in section 3.1.2.4 below.

Table 3.5 Raw material for deacetylation (deprotection).

No.	Name	Formula
1	Acetylated sugars	see Table **3.4**
2	Methanol	CH_3OH
3	Sodium methoxide	CH_3ONa
4	Resin	Amberlite IR 120 (H^+)

3.1.2 Synthesis

In this study 12 different glycolipids, shown in **Table 3.1**, were prepared according to literature described procedures (Hashim et al., 2006; Vill, 1989).

The studied glycolipids, except for the commercial dodecyl β-maltoside (β-MaltoC_{12}), were obtained in the laboratory in high purity. The anomeric purity was

examined by ^{1}H-NMR (Misran et al., 2013). The anomeric (α/β) purity of most compounds was equal or higher than 97%.

The synthesis of glycolipids comprises of four main stages. In the first stage all hydroxyl groups of the sugar molecule are acetylated to ensure solubility in non-polar organic solvents, suitable for the subsequent reaction with a hydrophobic alcohol, and to avoid condensation of sugar molecules during the glycosylation, which would lead to unwanted oligosaccharide side products. In the following Lewis-acid catalysed glycosylation step the acetalic, or glycosidic, acetate is exchanged with a hydrophobic alcohol. A ratio of 1:1.5 of sugar peracetate and alcohol is applied to create the acetylated glycolipid. The latter is subsequently purified by column chromatography on silica gel. The separation process is difficult owing to the similar elution property of anomeric impurities, which cannot be avoided entirely during the glycosylation process. The anomeric purity is evaluated by ^{1}H-NMR. In the final stage the acetate protection groups on the glycolipid are removed by trans esterification. Typically no side products are observed during this process.

3.1.2.1 Acetylation (protection)

During this step we use the six sugars (four disaccharides and two monosaccharides) that are shown in **Figure 3-1**. We used these six sugars because the optimization based on simulation uses the same sugars.

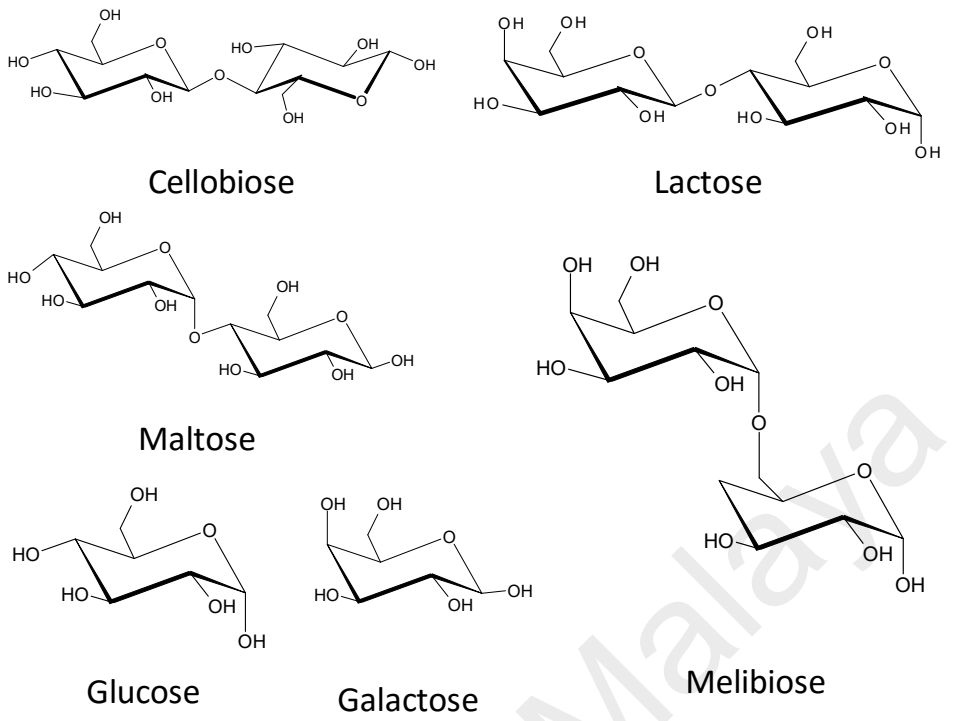

Figure 3-1 Structure of disaccharides.

We changed the hydroxyl groups (-OH) in the sugars to esters (acetylating) before the glycosylation. The reaction scheme of peracetylation is shown in **Figure 3-2**.

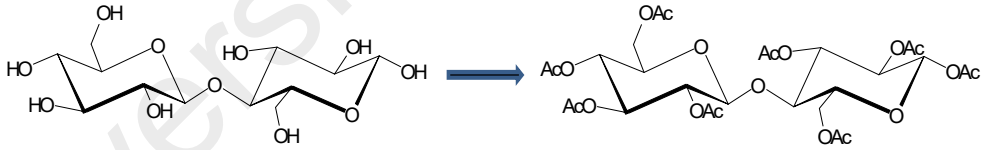

Figure 3-2 Reaction scheme of peracetylation cellobiose.

There are three reasons for the peracetylation prior to the glycosylation. That explain in below:

(a) Product choice:

To be able to produce β-enantiomer and to minimise the impurities of α-enantiomer, a neighbor active protection group at C-2 is required to block the unwanted α-attack. Esters, like acetates, are suitable protection groups.

(b) Reactant miscibility:

Given the nature of the polar disaccharides, they are soluble only in polar solvents, while the selected alcohols are non-polar, hence only soluble in non-polar solvents. However, both compounds need to be dissolved in the same solvent in order to enable an effective reaction. The acetylation of the sugar reduces its polarity and enables reactions inorganic solvents of low polarity.

(c) Destruction of the disaccharide:

The glycosylation of disaccharides requires the activation of the reducing anomeric carbon to ensure sufficient reactivity for the glycosylation without risking damage of a glycosidic bond between the two sugars. Glycosyl ester, in particular the β-anomers, are more reactive than normal glycosides and, therefore, provide this activation. The sugars, which were acetylated in the survey, are listed in **Table 3.6**.

Table 3.6 Acetylated moleculs.

No.	Compounds	Acetylated
1	β-Lactose	β-Lactose octaacetate
2	β-Cellobiose	β-Cellobiose octaacetate
3	β-Galactose	β-Galactose octaacetate

In the acetylation method, sodium acetate and acetic anhydride were heated to reflux and the sugar was added slowly. After complete addition of the sugar the reaction was heated for another hour and subsequently poured into ice water. The precipitating sugar acetate was collected and finally recrystallised from ethanol. The crystallization provided the peracetates in good yields and high chemical and optical purity.

3.1.2.2 Glycosylation

The glycosylation step was monitored by thin layer chromatography to check both reaction process and the purity of the compounds, with respect to formation of anomeric impurities. The requirement for column chromatographic purification of the product limits the reaction scale, because only up to 7g crude product can be purified at once. This translates to less than 3 g acetylated glycolipid, or less than 2 g final deacetylated glycolipid, based on the conversion rate and loss due to impurities. The reaction for the glycosylation is show in **Figure 3-3**.

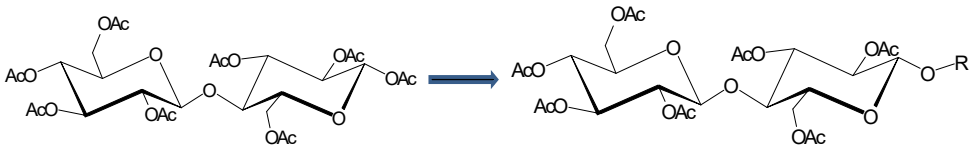

Figure 3-3 Reaction scheme of glycosylation cellobiose acetate.

BF_3 was used as Lewis acid catalyst to mediate the glycosylation. For kinetic controlled reactions of β-glycosides the reaction time has to be limited to about five to

six hours. In this method a solution of acetylated sugar and alcohol at ratio 1:1.5 is treated with access catalyst (equal or more than 1.5 equivalents based on the sugar) and is stirred at room temperature. For the preparation of α-glycosides significantly increased reaction times (up to two days) and higher Lewis acid concentration, or the application of $SnCl_4$ is required.

3.1.2.3 Purification (chromatography)

Column chromatography was used for the purification (**Figure 3-4**). In this study, silicagel with particle sizes in the range of 35-70 μm and three different column sizes, as specified in **Table 3.7** were used. To ensure a reasonable flow, moderate pressure was applied using a hand bellow. The eluent, hexane and ethylacetate, was adjusted to a R_f of about 0.2 for the targeted glycolipid. Samples were investigated by TLC to identify the correct fractions.

Table 3.7 Chromatography columns.

No.	Diameter	Height of Silica gel	Weight of Crude Product
1	3 cm	20 cm	0 – 3 g
2	5 cm	20 cm	3 – 5 g
3	7 cm	20 cm	5 – 7 g

Figure 3-4 Chromatography column.

Purification was achieved by column chromatography and subsequently evaluated by ^{1}H-NMR spectroscopy. The distinct difference of anomeric signals enables a good differentiation of these diastereomeric products, while the integration of signals enables a quantification of sugar and alkyl chain, respectively. This is the basis for the determination of both chemical purity and anomeric purity of the glycolipid. An example of a ^{1}H-NMR spectrum for an acetylated glycolipid is shown in **Figure 3-5**.

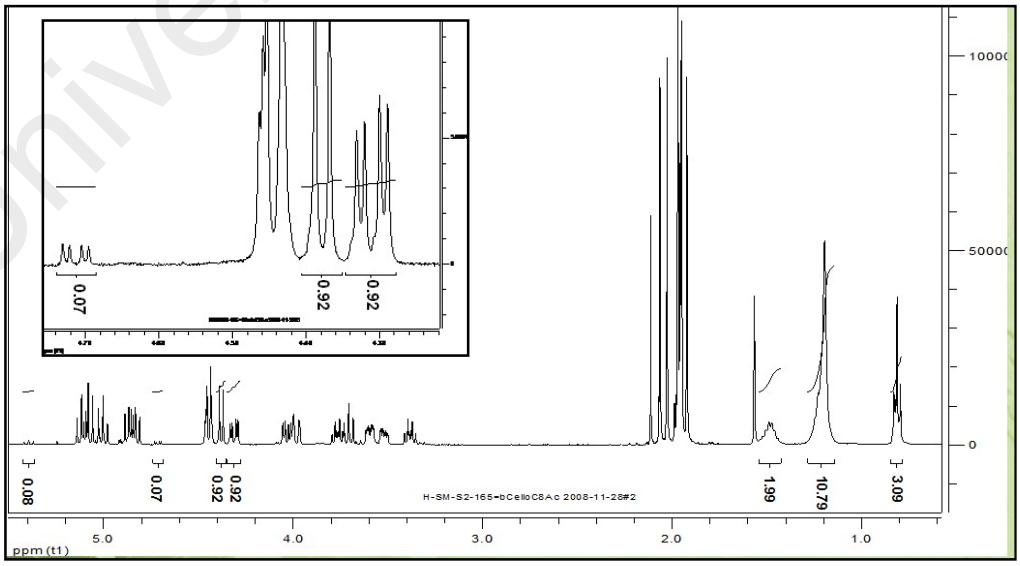

Figure 3-5 ^{1}H-NMR for chemical and anomeric (α/ß) purity.

For the chemical purity the integral for the CH_3 peak at 0.8 ppm was standardised to 3 (one CH_3 group). Based on a C_8 alkyl chain, the integration for the CH_2 peaks at 1.2 ppm and 1.45 ppm must be 10 (5 CH_2) and 2 (β-CH_2), respectively, and the anomeric sugar signals at 4.3 and 4.7ppm must be two in sum, since the spectrum refers to a disaccharide (one CH for each glucose unit). The anomeric purity can be determined by comparing the integrals for the characteristic signals for both anomers: the H-1 of the β-anomer appears as a doublet with about a coupling constant of about 8 Hz at around 4.4ppm, while the H-2 of the α-anomeric shows up at 4.65–4.75 ppm as double-doublet with a 10 Hz and a 4 Hz coupling constant.

3.1.2.4 Deacetylation (deprotection)

This reaction is fast and can be monitored by thin layer chromatography. A problem in this step is water impurity, because the glycolipids are hygroscopic. For this reason the compounds were dried in a vacuum oven for one night. The reaction scheme of the deacetylation is shown in **Figure 3-6**.

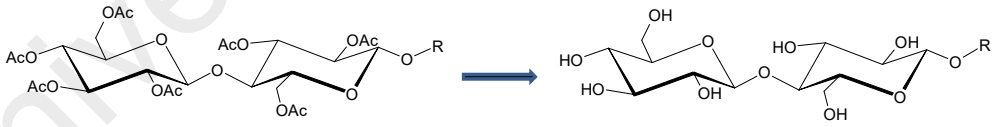

Figure 3-6 Reaction scheme of deacetylation.

The acetylated precursor was dissolved in methanol, and then sodium methoxide powder was added to obtain a pH of 8-9. The reaction was followed by TLC. It usually took about an hour. For workup, a proton charged ionic resin was applied to remove the sodium ions, whereas the solvent and the side product, methyl acetate, were evaporated at a rotary evaporator.

3.1.2.5 Synthesis monosaccharide glycolipids

(a) 2-Ethyl-1-hexyl-α-glucoside (α-glucoC$_6$C$_2$)

For the preparation of α-GlucoC$_6$C$_2$, first the amount of 7 grams of glucose pentaacetate in 50 ml was added to dichloromethane solvent (DCM) and was dissolved in it, and then the amount of 3.38 ml (ratio of 1: 1.5) alcohol (2-ethyl-1-hexanol) was added to it. Then 2.1 ml of $SnCl_4$ as catalyst was added slowly with a syringe. Solution was stirred for 24 hours. Then the reaction was stopped by adding Celite resin. And then acetonitrile and hexane solvents were used for the product's extraction. And then the amount of material after purifying, the separation and drying was 0.7 g (yield 9%). Then the column chromatography was used for separating and purifying, and the amount of substance 0.57 g (yield 81%) after purifying, then for deacetylation (DVD), it was dissolved in methanol, and sodium methoxide anhydrous was added and was stirred for 24 hours. Then with the increase of a little resin amberlite, pH was brought to 7 and 0.26 g of the dried α-GlucoC$_6$C$_2$ (yield 72%) was achieved, and the total reaction's yield was 5%.

(b) 2-Hexyl-1-decyl-α-glucoside (α-glucoC$_{10}$C$_6$)

For the preparation of α-GlucoC$_{10}$C$_6$, the same method of preparing α-GlucoC$_6$C$_2$ was used which was described in the previous section with the same amount, but 7.76 ml alcohol (2-hexyl-1-decanol) and the amount of 3.16 ml $SnCl_4$ were used. The yield for glycosylation was 14%, and for chromatography stage 80%, and for deacetylation was 89% and the total yield was 12%.

(c) 2-Octyl-1-dodecyl-β-glucoside (β-glucoC$_{12}$C$_8$)

The production method of α-GlucoC$_6$C$_2$ was used as the method of producing β-GlucoC$_{12}$C$_8$ but the amount of 7.74 ml alcohol (2-octyl-1-dodecanol) in a ratio of 1:1.2 was added, and 2.88 ml of boron trifluoride diethyl etherate (BF_3) as a catalyst was slowly added with a syringe. For stopping the reaction, saturated sodium bicarbonate and then a small amount of magnesium sulfate were used. The yield of reaction in glycosylation was 26% and it was 97% for the chromatography stage and it was 81% for deacetylation and the total production yield was 21%.

(d) 2-Decyl-1-tetradecyl-α-glucoside (α-glucoC$_{14}$C$_{10}$)

The production method of α-GlucoC$_6$C$_2$ was used for the synthesis of α-GlucoC$_{14}$C$_{10}$ but the amount of 11.36 ml of alcohol (2-decyl-1-tetradecanol) and 2.37 ml of $SnCl_4$ were used. The yield of reaction in glycosylation was 10% and it was 86% for the chromatography stage and it was 92% for deacetylation and the total production yield was 9%.

(e) 2-Ethyl-1-Hexyl-β-galactoside (β-galactoC$_6$C$_2$)

The production method of β-GalactoC$_6$C$_2$ was the same as producing method of β-GlucoC$_{12}$C$_8$, but 5 grams of galactose pentaacetate and 2.41 ml of alcohol (2-ethyl-1-hexanol) and 2.37 ml of BF_3 were used. The yield of reaction in glycosylation was 63% and it was 99% for the chromatography stage and it was 69% for deacetylation and the total production yield was 43%.

(f) Octyl-α-galactoside (α-galactoC$_8$)

Producing α-GalactoC$_8$ was not done by the use of $SnCl_4$ as a catalyst and the production rate of β enantiomer was more than α. The α enantiomer was produced by using BF_3 as a catalyst over the long period of time, though without a high yield. Therefore, the amount of 7 grams of Galactose pentaacetate was added in DCM solvent solution and 4.17 ml of alcohol (1-octanol) and 3.32 ml of BF_3 as a catalyst were added slowly with syringe and stirred for 9 hours. The rest of process was similar to β-GlucoC$_{12}$C$_8$ production processes. The yield of reaction in glycosylation was 26% and it was 57% for the chromatography stage and it was 79% for deacetylation and the total production yield was 12%.

3.1.2.6 Synthesis glycolipids disaccharide

(a) Octyl-β-cellobioside (β-celloC$_8$)

For producing β-CelloC$_8$, the cellobiose pentaacetate in the amount of 7 g was dissolved in DCM and the solvent ratio of 1:1.5 alcohol (1-octanol) in the amount of 2.43 ml was added, and the amount of 1.91 ml BF_3 as a catalyst was added slowly with syringe and was stirred for 7 hours. For stopping the reacted, the saturated sodium bicarbonate was added and then a small amount of magnesium sulfate was added and was extracted and dried by the solvents of acetonitrile and hexane (the yield of 87%). Then it was purified by using column of chromatography (the yield of 43%). Then it was dissolved in methanol for deacetylation(DVD) and a small amount of sodium methoxide anhydrous was added and was stirred for 12 hours. Then pH was raised to 7,

and 1.71 g of dried β-CelloC_8 was obtained with the slight increase in resin amberlite (the yield of 98%) and the total reaction yield was 36%.

(b) Dodecyl-β-cellobioside (β-celloC_{12})

Producing β-CelloC_{12} was in accordance with the method of β-CelloC_8 production, but 6.78 grams of cellobiose pentaacetate and alcohol (dodecanol) and 1.31 ml to 2.32 ml of BF_3 were used. The yield of reaction in glycosylation was 46% and it was 43% for the chromatography stage and it was 98% for deacetylation and the total production yield was 37%.

(c) Dodecyl-β-cellobioside (β-celloC_{12})(Tech.)

Producing β-CelloC_{12} (Tech.) was in accordance with producing β-CelloC_{12} with this difference that there is no chromatography stage for separating α and β enantiomers, and the product is the mixture of α and β. Also, the amount of 5 g of cellobiose pentaacetate was solved in the solvent, and 2.51 ml dose of alcohol (dodecanol) and 1.36 ml of BF_3 were used. The reaction yield of glycosylation was 58% and it was 95% for the deacetylation (DVD) and the total yield was 55%.

(d) 2-Butyl-1-octyl-β–maltoside (β-maltoC_8C_4)

The preparation of β-MaltoC_8C_4 was according with the method of producing β-CelloC_8. 3.46 ml of alcohol (2-butyl-1-octanol) was slowly added to the solutions of 7 g. Maltose pentaacetate in DCM, and 1.91 ml of BF_3 catalyst. The yield of reaction in

glycosylation was 79% and it was 49% for the chromatography stage and it was 88% for deacetylation and the total production yield was 34%.

(e) Dodecyl-β–lactoside (β-lactoC$_{12}$)

The production of β-LactoC$_{12}$ was done according to the production method of β-CelloC$_8$, but 7 grams of lactose pentaacetate and 3.47 ml of alcohol (dodecanol) and 1.95 ml of BF_3 catalyst were used. The yield reaction in glycosylation stage was 84% and it was 41% for the chromatography stage, and it was 59% for Deacetylation and the total yield was 20%.

(f) Dodecyl-β–melibioside (β-melibioC$_{12}$)

The preparation of β-MelibioC$_{12}$ was according to the production method of β-CelloC$_8$, but 6.78 g. of melibiose pentaacetate and 3.36 ml of alcohol (dodecanol) and 1.90 ml of BF_3 catalyst were used. The reaction yield in glycosylation was 74% and it was 27% for the chromatography stage and it was 95% for deacetylation and the total yield was 19%. This material was not purified by chromatography method.

3.1.3 Purity

The choice of preparative method of these glycolipids usually balance on costs and time rather than on optimised total yields. Highest priority was given to achieve high chemical purity, in particular with respect to the stereo-chemical configuration at the reducing sugar. Here anomeric (α/ß) purity was the main goal. This led the ^{1}H-NMR method to choose which chemical purity was measured with high accuracy and

anomeric (α/ß) purity was considerable. The latter is subsequently purified by column chromatography on silica gel. The separation process is difficult owing to the similar elution property of anomeric impurities, which cannot be avoided entirely during the glycosylation process. The anomeric purity is evaluated by ^{1}H-NMR. In the final stage the acetate protection groups on the glycolipid are removed by trans esterification. Typically, no side products are observed during this process. This technique follows a previously reported work (Hashim R. 2006). The purity of the sample was determined by ^{1}H-NMR and found to be greater than 97%. This is sufficient for the present work since it focused on physical characterization.

3.2 Methods

Three methods were used to study the physical behaviour of the glycolipids. They are described below. Besides the actual physical measurement, special care had to be taken for the sampling. Two methods were used to determine the bound water content. The methods evolved from literature studies; one is based on ^{2}H-NMR, while the other applies DSC measurements. For the identification of liquid crystalline phases textures were investigated under the optical polarised microscope (OPM).

3.2.1 Deuterium NMR (^{2}H-NMR)

One of the methods that was used in this study is based on the nuclear magnetic resonance spectroscopy of deuterium in heavy water (Zheliaskova et al., 1999).

The study was performed on a JEOL GSX 270 MHz spectrometer at different temperatures. For this study samples were prepared in the quartz tubes with a diameter

of 4 mm and a height of 5 cm (**Figure 3-18**) and measured in 5 mm NMR tubes. The calculation of the water content in the lamellar phase applied the following equation **Equation 1.8** (Rendall & Tiddy, 1984).

$$[(\mathbf{water/surfactant})\mathbf{molar\ ratio}] = (\mathbf{N} - \mathbf{1})$$

The quadrupole splitting of the deuterium nucleus in a lamellar phase depends on the angle between the D–X bond and director of the lamellar phase. The concentration effect of the quadrupole splitting enables the determination of bound water (**Figure 3-7**).

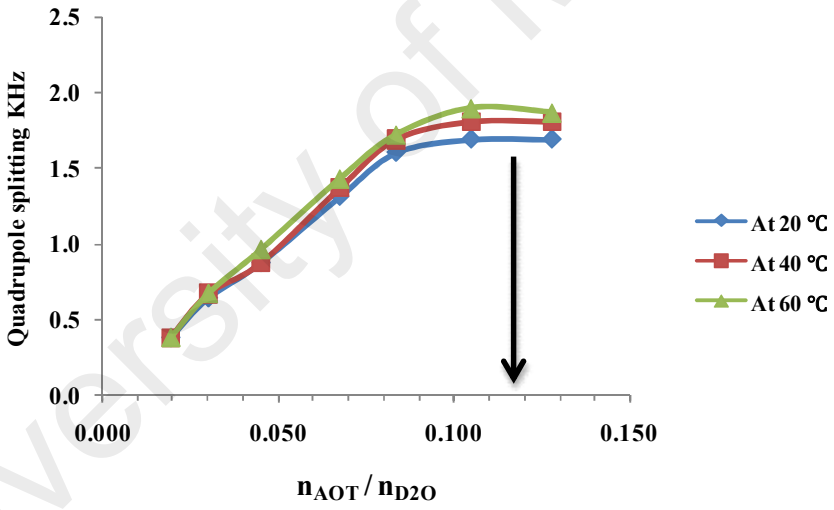

Figure 3-7 Water content was calculated by ^{2}H-NMR.

In the normal ^{2}H-NMR the deuterium probe is bound to a liquid crystalline molecule. Neglecting imperfect molecular alignments in liquid crystalline phases, this arrangement leads to a fixed angle between the director and the X–D bound, hence the angle does not vary. However, in the current research D_2O is not fixed chemically but associated through hydrogen bonding only. It is assumed that D_2O molecules obtain a preferred orientation in the lamellar phase due to the H-bonding with the sugar head.

Because the sugar is fixed and the water interacts with the sugar, it is assumed that there is also preferred direction for the water. This assumption, however may not always apply. The experiment averages over a large number of OH-groups, for which a distribution around a preferred orientation is expected. The presence of different interaction sites complicates the situation further. However, the orientation is supposed to be not zero, if the direction of water molecules at various binding sites does not cancel out each other. Otherwise no quadrupole splitting can be observed.

Formulations were prepared in 4 mm NMR tubes by measuring both the amount of surfactant and water/deuterium oxide on a high precision balance. The samples were immediately flame sealed and homogenised by several cycles of heating to 90 ℃ to 100 ℃ for about 30 min followed by repeated centrifugation (1 min @ 11000 rpm) up and down. Samples were left to equilibrate at room temperature for several days before analysis. All samples appeared homogenous on visual inspection and exhibited anisotropic behaviour under crossed polarisers, indicating the presence of a liquid crystalline phase.

NMR samples of about 100 mg formulation were run on a JEOL GSX 270 MHz spectrometer at various temperatures. Measurements were recorded after a thermal equilibration time of about 15-30 min both in heating and in cooling mode based on 5-10 ℃ per minute temperature increments.

3.2.2 Optical polarizing microscope (OPM)

For the measurement, the polarised microscope was used Olympus BX52 polarizing microscope with thermal cell Mettler FF82 hot stage (**Figure 3-8**).The schematic of a polarizing microscope is shown in **Figure 3-9**.

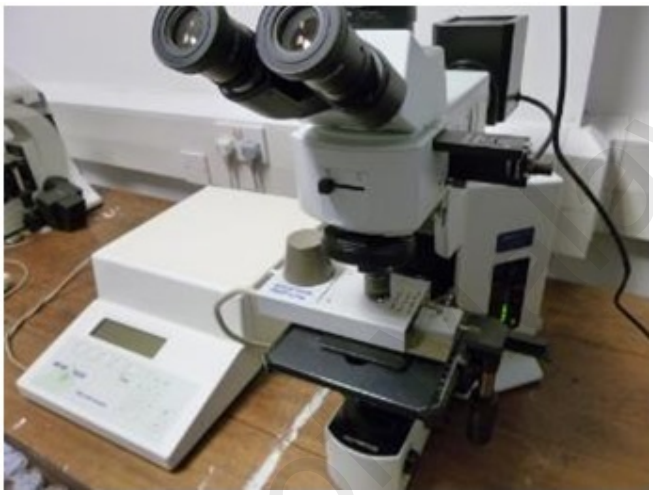

Figure 3-8 Optical polarizing microscope.

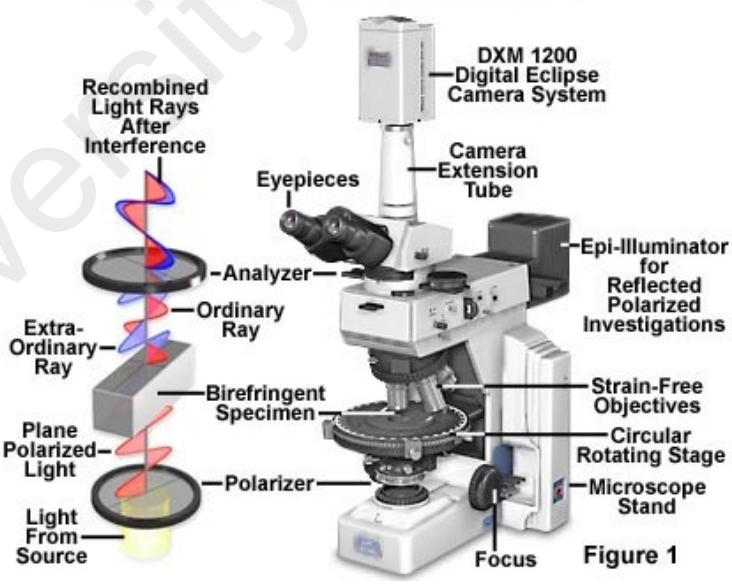

Figure 3-9 Polarised light microscope configuration.

The used device is equipped with a sample holder system (hot stage) or cell with the ability of thermal programming (**Figure 3-10**) and camera for taking picture from the sample during heating.

Figure 3-10 Mettler FF82 hot stage.

The liquid crystals were measured and examined by using OPM polarised light microscope in the method of thermotropic and lyotropic.

3.2.2.1 Thermotropic phase behaviour

The thermotropic phase behaviour was achieved through using optical polarizing microscope (OPM) by controlling the temperature on a hot stage. Thus, a thin sample of a glycolipid material placed between a glass microscope slide and a glass cover slip was analysed. The thin layer of the sample is obtained by pressing the cover slip carefully. The slide containing the material under examination is placed on the hot stage and the different phases were identified by their characteristic textures which are generallybetter

recognised on cooling while the transition temperatures are more precisely determined on heating.

3.2.2.2 Lyotropic phase behaviour

The contact penetration method (Von Minden et al., 2000) was used to investigate the lyotropic phase behaviour. It was performed using a small amount of sample that was placed on a microscope slide before being covered with a cover glass. The sample was heated until isotropic before being cooled to room temperature. Then solvent was introduced at the edge of the covered glass. The solvent moves under the cover glass by capillary action surrounding the sample before penetrating it. The phase behaviour was subsequently investigated by optical polarizing microscopy. For homeotropic compounds (homeotropic alignment liquid crystalline is one of the ways of alignment of molecules which is the state in which a rod-like liquid crystalline molecule aligns vertically to the substrate) (Kuhnau et al., 1997), the sample was heated before isotropic point and cooled afterwards before solvent being introduced. The solvents used in this experiment were water, DMSO (polar solvent) and 1-undecanol (non-polar solvent). Although the concentration of the sample is unknown the concentration gradient with lowest glycolipid concentration at the outside and highest concentration at the centre of the sample enables the determination of different phases, while the composition remains unknown. The different lyotropic phases were recorded at room temperature.

3.2.3 Differential scanning calorimetry (DSC)

Differential scanning calorimetry measurements were carried out by using a Mettler Toledo, DSC 82i equipped with a Haake EK90/MT intra-cooler. The applied software for analysis was STARe Thermal Analysis System. The temperature range varied from one material to another depending on the temperature range of existence of the thermotropic liquid crystal texture (s) previously identified by optical polarizing microscopy. Sample between 6-10mg were applied and placed in standard aluminium pans of 40µl size and sealed with a pinhole cover. DSC was run for the individual branched chain alkyl glycosides after deacetylation (thermotropic phase behaviour).

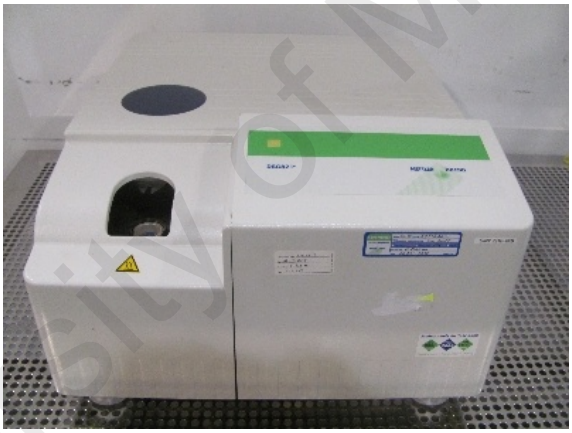

Figure 3-11 Mettler toledo differential scanning calorimetry (DSC).

3.3 Sampling

In this study, the sample preparation is very important and a lot of samplings were carefully and patiently prepared. In fact, series of samples varying in concentration were provided as liquid crystal lamellar phases.

In order to confirm that the samples were in a liquid crystalline state, the sample was investigated between two perpendicular polariser sheets. The in complete extinction

of light confirmed the presence of a liquid crystalline phase, while otherwise the sample appears black. The sample of liquid crystals was clearly seen between the two polariser sheets, as shown in **Figure 3-12**.

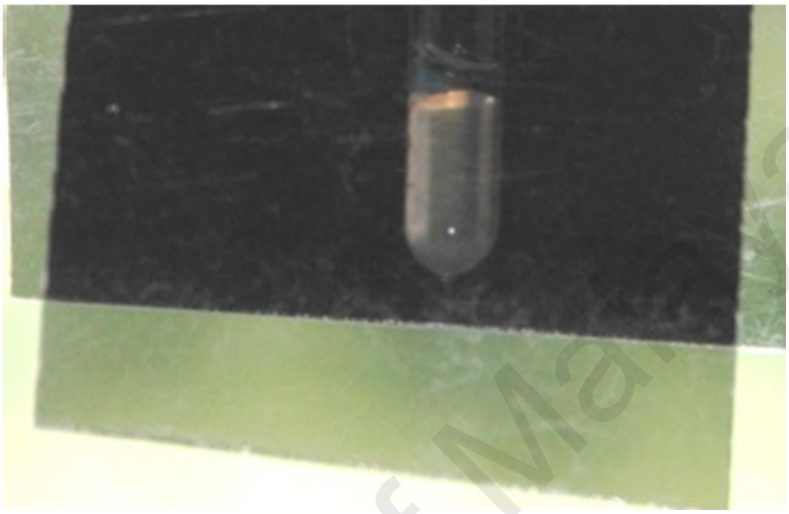

Figure 3-12 A 4 mm tube after sealing in cross polar plates.

3.3.1 Sampling ^{2}H-NMR

In my investigation I used three methods to prepare the samples. For ^{2}H-NMR all three methods were applied, but for DSC measurements only one of them was used.

Samples for ^{2}H-NMR were prepared by two methods: in the first method, the sample, containing a hand-homogenised mixture of glycolipid and water, was heated on anoil bath for evaporating water (**Figure 3-15**) and thus reaching the targeted water content. The mechanical stirrer for the homogenisation of the initial glycolipid-water mixture (**Figure 3-17**) was specially prepared (**Figure 3-16**). The Karl-Fisher method was used to determine the water content. In the second approach, glycolipid and a certain amount of water were placed in the 4mm tube. The tube was subsequently sealed

and mixed (**Figure 3-18**). These two methods are explained in detail because of their importance.

3.3.1.1 Method 1:

Figure 3-13shows the four steps for the preparation of samples. First the glycolipid was weighed into an empty NMR tube (4mm diameter and 4cm height). After that water was carefully added with a special handmade dropper and subsequently centrifuged down into the solid (glycolipid). The amount of water recorded and the tube was sealed with a lightweight torch very carefully without evaporating any water. Finally the sample was weighed again to ensure that no water has evaporated. The sealed tube was heated with a hot air gun using medium heat and after that centrifuged upside down at high speed (12000 rpm) for about 1min. To achieve good homogenization, heating and centrifuging are repeated numerous times. This preparation led to a problem owing to the hot air gun, because the sample heating could not be controlled well giving rise to a change in colour was associated with partial degradation.

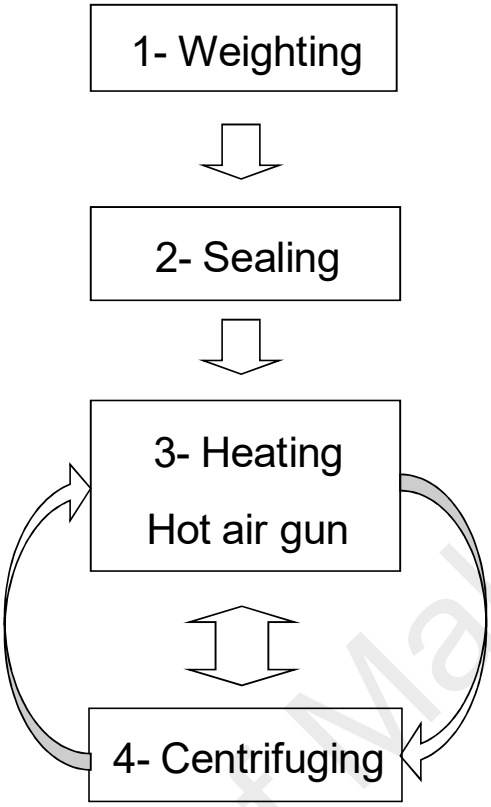

Figure 3-13 Method 1.

3.3.1.2 Method 2 (Karl Fischer) K.F

This technique provides good samples but it is difficult to achieve low water concentrations, because the evaporation of water cannot be controlled well enough (**Figure 3-14**).

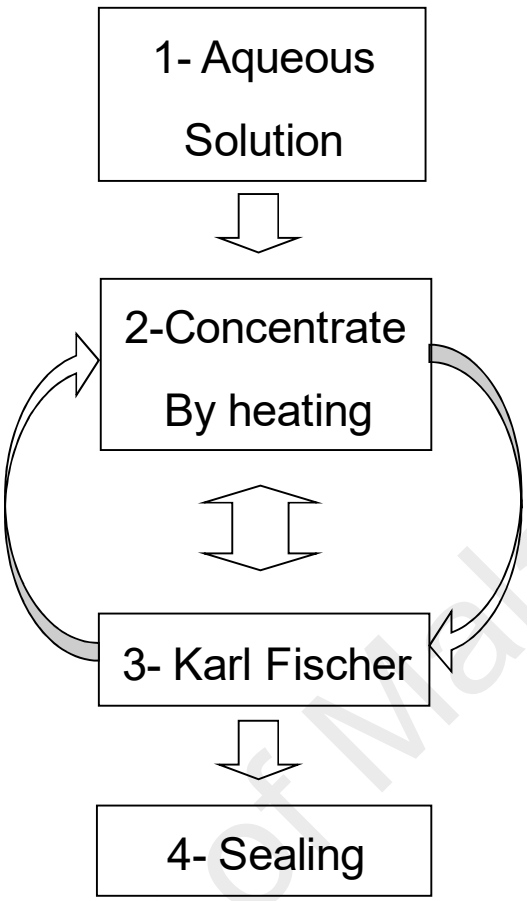

Figure 3-14 Method 2 (Karl Fischer) K.F.

In this method, first, the glycolipid was carefully weighed in an empty vial (**Figure 3-15**).

Figure 3-15 Empty vial.

Then heavy water (D_2O) was added and frequently blended with the already described self-made mixer (**Figure 3-16**) at high temperature (**Figure 3-17**).Water was

slowly evaporated on an oil bath, and the water content of the sample was experimentally determined using a Karl-Fischer titrator.

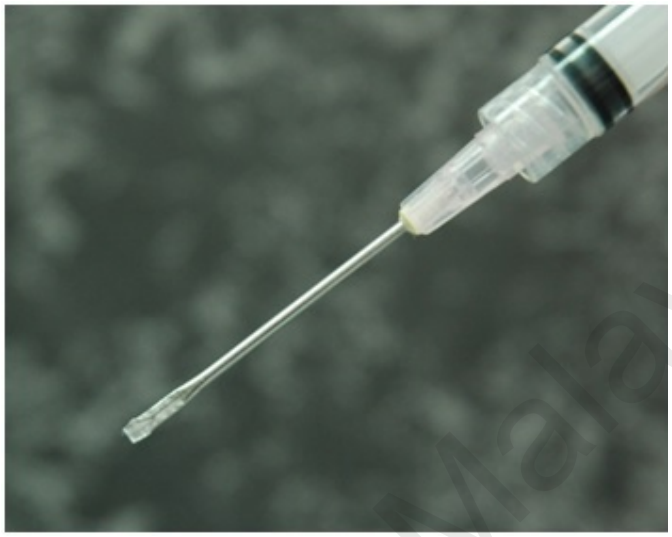

Figure 3-16 Stirrer made.

Figure 3-17 Hand stirring.

^{2}H-NMR samples were prepared in the previously indicated 4 mm tubes. The latter were obtained from commercial 4 mm diameter NMR tubes of length 15 cm, which were divided into 5 cm tubes by the glass section of university. The sample was carefully added and the tube was sealed by flame. A sample of the sample tubes is shown in **Figure 3-18**.

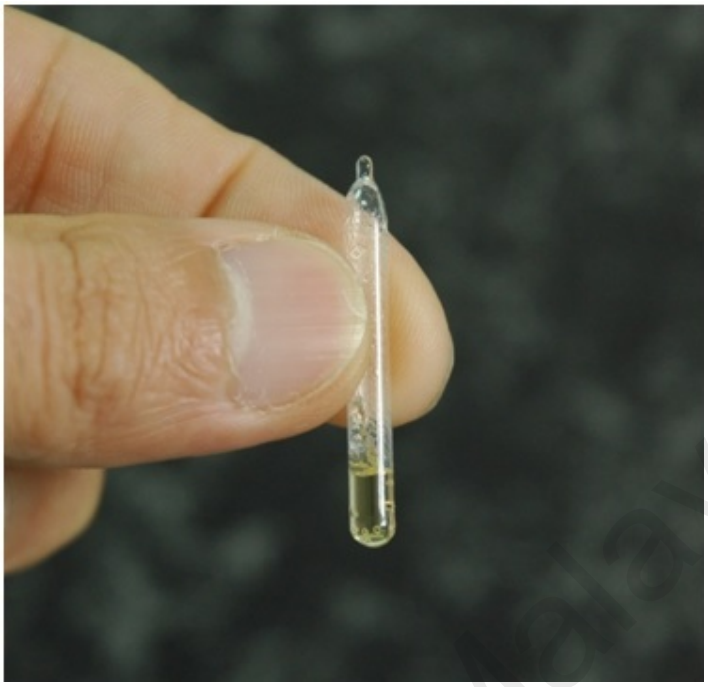

Figure 3-18 ^{2}H-NMR sample tube.

The sample was placed into a 5 mm standard NMR tube for measurement of the ^{2}H-NMR spectrum.

3.3.1.3 Method 3:

This procedure takes a long time but it is the best, because it can achieve good homogenised samples of almost any composition (**Figure 3-19**).

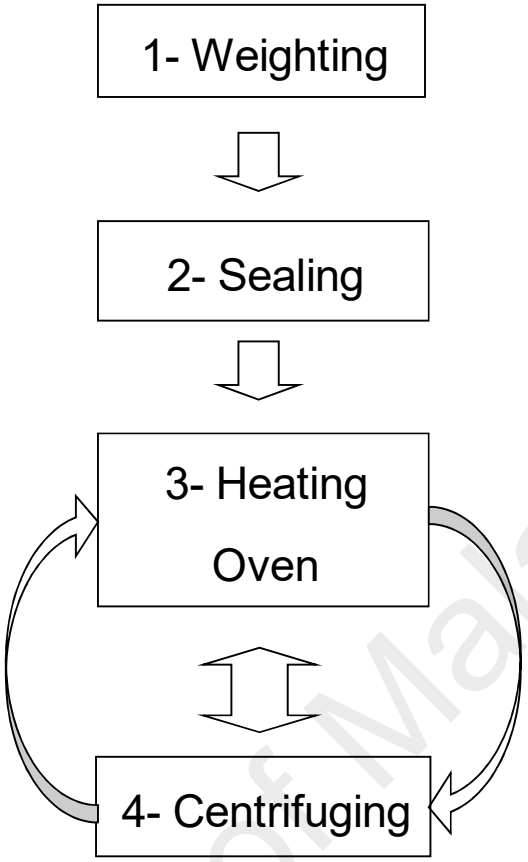

Figure 3-19 Method 3.

In this method, the glycolipid carefully weighed in the previously described 4 mm tubes of 5 cm height, and a certain amount of heavy water (D_2O) was added with accuracy. Afterwards the mixture centrifuged immediately and the tube was subsequently sealed by flame (**Figure 3-18**). Homogenisation was obtained by placing the sample inside a preheated oven at 98 ℃ for one hour and then centrifuging it to the other side at 12000 rpm. This procedure was repeated a couple of times to ensure good homogeneity.

3.3.2 Sampling OPM

There are two types of survey with OPM: thermotropic and lyotropic. When pure sample is examined without water it is called thermotropic, and when water is

added under a microscope and the water penetrates into the glycolipid it is called lyotropic.

Besides the contact penetration scans specific lyotropic samples were also investigated. For this sample tubes prepared for ^{2}H-NMR spectra were broken and their content was then investigated on the OPM.

3.3.2.1 Thermotropic sampling

In the thermotropic study, the glycolipid was placed on a glass slide and covered loosely with a slip. The slide was then placed on the hot stage and is carefully heated to a temperature close to the clearing point (the temperature at which the transition between the mesophase with the highest temperature range and the isotropic phase occurs [IUPAC Compendium of Chemical Terminology, 2005]), before the coverslip was pressed on the sample to obtain a thin sample film between the slide and coverslip. The sample is then heated slowly and changes of the texture were traced under a microscope. Pictures of the textures were recorded and subsequently analysed.

3.3.2.2 Lyotropic sampling

In the lyotropic study the sample preparation followed the approach previously described for thermotropic investigations, except that a small amount of water was dropped on the slide glass, precisely at the coverslip edge, using a self-made dropper. The water was sucked into the sample by capillary force and penetrated in the sample. Owing to the penetration of water into the sample regions differing in water content, with lowest values at the centre and highest water concentration at the outside, were

obtained. The study can be applied at various temperatures. This investigation is called penetration (Laughlin, 1992; Rendall et al., 1983).

3.3.3 Sampling DSC

Method 3, previously described in chapter 3.3.1.3, was used for DSC measurements with the following modification: after the homogenization the tube is cut and material is placed into the special container (Al-Crucible 4 µl) aluminium crucibles (**Figure 3-20**) and weighed carefully in range of 6-10 mg. The crucible is sealed afterwards by a special pressure sealing tool (**Figure 3-21**).

Two kind of samples were used for DSC measurements; the first were pure glycolipids, while the other were homogeneous lamellar phases based on glycolipid and water. About 5-10 mg of material was transferred into aluminium crucibles in both cases. The lid was then attached and the sample was placed in a DSC for measurement.

Figure 3-20 Al-Crucible 4 µl for DSC sampling.

Figure 3-21 Mettler toledo pressing crucible.

Each sample was heated and cooled in accordance with a temperature program. The applied temperature program of each sample is shown beside the corresponding DSC spectrum.

CHAPTER 4:RESULTS AND DISCUSSION

In pursuit of determining the bound water content around glycolipid molecules in the lamellar phase ^{2}H-NMR and DSC investigations were performed on a selection of disaccharide-based surfactants. The methodology for the ^{2}H-NMR approach was evaluated using a well investigated surfactant, i.e. AOT, as a model. The investigation applied different probes and a wide temperature range. Results are presented in chapter 4. DSC investigations focussed on molar melting and freezing enthalpies of water within the lamellar phase, which were related to those of pure bulk water. The results are presented in chapter 4.

4.1 Investigation of bound water for disaccharide glycolipid

The synthesised disaccharides are shown in Table **4.1** while their descriptions are given in section 3.1.2.5 of this thesis.

Table 4.1 Synthesised disaccharide moleculs.

No.	Compounds	Yield(%)	Catalyst
1	β-CelloC_{12}	31	BF_3
2	β-CelloC_{12}(Tech)	19	BF_3
3	β-MeliC_{12}	19	BF_3
4	β-CelloC_8	39	BF_3
5	β-LactoC_{12}	20	BF_3
6	β-MaltoC_8C_4	34	BF_3

4.1.1 Phase behaviour

4.1.1.1 Thermotropic phase behaviour

(a) Optical polarizing microscopy

All five compounds exist as a whitesolid powder at the room temperature. Upon heating, various types of liquid crystalline phases were observed. Some examples of the OPM textures for these compounds are given in **Figure 4-1**. The OPM texture for β-CelloC_8 at 125 ℃ is given in **Figure 4-1**a. The clearing point of β-CelloC_8 occurs at 175 ℃. For β-CelloC_{12} (see typical texture in **Figure 4-1**b), the compound melted into the liquid crystal phase at 90 ℃, which is much higher than that for β-CelloC_8. This result is expected due to the effect of chain lengthening from C8 to C12. The typical OPM image is given in **Figure 4-1**b. The clearing transition for this compound was found to be 195 ℃, and this is comparable to within the error of that found by (Koeltzow & Urfer, 1984). The OPM image (**Figure 4-1**c) for neat β-LactoC_{12} at 220 ℃ displayed a birefringent line at the edge of the sample, characteristic of a fluid lamellar phase (L_α). Upon heating, the sample slowly transformed to an isotropic phase at 255 ℃. Based on the OPM investigation no liquid crystal phase was observed at low temperatures for β-LactoC_{12}. And the formation of the ordered liquid crystal phase occurs at a high temperature. The β-MaltoC_{12} was found to undergo a phase transition into the liquid crystal phase at 110 ℃. The thermotropic texture of β-MaltoC_{12}, is given by OPM (**Figure 4-1**d) at 185 ℃, before the clearing temperature at 244 ℃ and this is almost comparable to that found by (Auvray et al., 2001)Thermotropic research related to β-MaltoC_8C_4, in OPM texture (**Figure 4-1**e) at 115 ℃. The clearing point for this compound is 180 ℃. The summary of this investigation is give in **Table 4.2**.

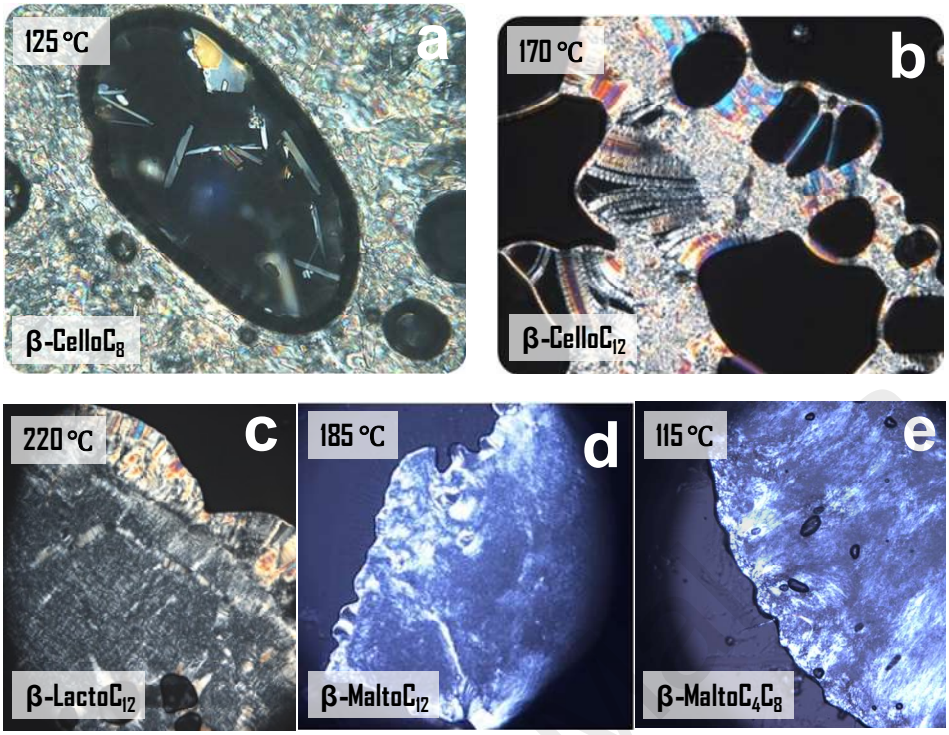

Figure 4-1 The liquid crystalline textures (on cooling) of 5 compounds. The names are (β-CelloC$_8$, β-CelloC$_{12}$, β-LactoC$_{12}$, β-MaltoC$_{12}$, β-MaltoC$_8$C$_4$) at selected tempertaures.

Table 4.2 Thermotropic phase transition temperatures by OPM. [Ref] 1: (Koeltzow & Urfer, 1984) 2:(Auvray et al., 2001) 3:(Hashim, 2004)

No.	Compounds	Phase and transition temperature (±1 ℃)	Comparison with literature
1	β-CelloC$_8$	Cr 70 L_α 175 I	N/A
2	β-CelloC$_{12}$	Cr 90 L_α 195 I	Cr N/A L_α 208[1] I
3	β-LactoC$_{12}$	Cr 192 L_α or Hex 255 I	N/A
4	β-MaltoC$_{12}$	Cr 110 L_α 244 I	Cr 103[2] L_α 245[2] I
5	β-MaltoC$_8$C$_4$	Cr 25 L_α 180 I	Cr N/A L_α 188[3] I

(b) Differential scanning calorimetry

In general, the results obtained from OPM were confirmed by DSC and both methods showed almost the same results. Slight differences in temperatures were attributed mostly to the difference in the heat transfer between the sample and supporting substrate (glass slide in OPM vs. aluminium pan in DSC). The DSC scan for each of the compounds started at -60 ℃ with a scan rate of 10 ℃/min. The transition

temperatures were obtained from the peak maxima of the second heating cycle to remove the thermal history whereas the enthalpies were obtained by integrating the sample transition peaks for β-MaltoC_{12} as shown in **Figure 4-2**. The complete DSC scans for these compounds is given in **Figure 5-1** - **Figure 5-5** of the Appendix A.

Upon heating, β-CelloC_8 changed from its liquid crystalline phase to an isotropic phase at 57 ℃ with ΔH=17.58 J/g. The enthalpy value for this transition was significantly larger than that of liquid crystalline to isotropic state transition. At around 211 ℃ there are two peaks, which are close together with small enthalpy value (ΔH=1.34 J/g) which were not detected by the OPM technique. From DSC, β-CelloC_{12} changed from the crystal to the L_α phase at 85 ℃ and on a further heating the L_α phase becomes isotropic at 180 ℃. Similarly, no other phase transitions were observed upon subsequent heating and cooling. Unlike the corresponding cellobiosides, β-LactoC_{12}does not have melting transition at low temperatures and showed the first melting transition to the L_α at 181 ℃ (ΔH = 58.65 J/g) then followed by a transition into the isotropic state at 260 ℃. Similar to theβ-CelloC_{12}, the β-MaltoC_{12} had two transition temperatures; first it melted at 94 ℃ with ΔH=4.34 J/g from the crystal phase. The second transition into the isotropic state occurred at 246 ℃ with ΔH=5.08 J/g that also shows in OPM texture. In the following DSC investigation, it was confirmed that β-MaltoC_8C_4 changed from liquid crystalline phase at 54℃ with ΔH=0.82 J/g but this transition was not found in the OPM texture. It also has a second transition into the isotropic state at186 ℃ with ΔH=3.58 J/g. This transition matched that was determined by the OPM technique. The phase transitions for these compounds are tabulated in **Table 4.3**.

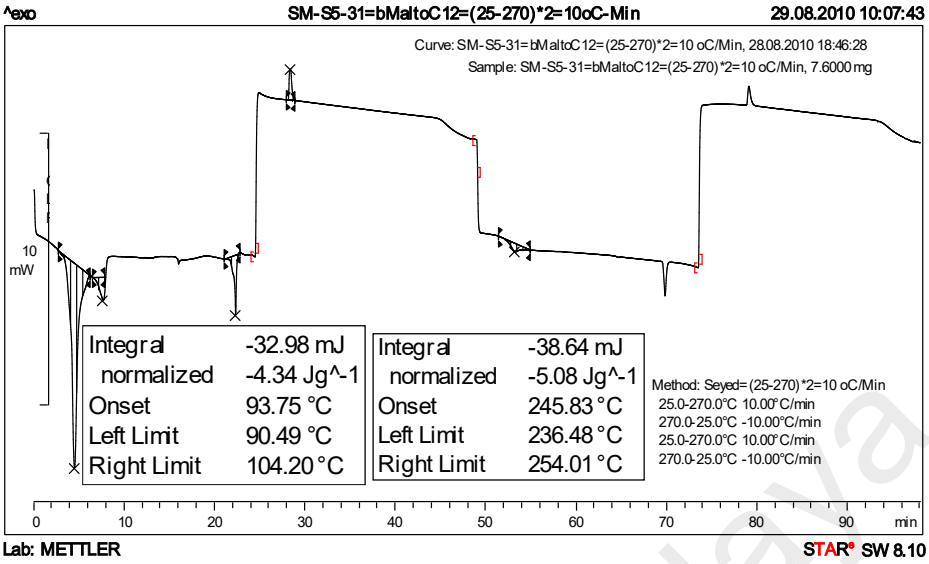

Figure 4-2 DSC thermogram for pure β-MaltoC_{12} (2 times).

Table 4.3 Thermotropic phase transition ℃ & ΔH at heating rate of 10 ℃/min.

No.	Compounds	Transition temperature, (±1 ℃) [Enthalpy, (J/g)]
1	β-CelloC_8	Cr 57[17.58]L_α211[1.34] I
2	β-CelloC_{12}	Cr85L_α 180 I
3	β-LactoC_{12}	Cr 181[58.65]L_α or Hex 260 I
4	β-MaltoC_{12}	Cr 94[4.34]L_α246[5.08] I
5	β-MaltoC_8C_4	Cr54[0.82]L_α 186[3.58]I

4.1.1.2 Lyotropic phase behaviour (water penetration)

The technique of water penetration scan was used to establish the lyotropic phase diagram qualitatively (Burgoyne et al., 1995; Funari et al., 1994). The sample is prepared similarly as for thermotropic measurement, but during the second run, when it was cooled to the room temperature and a clear texture image emerges, a drop of distilled water (the solvent) is placed at the edge of cover slip. Due to the capillary action, the water penetrated gradually and brought into contact with the sample. Various liquid crystal phase textures formed the concentration gradient. Although the exact concentration of the sample could not be determined, qualitatively the most diluted area is located on the outside of the material and it gets more concentrated towards the centre

of the sample. The mesophase textures were recorded at variable temperatures, and typically these are given as follows.

Typical OPM textures using the water penetration technique are given in Figure **4-3** for four compounds namely (a) β-CelloC$_8$ at 29 ℃, (b) β-CelloC$_{12}$at 27 ℃, (c) β-LactoC$_{12}$ at 35 ℃ and (d) β-MaltoC$_8$C$_4$ at 30 ℃. At low temperatures in Figure **4-3**a, b & d, there are only three phases, namely water (W), an ordered lamellar phase (L$_\alpha$) and the solid lipid phase (Lipid) for both cellobiosides, β-CelloC$_8$, β-CelloC$_{12}$ and β-MaltoC$_8$C$_4$. Similarly for β-LactoC$_{12}$ three phases were observed at 60 ℃ (Figure **4-3**c). More contact penetration scan OPM textures are given in Appendix C.

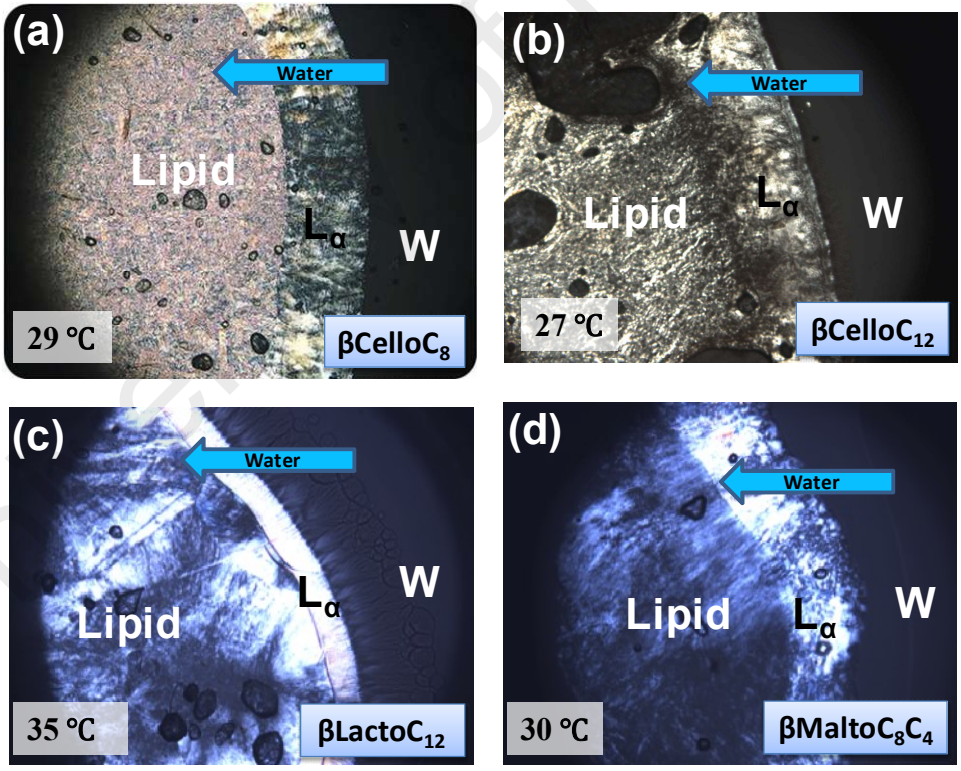

Figure 4-3 OPM textures water penetration technique.

Figure 4-4 gives the contact penetration scan textures of β-MaltoC$_{12}$ at four different temperatures namely 36 ℃, 70 ℃, 103 ℃, 124℃. We observed four phases

namely, water (W), hexagonal (H_α), cubic (Q_1) and Lipid at 36 ℃ (**Figure 4-4a**) and 70 ℃ (**Figure 4-4b**), These results agree with those determined by Auvray (see red lines in **Figure 4-4e**). Furthermore, at 103 ℃ we observed five phases W, Q_1, L_α, $Q_2$and Lipid (**Figure 4-4c**). These results were not indicated in Auyray report since the latter phase diagram was determined below lower than 100 ℃. At 124 ℃, we observed three distinct bands **Figure 4-4d**, which correspond water (W), and ordered phase and Lipid phase. In this case the texture corresponds to the ordered phase is distinctly different from the others in **Figure 4-4a-c**. Thus, we identify this phase to be the L_α phase. These assignments agree with those found by Auvray (X. Auvray et al., 1995). In their work, which was supported by X-ray data, the lipid phase is in co-existance with the L_α.

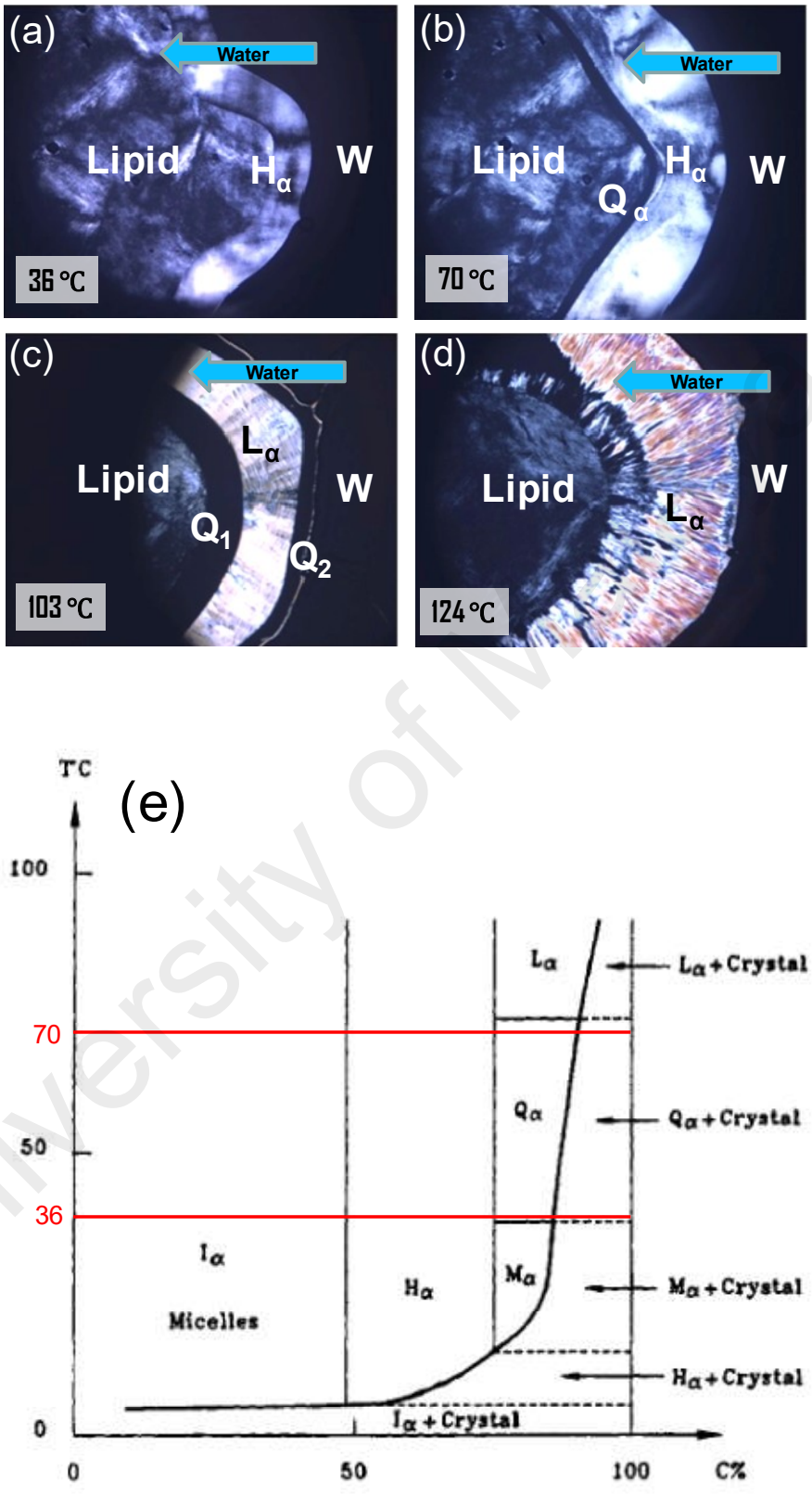

Figure 4-4 OPM phase diagram studies of β-MaltoC_{12}.
(a) contact penetration technique observed (b) by Auvray (Auvray et al., 1995).

4.1.2 Determination of bound water by deuterium NMR (^{2}H-NMR)

In order to get familiar with the ^{2}H-NMR technique, a well investigated compound, AOT, was used as a model. Application of AOT in D_2O provided the expected ^{2}H-NMR spectra indicating the presence of a liquid crystalline phase. Following this, the synthesised β-CelloC_{12} was investigated. Although the samples indicated the presence of a liquid crystalline phase based on evaluation under crossed polariser sheets the ^{2}H-NMR revealed no quadrupole splitting. Therefore a suitable replacement for D_2O was sought. Instead of D_2O a solution of CD_3OD (5% by weight) was chosen. The CD_3OD probe was successfully tested on AOT, thus proving it suitable for the investigation-task.

However, the application of the new probe on ßCelloC_{12} did not provide any quadrupole splitting either. In the attempt to obtain better results a shorter hydrophobic chain was applied, by replacing the C_{12} alcohol with a C_8 analogue. Unfortunately, again there was no splitting in ^{2}H-NMR spectrum. Instead of the hydrophobic domain the sugar configuration was altered and the β-cellobioside replaced by a β-lactoside. Various samples of the glycolipid β-LactoC_{12} with different D_2O contents in the lamellar phase were prepared and the ^{2}H-NMR spectra were subsequently recorded. Again no quadrupole splitting was found in the spectra. However, the peaks were not sharp but wide, which could originate from unresolved very small quadrupole splittings. Meanwhile, significant splitting were observed a thigh temperature between 120℃ to 180 ℃. To compare straight chain glycosides with branched analogues, a previously investigated maltoside, β-MaltoC_{12}, was reinvestigated. It exhibited the expected quadrupole splitting very clearly. However, when the straight alkyl chain was changed into a branched analogue, the resulting β-MaltoC_8C_4 did not exhibit the splitting. Instead, again, only broad peaks were observed.

Following is a complete description of the ^{2}H-NMR investigations on series of lamellar phases differing in water concentration for a selection of glycolipids, as well as the model surfactant, AOT.

4.1.2.1 Results

(a) Sodium bis (2-ethylhexyl) sulfosuccinate (AOT) with D_2O

The molecular structure of sodium 1,4-bis(2-ethylhexoxy)-1,4-dioxobutane-2-sulfonate, also known as docusate sodium or Aerosol OT, short AOT, is shown in **Figure 4-5**.

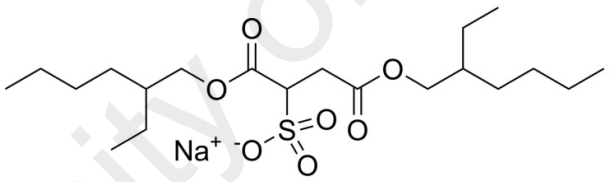

Figure 4-5 Aerosol OT or AOT.

AOT was used as reference material to evaluate the ^{2}H-NMR method. The investigated formulations, comprising of different compositions of AOT and D_2O, are shown in **Table 4.4**.

Table 4.4 Sampling of AOT + %D_2O for ^{2}H-NMR.

No.	Sample	% D_2O	Temperature ℃
1	AOT	15	20 , 40
2	AOT	18	21,25
3	AOT	26	21(2) ,40, 60
4	AOT	30	21 ,40, 60
5	AOT	35	21(3) ,40, 60
6	AOT	40	21,40, 60
7	AOT	50	21,40, 60
8	AOT	60	21,40, 60
9	AOT	70	21,40, 60
10	AOT	80	21,25

^{2}H-NMR spectra were recorded at 20 ℃, 40 ℃ and 60 ℃. Sample spectra, taken at 40 ℃, are shown in **Figure 4-7**. There is also good reason to suggest that the splitting in the spectrum of filaments composed and prototyping phase selection method in the number three is acceptable.The lamellar phase for AOT is reported to cover the concentration range of surfactant between 15% and 75% (**Figure 4-6**) (Nees & Wolff, 1996).

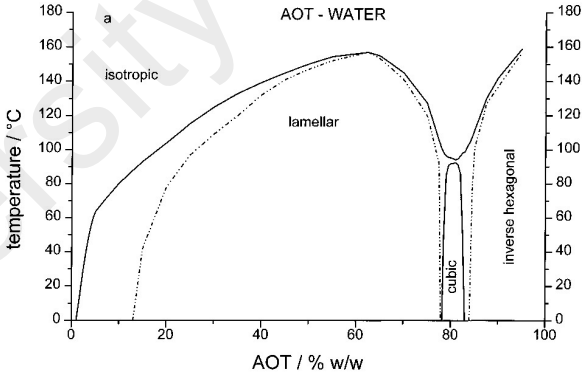

Figure 4-6 Phase diagram of the binary system AOT- water.
Figure from (Nees & Wolff, 1996).

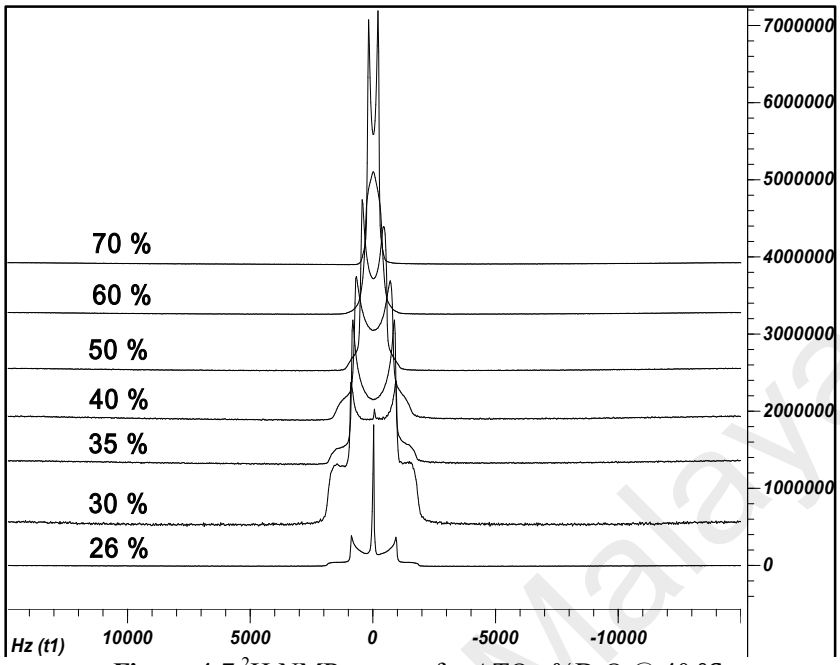

Figure 4-7 ^{2}H-NMR spectra for ATO+ %D_2O @ 40 ℃.

Also, the evaluation of the spectra showed that the quadrupole splitting increased slightly with the increasing temperature, as shown in **Figure 4-8**.

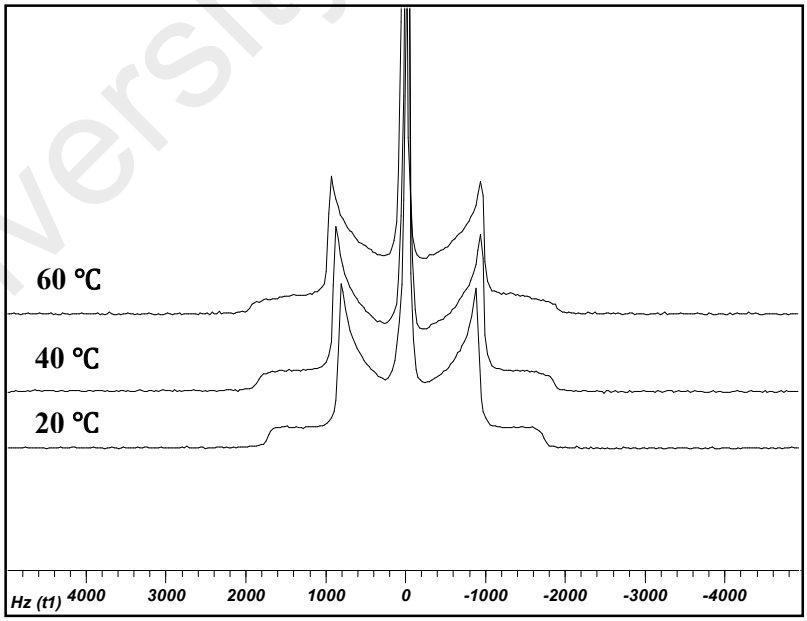

Figure 4-8 ^{2}H-NMR spectra for AOT + 26 % D_2O.

The determination of the bound water content requires a systematic investigation of the quadrupole splitting over a concentration range. The investigation was performed at all the previously indicated temperatures. Data are provided in **Table 4.5**.

Table 4.5 Spliting (Δ KHz) of ^{2}H-NMR spectroscopy of AOT + %D_2O.

%AOT	n_{AOT}	n_{D2O}	n_{AOT} / n_{D2O}	T = 20 ºC	T = 40 ºC	T = 60 ºC
30	0.07	3.50	0.019	0.380	0.380	0.380
40	0.09	3.00	0.030	0.644	0.673	0.673
50	0.11	2.50	0.045	0.878	0.878	0.966
60	0.13	2.00	0.067	1.317	1.375	1.434
65	0.15	1.75	0.084	1.609	1.697	1.726
70	0.16	1.50	0.105	1.697	1.814	1.902
74	0.17	1.30	0.128	1.697	1.814	1.873

As seen in **Table 4.5**, the splitting increases with decreasing water content, i.e. increasing AOT concentration. **Figure 4-9** displays the data in a way enabling the determination of the bound water content. The saturation of the quadrupole splitting indicates the maximum AOT-D_2O interaction. The respective ratio $n_{(D_2O)}/n_{AOT}$ translates to a bound water content of around ~10 molecules by using the **Equation 1.8**. This is in agreement with previous investigations (Hauser et al., 1989) and, proves that the method is correct.

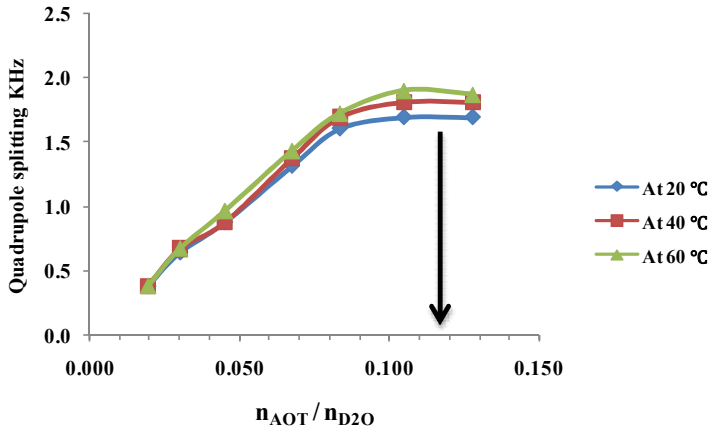

Figure 4-9 Water content D_2O.

As seen in **Figure 4-8**, in 26% of D_2O, an isotropic peak, is at the centre of the spectrum, which represents the cubic phase. When we use CD_3OD, instead of D_2O, we still observe an isotropic peak which may indicates the presence of the cubic phase in co-existence with the lamellar phase (**Figure 4-12**). However, since the aim of this study is to measure the bound water for the glycolipid system, we shall not discuss the bound water of AOT in great details as these have been reported(Nees & Wolff, 1996). Here these measurements are used simply as a standard to check the methodology.

(b) Dodecyl-β-cellobioside (β-celloC_{12}) with D_2O

Numerous examples of β-CelloC_{12} with different percentages of D_2O were prepared and each of them was investigated by ^{2}H-NMR at different temperatures. The scope of the investigation is shown in **Table 4.6**.

Table 4.6 Sampling of ß-CelloC_{12}+ %D_2O for ^{2}H-NMR.

No.	Sample	%D_2O	Temperature ℃
1	ß-CelloC_{12}	4	18.5,20,25,30,35,40,45,50, 60,90,100,140,160,170,180
2	ß-CelloC_{12}	20	20,25,30,35,40,4550(3),55,60,65,75
3	ß-CelloC_{12}	23	20,25,30,35,40,4550(3),55,60,65,75
4	ß-CelloC_{12}	30	20,25,30,35,40,4550(3),55,60,65,75
5	ß-CelloC_{12}	32	20,25,30,35,40,4550,55,60,65,75
6	ß-CelloC_{12}	41	20,25,30,35,40,4550,55,60,65,75
7	ß-CelloC_{12}	47	20,25,30,35,40,45,60,65
8	ß-CelloC_{12}	49	20,25,30,35,40,45,50,55,60,65
9	ß-CelloC_{12}	57	21 , 40 , 60,80,100
10	ß-CelloC_{12}	63	20,25,30,35,40,4550,55,60,65,75

Spectra were taken at various concentrations and at different temperatures. However, no quadrupole splittings were observed at low temperatures. Instead only singlets were recorded (**Figure 4-10**). Only at the high temperatures the peak flattened slightly. This is indicated with the term W in **Table 4.7**, which represents a broad peak.

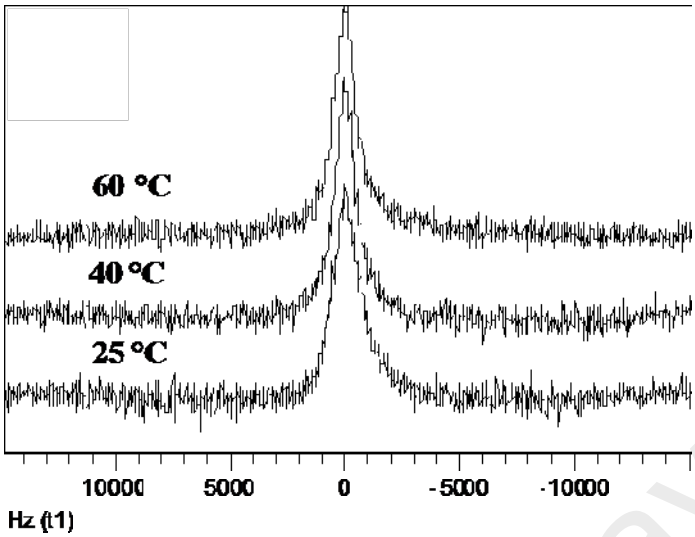

Figure 4-10 ^{2}H-NMR spectra for β-CelloOC$_{12}$ @ 4 % D_2O.

Despite anisotropic sample behaviour only single line spectra were obtained at temperatures below 100 ℃.

Table 4.7 β-CelloC$_{12}$ at low temperatures.
The N= no splitting & W=wide peak.

% D_2O	Temperature													
	20	25	30	35	40	45	50	55	60	65	70	80	90	100
4	N	N	N	N	N	N	N		N				W	W
20	N	N	N	N	N	N	N	N	N	N				
23	N				N				N					N
30	N				N		N		N		N	N	N	N
32	N	N	N	N	N		N		N	N				
42	N				N				N	N			N	
47	N	N	N	N	N	N	N	N	N	N				
49	N	N	N	N	N	N	N	N	N	N				
57	N				N				N			N		N

The measurements did not reveal the expected quadrupole splittings that form the basis for the determination of the bound water content, as previously demonstrated for AOT. β-CelloC$_{12}$ did not exhibit any quadrupole splitting within the temperature range from 20 ℃ to 100 ℃. Instead only single signals, usually found for isotropic media, were recorded, as indicated in **Table 4.8**. However, at very high temperature, i.e.

above ~150 ℃, the typical powder pattern with its quadrupole splitting was observed, as shown in **Figure 4-11**.

Table 4.8 β-CelloC_{12} at high temperatures.
The W=wide peak & Y= have splitting.

% D_2O	Temperature												
	100	105	110	120	125	140	150	155	160	165	170	175	180
4	W					W			Y		Y		Y

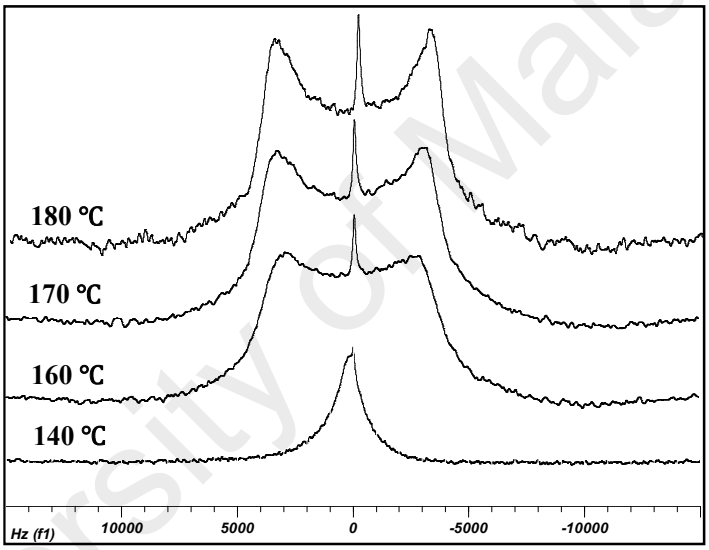

Figure 4-11 ^{2}H-NMR spectra for β-CelloC_{12} @ 4 % D_2O.

(c) Sodium bis(2-ethylhexyl) sulfosuccinate (AOT) with CD_3OD

The reason to use CD_3OD as a probe was due to the previous failure to obtain quadrupole splittings with the D_2O probe for lamellar phases of aqueous β-CelloC_{12} at ambient or slightly elevated temperature. Like for D_2O before, the CD_3OD probe was initially investigated on its ability to study the bound water content using AOT formulations as a model system.

In this research, a 5 % aqueous solution of CD_3OD was used as probe to study lamellar AOT formulations of varying water concentrations. The investigation scope in terms of both concentration and temperature is displayed in **Table 4.9**, while sample spectra are shown in **Figure 4-12**.

Table 4.9 Sampling of AOT + %CD_3OD for ^{2}H-NMR.

No.	Sample	% (CD_3OD+H_2O)	Temperature ℃
1	AOT	15	20 , 40
2	AOT	19.2	20 , 40 , 80
3	AOT	23	20 , 40
4	AOT	25.1	21
5	AOT	31	21
6	AOT	42	21
7	AOT	49	21
8	AOT	57	21
9	AOT	65	21
10	AOT	73	21
11	AOT	80.6	21

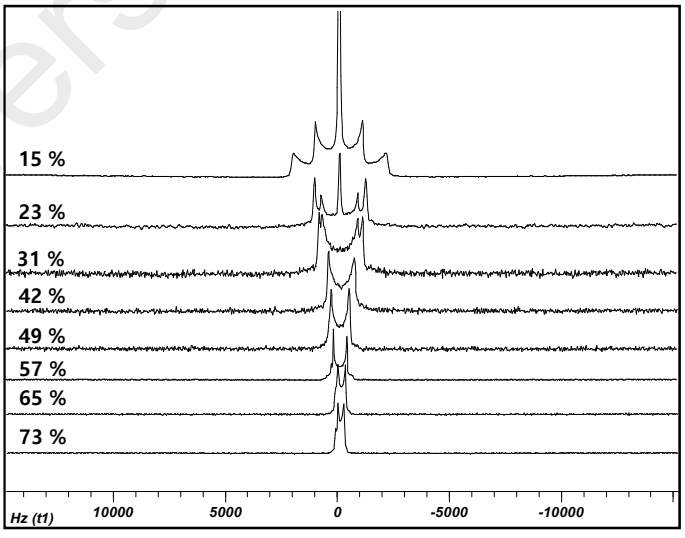

Figure 4-12 ^{2}H-NMR spectra for ATO+CD_3OD @ 20 ℃.

Deuteriated methanol is larger and heavier than water and has less H-bonding opportunities. Deuterium methanolCD_3OD has two different types of deuterium, one is associated with OD and the other is connected to CD_3. The binding to glycolipids will be very different from that of water. Thus there are two set of deuterium peaks (one from the CD_3 and the second from the OD in exchange with water) for CD_3OD at all concentrations, especially those less than 30 percent. For example, two splitting are clearly observed in the spectra at 23% and 31% water. These AOT results are interesting but will not be discussed further since the aim of this thesis is on glycolipids.

Figure 4-12 indicates a systematic variation of the quadrupole splitting upon the change of water concentration. The quadrupole splittings (Δ) and the corresponding calculations of contents for the formulations are shown in **Table 4.10**.

Table 4.10 Splitting (Δ KHz) of AOT + %(CD_3OD+H_2O).
In ^{2}H-NMR spectroscopy.

%AOT	n_{AOT}	m_{CD3OD}	n_{CD3OD}	m_{H2O}	n_{H2O}	$n_{(CD3OD+H2O)}$	n_{AOT}/ $n_{(CD3OD+H2O)}$	quadrupole splitting (in KHz)	
								T = 20 °C	T = 40 °C
27	0.06	3.7	0.10	69	3.9	4.0	0.02	0.26	0.29
35	0.08	3.3	0.09	62	3.4	3.5	0.02	0.35	0.41
43	0.10	2.9	0.08	54	3.0	3.1	0.03	0.59	0.70
51	0.11	2.5	0.07	47	2.6	2.7	0.04	0.82	0.91
58	0.13	2.1	0.06	40	2.2	2.3	0.06	1.1	1.2
69	0.16	1.6	0.04	29	1.6	1.7	0.09	2.0	2.0
75	0.17	1.3	0.03	24	1.3	1.4	0.12	2.3	2.3
77	0.17	1.2	0.03	22	1.2	1.2	0.14	2.3	2.2

The data from **Table 4.10** were subsequently displayed in a graph (**Figure 4-13**) to determine the bound water content.

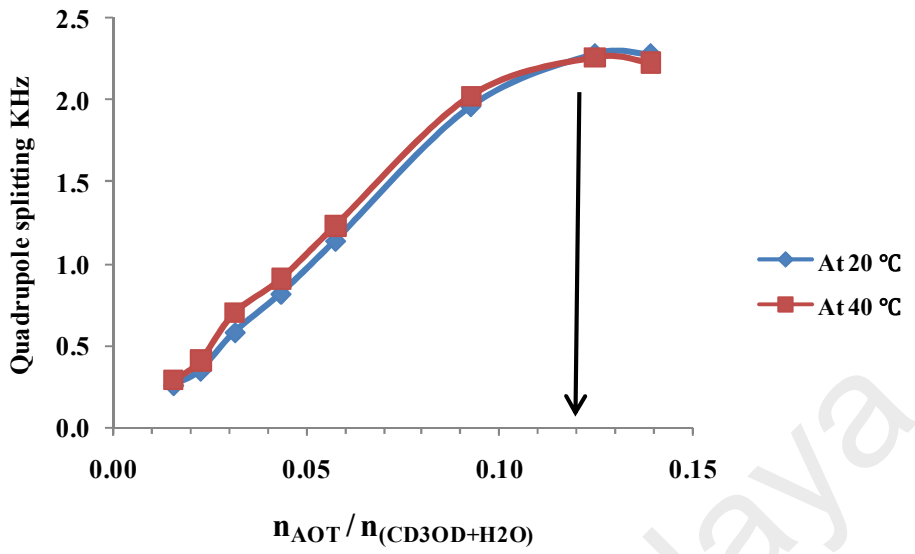

Figure 4-13 Bound water content (CD_3OD+H_2O).

As can be seen, the latter is about 9, thus matching the previous investigation using the D_2O probe. This study shows that deuterium methanol can be applied as an alternative probe instead of heavy water.

(d) Dodecyl-β -cellobioside (β-celloC_{12}) with CD_3OD

After the successful test of the CD_3OD probe for aqueous AOT formulations the probe was applied on aqueous lamellar phases of dodecyl β-cellobioside. The investigation scope is displayed in **Table 4.11**. However, like for the previous investigation with the D_2O probe, no quadrupole splitting could be observed. Instead only single peaks were detected, as shown in **Figure 4-14**.

Table 4.11 Sampling of β-CelloC_{12}+ %(CD_3OD+H_2O) for ^{2}H-NMR.

No.	Sample	% (CD_3OD+H_2O)	Temperature ℃
1	β-CelloC_{12}	10	20 , 60 , 80 , 100 , 120
2	β-CelloC_{12}	13	20 , 60 , 80 , 100 , 120
3	β-CelloC_{12}	19.4	20 , 60 , 80 , 100 , 120
4	β-CelloC_{12}	31	60

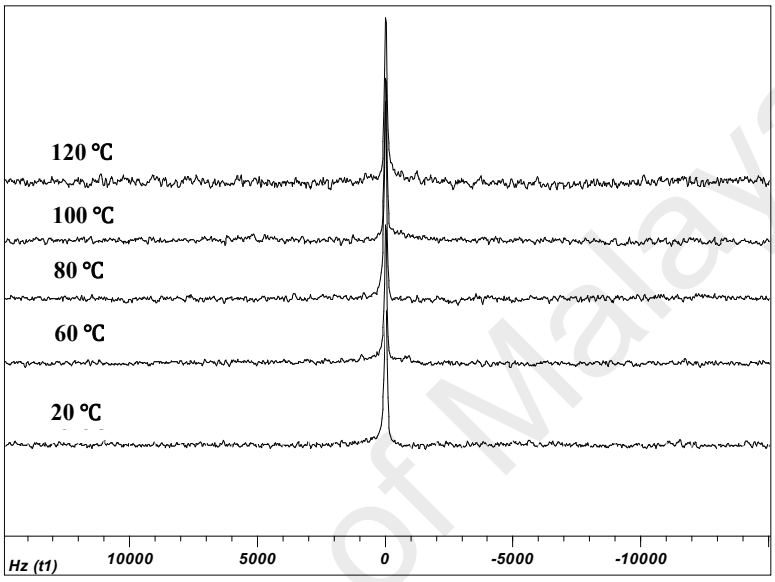

Figure 4-14 ^{2}H-NMR spectra for β-CelloC_{12} + 10 % (CD_3OD+H_2O).

(e) Octyl-β-cellobioside (β-celloC_8)

Owing to the failure to obtain quadrupole splittings for the C_{12} cellobioside an alternative glycolipid was investigated. Since the investigation objective involved the determination of bound water for a certain sugar configuration, i.e. β-lactoside, only the length of the alkyl chain could be changed. Instead of the C_{12} alcohol the C_8 analogue was chosen. This choice originated from the requirement of high structural consistency,e.g. to avoid potential packing effects due to chain branching, and synthetic accessibility, which favours shorter chained glycolipids. The investigation applied the D_2O probe, based on simplicity, as the CD_3OD probe did not exhibit advantages in the

previous investigation. The scope is displayed in **Table 4.12**. Unfortunately the results matched those previously obtained for ßCelloC$_{12}$, as demonstrated in **Figure 4-15**.

Table 4.12 Sampling of β-CelloC$_8$+ %D$_2$O for ^{2}H-NMR.

No.	Sample	% D_2O	Temperature ℃
1	β-CelloC$_8$	17	20,25,55,60,100,120,160
2	β-CelloC$_8$	29	25,55,60,120
3	β-CelloC$_8$	37	60

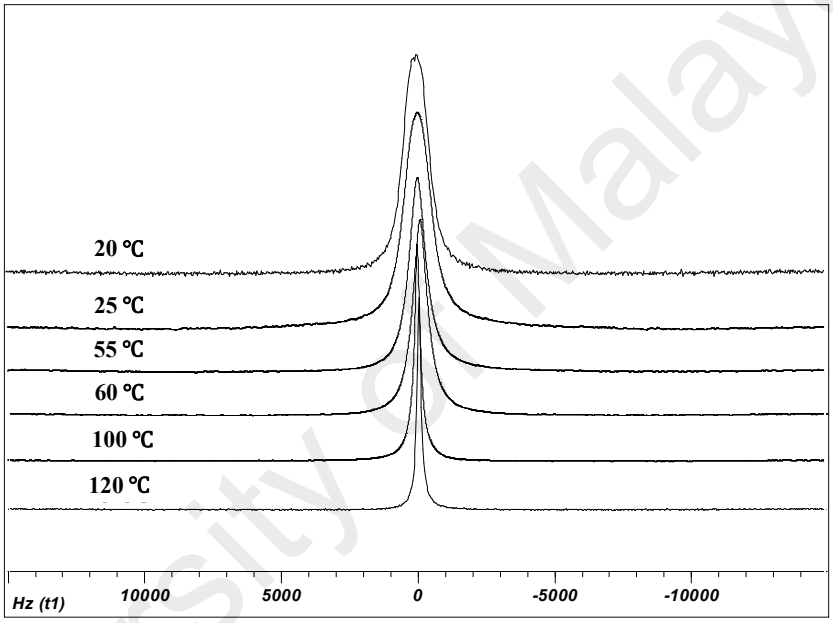

Figure 4-15 ^{2}H-NMR spectra for β-CelloC$_8$ @ 17 % D$_2$O.

(f) Dodecyl-β–lactoside (β-lactoC$_{12}$)

Despite the failure to determine the bound water content for β-cellobiose-based glycolipids, the investigation of different sugar configurations was continued. In view of structural similarities the study focused on β-LactoC$_{12}$, as C-4-epimer of β-CelloC$_{12}$. Several lamellar phases of the lactoside varying in water content were formulated and subsequent investigated by ^{2}H NMR spectroscopy. The investigation scope is shown in **Table 4.13**.

Table 4.13 Sampling of β-LactoC_{12}+ %D_2O for ^{2}H-NMR.

No.	Sample	% D_2O	Temperature ℃
1	β-LactoC_{12}	2.77	150,160,165,170,175,180
2	β-LactoC_{12}	5.08	19,60,120,140,160,180
3	β-LactoC_{12}	7.30	160,165,170,175
4	β-LactoC_{12}	9.79	19,60,120,140,150,140 160,165,170,175.180
5	β-LactoC_{12}	12.64	150,160,165,170,175.180

In agreement to the previous investigations no quadrupole coupling were observed at ambient and moderately elevated temperature. However, significant quadrupole splittings were recorded at high temperatures. Selected spectra are displayed in **Figure 4-16**, **Figure 4-17** & **Figure 4-18**. According to **Figure 4-16**, the splitting decreases with increasing concentration of D_2O. This trend matches the previous observation for the AOT molecule (**Figure 4-7**). Moreover, the increase of the quadrupole splitting upon heating, as shown in **Figure 4-17** and **Figure 4-18**, reflected a previous observation for AOT, as shown in **Figure 4-8**. However, the quadrupole splitting appears to change comparably rapidly upon changing concentration for β-LactoC_{12} compared to the AOT. Besides the resolution of the spectra is significantly reduced for the glycolipid, perhaps is a consequence of the high temperature. Most remarkable, however, is the drastic increase of the quadrupole splitting upon rising temperature. This feature is believed to be the reason for the previous failure of determining the bound water content in cellobioside-based glycolipids. The behaviour limits ^{2}H NMR investigations of the investigated glycolipids to lower water contents owing to the possible development of pressure inside the NMR-tube.

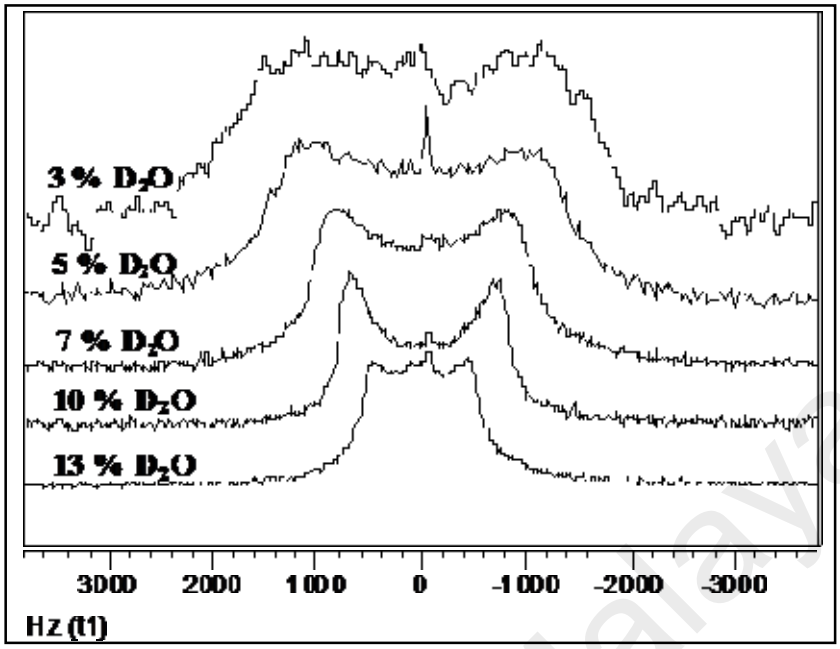

Figure 4-16 Quadrupole splitting vs. D_2O concentration for β-LactoC_{12}. At 175 ℃ ^{2}H-NMR spectra at various water concentration.

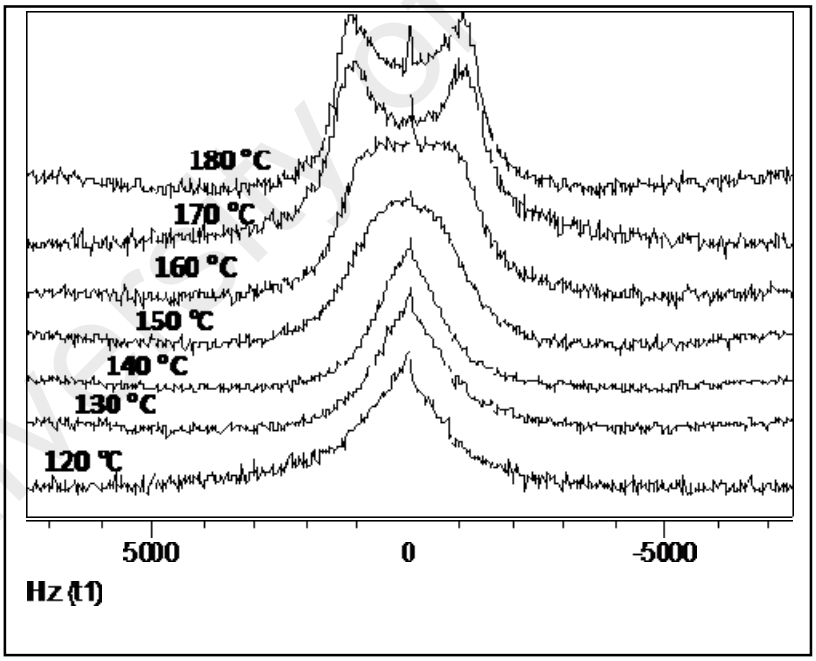

Figure 4-17 Quadrupole splitting β-LactoC_{12}+ 5%D_2O @ high temperatures.

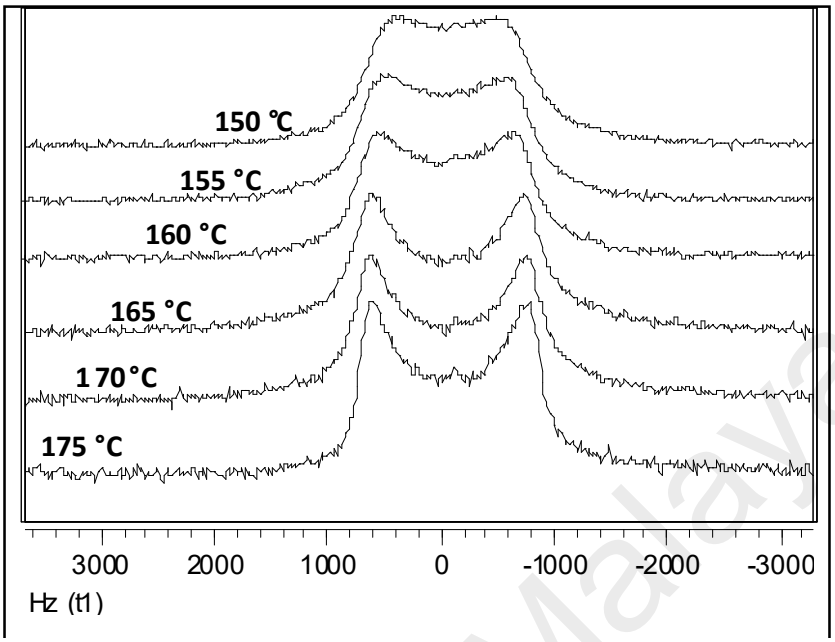

Figure 4-18 Quadrupole splitting β-LactoC_{12}+10%D_2O @ high temperatures.

Table 4.14 Splitting (Δ KHz) of β-LactoC_{12}.
The N= no splitting & W=wide peak & Y= have splitting.

% D_2O	Temperature											
	20	60	120	125	140	150	155	160	165	170	175	180
3						W					Y	
5	N	N	W		W	W		Y	Y	Y	Y	Y
7								W	W	Y	Y	
10						Y	Y	Y	Y	Y	Y	Y
13								Y	Y	Y	Y	Y

Table 4.14 the findings of the ^{2}H-NMR measurements for β-LactoC_{12}, while the concentration dependence of the quadrupole splitting is displayed in **Figure 4-19**.

Table 4.15 Quadrupole splitting β-LactoC_{12} at high temperatures.

% β$LactoC_{12}$	Temperature ℃				
	160	165	170	175	180
97	–	–	–	2.9	–
95	1.4	1.7	1.9	2.3	2.2
93	1.2	1.4	1.5	1.7	–
90	1.2	1.3	1.3	1.4	–
87	0.62	0.73	0.72	1.1	0.89

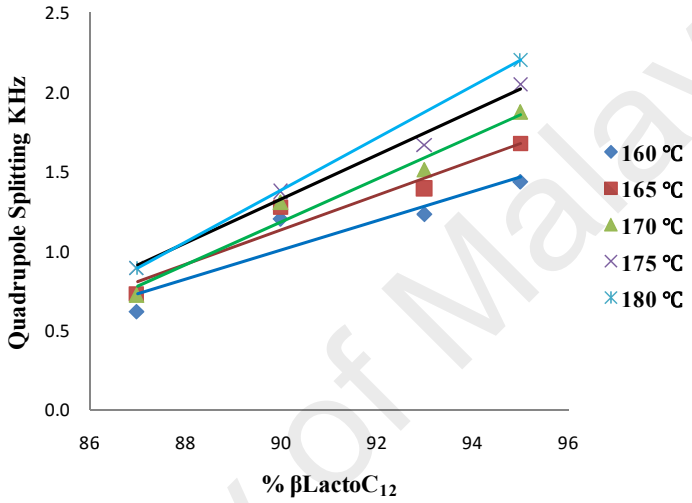

Figure 4-19 Quadrupole splitting (KHz) of β-LactoC_{12}.
In different persent of D_2O at different temperature.

Although the number of data is limited, it is possible to estimate the bound water content based on the trend of the quadrupole splitting with the molar ratio of glycolipid and water. The calculated concentrations are displayed in **Table 4.16**, while the corresponding plot is displayed in **Figure 4-20**. The quadrupole splitting appears to increase up to an equimolar ratio of glycoside and water. This translates to a bound water content of 2 mol water per glycoside, according to **Equation 1.8** (Rendall & Tiddy, 1984).

$$[(\boldsymbol{water/surfactant})\boldsymbol{molar\ ratio}] = (\boldsymbol{N-1})$$

Table 4.16 Splitting (Δ KHz) of β-LactoC_{12} + % D_2O.
In ^{2}H-NMR spectroscopy.

%D_2O	$n_{\beta LactoC12}$	n_{D2O}	$n_{\beta LactoC12} / n_{D2O}$	Δ (in KHz) T = 175 °C
3	0.19	0.2	1.3	2.9
5	0.19	0.3	0.7	2.3
7	0.18	0.4	0.5	1.7
10	0.18	0.5	0.4	1.4
13	0.17	0.7	0.3	1.1

The result matches previous experiments on monoglycoside glycosides (Misran et al., 2013). However, with respect to the significantly increased size of the head-group, higher bound water content should be expected.

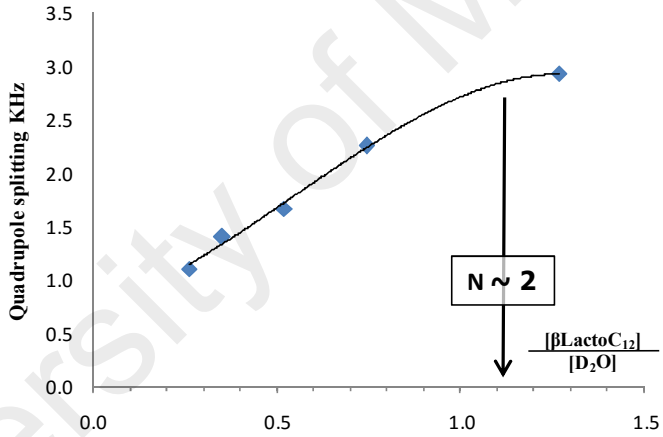

Figure 4-20 Quadrupole splitting vs. D_2O concentration for β-LactoC_{12}.
At 175 ℃ trendline of quadrupole splitting with increasing surfactant-water ratio.

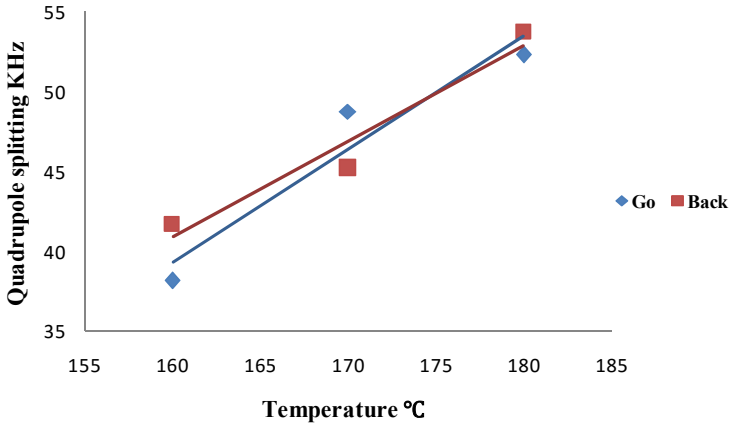

Figure 4-21 Quadrupole splitting β-LactoC_{12} +5%D_2O.
Go to high temperature and back to low temperature.

(g) β–Maltoside (β-maltoC_8C_4)

The assembly behaviour of branched chain glycolipids differs from those of straight chain analogues (R. Hashim et al., 2006). This could be reflected in the different bound water content of these glycolipids. In order to evaluate this Guerbet maltoside, i.e. β-MaltoC_8C_4, was investigated. The choice of the maltoside was based on the observations of quadrupole splittings for the straight chain maltoside at ambient and slightly elevated temperature (Manickam Achari et al., 2011 (unpublished)), whereas cellobiosides and lactosides only exhibited anisotropic behaviour in the ^{2}H-NMR spectra at high temperatures. **Table 4.17** shows the investigation scope in view of sample concentrations and temperatures.

Table 4.17 Sampling of β-MaltoC_8C_4+ %D_2O for ^{2}H-NMR.

No.	Sample	% D_2O	Temperature ℃
1	β-MaltoC_8C_4	3.60	20,40,80
2	β-MaltoC_8C_4	5.60	20,50,20
3	β-MaltoC_8C_4	9.92	20,40,60,80
4	β-MaltoC_8C_4	15.0	20,40,60,80,120
5	β-MaltoC_8C_4	20.5	20 , 40,50,60,80
6	β-MaltoC_8C_4	25.6	20,40,80
7	β-MaltoC_8C_4	29.2	20,40,80

It was expected that the branched hydrophobic domain of β-MaltoC_8C_4, which increases the molecular surface area with respect to the straight chain analogue β-MaltoC_{12} (Nguan et al., 2010) enhances the interaction with water and, hence, potentially increases the bound water content. In comparison with the cellobiose and lactose based glycolipids, higher water interaction was expected for the non-linear maltoside, owing to increased packing constraints of the head-group.

Table 4.18 Broad peaks (Δ KHz) of β-MaltoC_8C_4+% D_2O.
In ^{2}H-NMR spectroscopy at different temperature.

% βMalto#2	% D_2O	Quadrupole Splitting (in KHz)					
		20	40	60	80	120	150
94	5.6	5.4	5.1	5.0	4.1	1.7	2.5
90	9.9	6.8	6.6	3.8	2.5	–	–
85	15	5.4	3.1	2.1	1.8	1.2	–
80	21	3.5	2.4	1.8	1.3	0.87	0.71
74	26	2.7	1.7	–	1.0	–	–
71	29	1.8	1.4	–	0.84	–	–

The peak width increased with increasing concentration as shown in **Figure 4-22**. Interestingly, unlike for the previously investigated glycolipids, the peak width, reflecting a poorly resolved powder spectrum, decreased with the temperature.

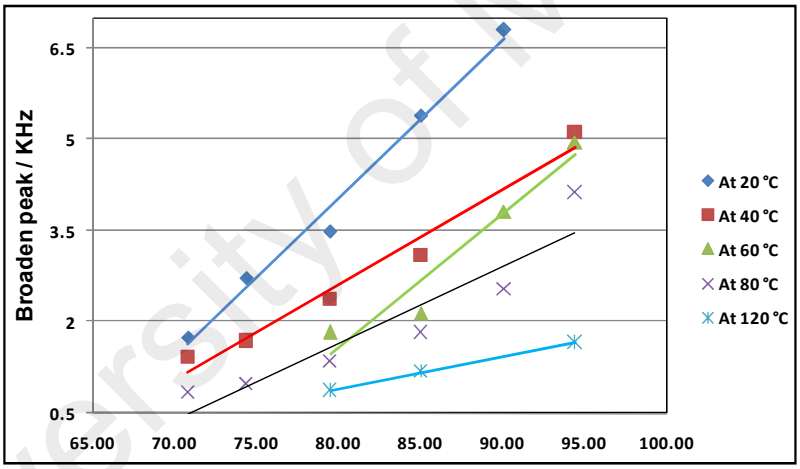

Figure 4-22 Broad peak β-MaltoC_8C_4 + %D_2O at different temperature.

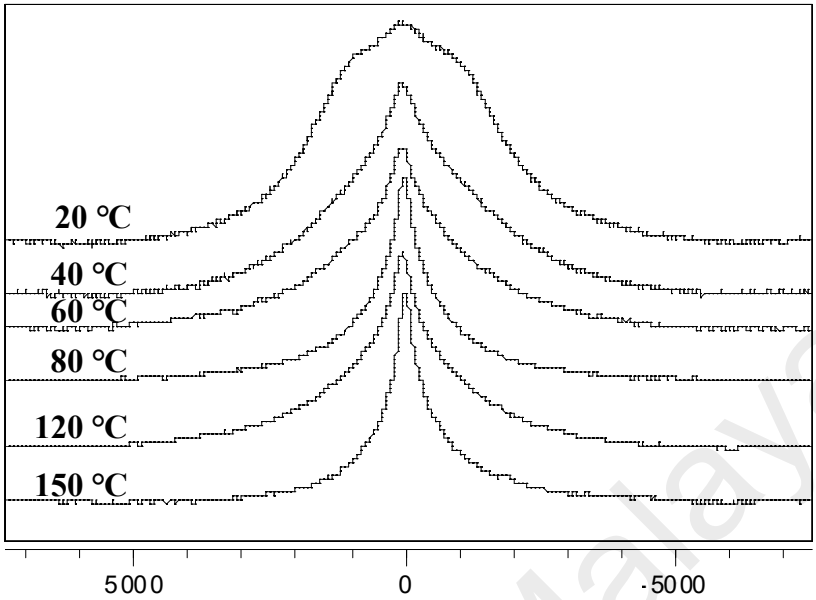

Figure 4-23 Quadrupole splitting for β-MaltoC_8C_4+ 20 % D_2O.
In ^{2}H-NMR spectroscopy at different temperature.

A correlation of concentration, molar ratio and estimated quadrupole splitting is provided in **Table 4.19**. A plot of the data, displayed in **Figure 4-23**, enables the determination of the bound water content, as previously discussed. The data indicate a bound water content of only 3 molecules water per surfactant.

Table 4.19 Broad peaks (Δ KHz) of β-MaltoC_8C_4 + % D_2O.
In ^{2}H-NMR spectroscopy .

%D_2O	$n_{\beta MaltoC8C4}$	n_{D2O}	$n_{\beta MaltoC8C4} / n_{D2O}$	Quadrupole Splitting (in KHz)		
				T = 20 ºC	T = 40 ºC	T = 60 ºC
5.6	0.18	0.28	0.66	5.4	5.1	5.0
9.9	0.18	0.50	0.36	6.8	6.6	3.8
15	0.17	0.75	0.22	5.4	3.1	2.1
21	0.16	1.0	0.15	3.5	2.4	1.8
26	0.15	1.3	0.11	2.7	1.7	–
29	0.14	1.5	0.10	1.8	1.4	–

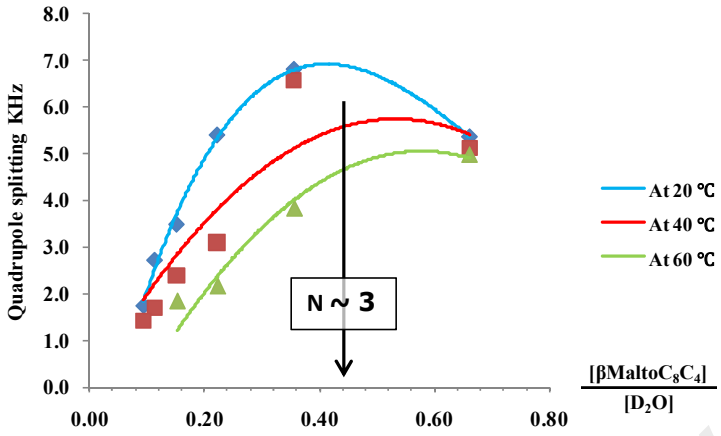

Figure 4-24 Quadrupole splitting vs. D_2O concentration for β-MaltoC_8C_4. Trendline of quadrupole splitting with increasing surfactant-water ratio.

The relative results for β-MaltoC_8C_4 and β-LactoC_{12} are in line with the expectation of a larger surface area for the former. However, the bound water content is surprisingly small. Moreover, a recent ^{2}H-NMR investigation of bound water content for β-MaltoC_{12} led to a significantly higher value (Manickam Achari et al., 2011 (unpublished)). This puts doubts in the reliability of the results. In order to evaluate the data, an alternative approach for the determination of bound water based on the melting enthalpy of 'free' water was applied.

4.1.2.2 Discussion

The deuterium NMR technique make use of the quadrupole splitting (Δ) for D_2O as a function of composition. It must be noted that the solute (glycolipid) contains highly moving OH (OD) groups. Therefore in addition of the signal due to the deuterated water, there will be also signals from ODs of the glycolipids which undergo some rapid exchange with the deuterated water, leading to an average Δ value. At low water concentration, the glycolipid OD groups are likely to provide the major contribution to Δ because the OD groups are rigidly attached by a permanent chemical

bond rather than by a loose H-bond. Each different OD group could provide a separate contribution. The spectra from β-LactoC_{12} with 3% and 5% water are likely to be dominated by the lipid contribution. For example for 5%, we can see these extra seven peaks in **Figure 4-25**. It is difficult to assign these peaks precisely. However, it is believed that the outer most peak with the largest Δ (hence more ordered) is due to the OD at the C4 carbon position, while the innermost peak with the smallest Δ (hence least ordered), is usually attributed to the OD associated with the exocyclic -CH_2-OD groups (on the C6 position) (Loewenstein & Igner, 1993; Misran et al., 2013; Morley & Tiddy, 1993).

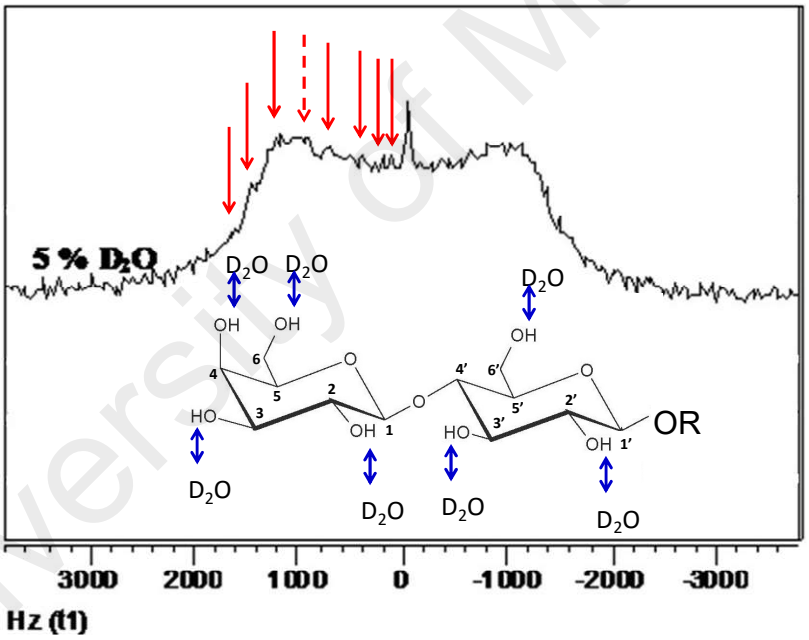

Figure 4-25 Shows extra peaks for β-LactoC_{12}.

A series of surfactants, listed in **Table 4.20**, was studied by ^{2}H-NMR. The concentration depending size of the quadrupole splitting enabled the determination of bound water content for the lamellar phase of AOT. Both D_2O and CD_3OD can be applied as probe. The obtained value of about 9 water molecules per surfactant is in reasonable agreement with a previous report on bound water for AOT in reverse

micelles, which applied a chemical shift-based approach using ^{2}H-NMR (Hauser et al., 1989). The difference of the values of the current and the previous investigation may reflect changes with respect to the applied probing approach. Besides, the different morphology of the interface of reversed micelles with respect to a lamellar assembly can contribute as well.

Table 4.20 Bound water by ^{2}H-NMR technique. Ref = (Hauser et al., 1989).

No.	Name	B.W. ^{2}H-NMR
1	AOT	8.56 (8-9), $(11)_{Ref}$
2	β-CelloC_8	No Splitting
3	β-CelloC_{12}	No Splitting
4	β-LactoC_{12}	1.89 (~ 2)
5	β-MaltoC_8C_4	3.22 (~ 3)

The disaccharide-based glycolipids β-CelloC_8 and β-CelloC_{12} were investigated by the ^{2}H-NMR method, applying a wide range of concentrations temperatures, but failed to provide the required quadrupole splitting. Only at very high temperature a quadrupole splitting could be noticed. These conditions, however, are incompatible with a systematic investigation of spectra over particularly samples with higher water concentration. The reason for missing quadrupole splittings at ambient and moderately elevated temperature is unknown. A possible explanation might be the spatial orientation of the head-group. The multiple interaction sites of the disaccharide head-group may cause a cancelation of directors for water molecules bound at different positions, resulting in no 'macroscopic' orientation. The large head-group can cause wrinkles at the surface, leading to the disappearance of a direction for the O-D bond. Increasing molecular surface area for the hydrophobic domain of the surfactant, however, might straighten the molecular surface at high temperature, resulting in observable quadrupole splittings.

The behaviour of β-LactoC_{12} mostly resembled that of the cellobiose analogues. Nonetheless, it was possible to determine the bound water content at high temperature. β-MaltoC_8C_4, on the other hand, differed substantially from the previous glycolipids. Unlike in the latter, the branched chain maltoside exhibited poorly resolved quadrupole splittings at low temperature, which decreased and disappeared at higher temperature. The reason of wide but not resolved ^{2}H-NMR signals is not clear, although it has been reported that widened peaks may result from a non-uniformly aligned molecular orientation but a wide distribution of the director (Hamasuna et al., 2008). The bound water contents for both the straight lactoside and the branched maltoside were with 2 and 3, respectively, surprisingly small, rather matching than exceeding those of a previously studied monosaccharide-based glycolipid (Misran et al., 2013).

4.1.3 Differential scanning calorimetry (DSC) (bound water)

Differential scanning calorimetry enables the determination of enthalpy changes, e.g. the enthalpy of melting water in the lamellar phase. It is assumed that there are two types of water in the lamellar phase of glycolipids; free water and water bound to the surfactant head-group. By measuring the melting enthalpy of water in the lamellar phase the free water can be determined by DSC. Knowledge of the total water enables the calculation of the bound water. The scope of the investigation is shown in **Table 4.21**.

Table 4.21 Sampling with different concentration of H_2O for DSC.

No.	Sample	% H_2O
1	β-CelloC_8	22, 31, 15, 45, 16, 24, 35
2	β-CelloC_{12}	15, 17, 20, 21, 26, 30 37, 44, 46, 72, 73
3	β-LactoC_{12}	5, 10, 15, 20, 25, 40,
4	β-MaltoC_{12}	5, 10, 16, 18, 20, 25, 30, 35, 41

4.1.3.1 Results

(a) Comparison of water and deuterated water

The DSC spectrum of pure water was examined. Pure water samples were cooled to a temperature of -40 ℃ and then heated back to 25 ℃. This procedure was repeated three times and the peaks for melting point and freezing point were recorded (**Figure 4-26**).

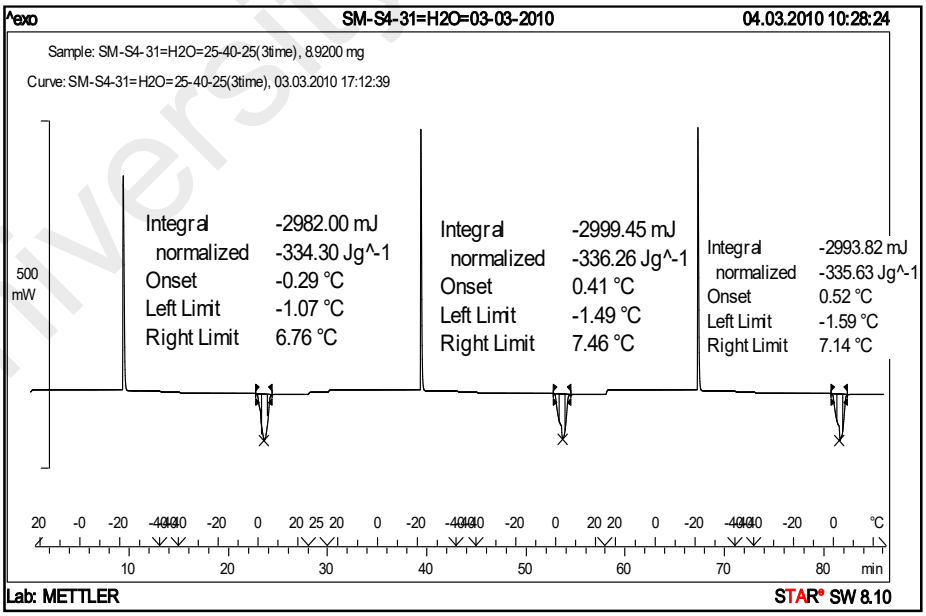

Figure 4-26 DSC of H_2O (Triple Scans).

The enthalpy of the melting was calculated. The determined values (**Figure 4-27**) of 335.40 and 335.13 joules per gram (J/g) matched with only 0.42% and 0.34% error the literature reported standard of 334.01 J/g (Eggenhoffner, 1982; Lide, 2004).

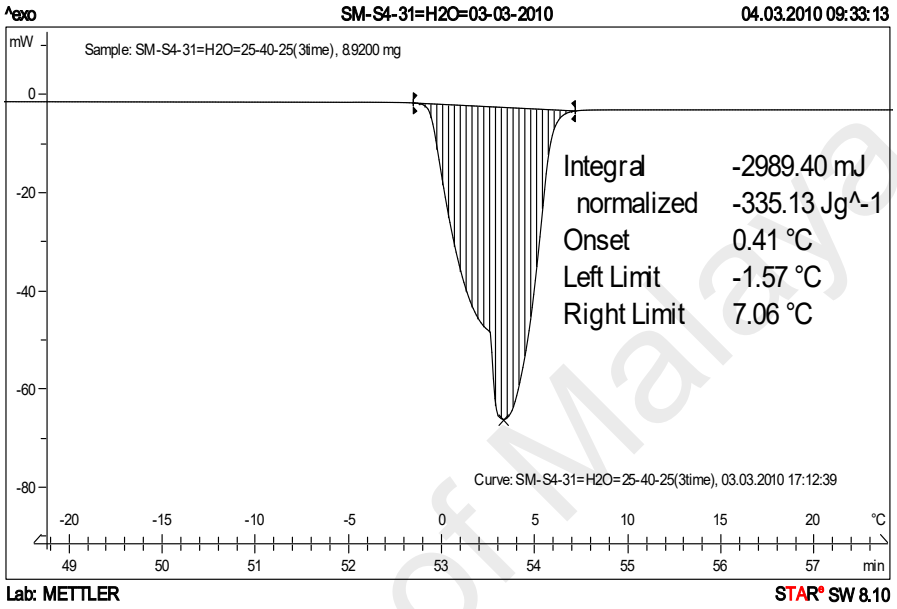

Figure 4-27 DSC of H_2O (Single Scan).

For the DSC investigation the melting enthalpy of H_2O, D_2O and free water in a lipid formulation were compared. As can be seen in **Figure 4-28** the melting peaks differ slightly. These shifts are due to the isotopic effect of deuterium, because heavy atoms require more energy to move causing an increase in melting temperature, on the one hand and melting point depression due to interaction with solutes (glycolipid molecules) on the other.

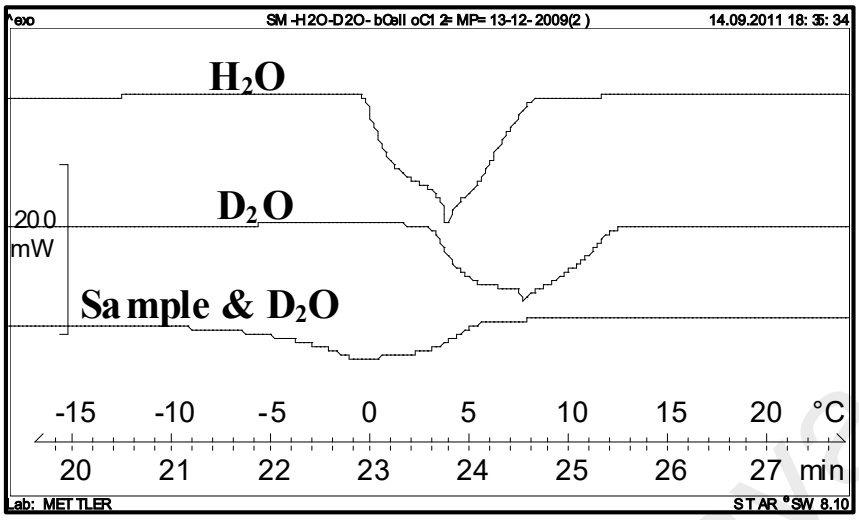

Figure 4-28 DSC melting temperature ranges.
For pure water, deuterium oxide and free water in lipid formulation.

(b) Dodecyl-β-cellobioside (β-celloC$_{12}$)

Numerous DSC samples with β-CelloC$_{12}$were prepared, differing in the content of heavy water (D_2O) based on the second method (i.e. using Karl Fischer titration method); some are shown in **Table 4.22**. In addition several samples of β-CelloC$_{12}$ with different percentage of a little water (H_2O) were measured as well. These are shown in **Table 4.23**. The latter were prepared by the third method using normal water (H_2O).

Table 4.22 Sampling of β-CelloC$_{12}$+ %D_2O for DSC.

No.	Sample	% D_2O	Sample weight / mg
1	β-CelloC$_{12}$	21	7.27 , 6.84
2	β-CelloC$_{12}$	32	7.35 , 6.92
3	β-CelloC$_{12}$	47	8.39 , 6.52
4	β-CelloC$_{12}$	49	8.83 , 7.10
5	β-CelloC$_{12}$	63	6.86
6	β-CelloC$_{12}$	69	6.88

Surprisingly, the recorded spectra for the D_2O-containing samples revealed double peaks. An example is shown in **Figure 4-29**. The reason for the doubled peaks is not known. It may be an indicative for the presence of two different types of water; free water within the lamellar phase on the one hand and water molecules at the inter phase

of the glycolipid on the other, which are, however, not completely bound by the sugar head-group, as the latter should not freeze.

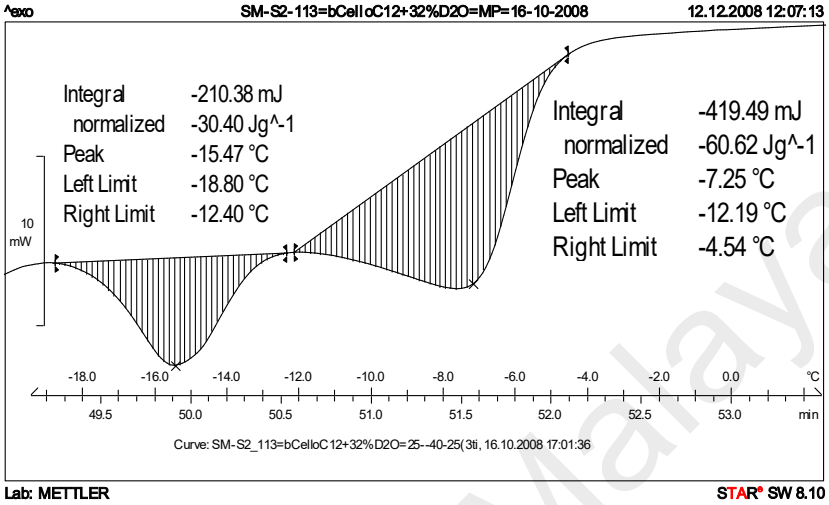

Figure 4-29 DSC of β-CelloC_{12}+32%D_2O.

Table 4.23 Sampling of β-CelloC_{12}+ %H_2O for DSC.

No.	Sample	% H_2O	Sample weight / mg
1	β-CelloC_{12}	15	9.37 , 7.12
2	β-CelloC_{12}	17	7.69 , 8.65
3	β-CelloC_{12}	20	7.65 , 7.06
4	β-CelloC_{12}	21	10.09 , 9.67 , 9.74
5	β-CelloC_{12}	26	7.21 , 8.60
6	β-CelloC_{12}	30	5.91 , 8.20
7	β-CelloC_{12}	37	8.43 , 7.75 , 9.39
8	β-CelloC_{12}	45	6.97 , 8.48

Table 4.24 DSC data analysis & calculation of bound water for β-CelloC_{12}.

No.	weight / mg	H_2O			βCelloC_{12}	n_{H2O} / $n_{\beta CelloC12}$	Enthalpy / J
		%	mg	µmol	µmol		
1	9.4	15	1.4	78	16	5.0	0.00
2	7.7	20	1.5	85	12	7.1	0.05
3	8.6	26	2.2	122	13	9.7	0.13
4	8.2	30	2.5	137	11	12	0.16
5	8.5	45	3.8	212	9.1	23	0.61

The DSC measurements on the H_2O-containing samples of β-CelloC_{12} are summarised in **Table 4.24**. The melting enthalpy increased with the amount of water in the sample. At 15 % water content no ice melting peak was observed, thus suggesting the absence of free water or that all water in this sample is bound. For samples above that water content the ice melting peak indicates presence of free water. A plot of the

melting enthalpy against the glycolipid-water ratio, as shown in **Figure 4-30** enables a good estimation of the maximum bound water content, according to: **Equation 1.9** below (Hatakeyama et al., 1988).

$$W_t = W_f + W_b$$

The result indicates about 6.5 water molecules to be bound by the glycolipid β-CelloC_{12}.

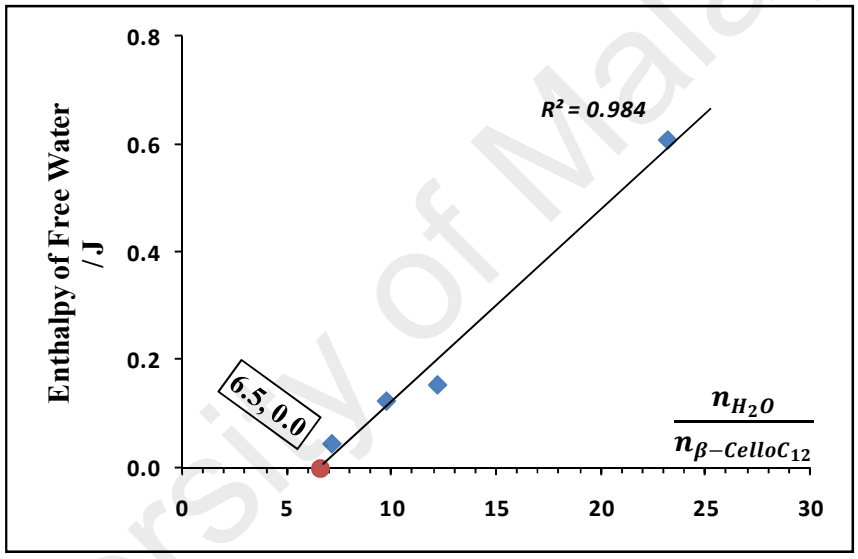

Figure 4-30 DSC data analysis: ice melting enthalpy.
In diferent water concentration for β-CelloC_{12}.

(c) Octyl-β-cellobioside (β-celloC_8)

The following samples were prepared and DSC spectra were taken according to **Table 4.25**.

Table 4.25 Sampling of β-CelloC_8+ %H_2O for DSC.

No.	Sample	% H_2O	Sample weight / mg
1	β-CelloC_8	16	6.55 , 9.02
2	β-CelloC_8	22	8.61 , 9.42
3	β-CelloC_8	24	6.22 , 9.02
4	β-CelloC_8	31	9.60 , 9.70

The DSC spectra (**Figure 4-31**) for at least two samples indicated the presence of increasing amounts of free water.

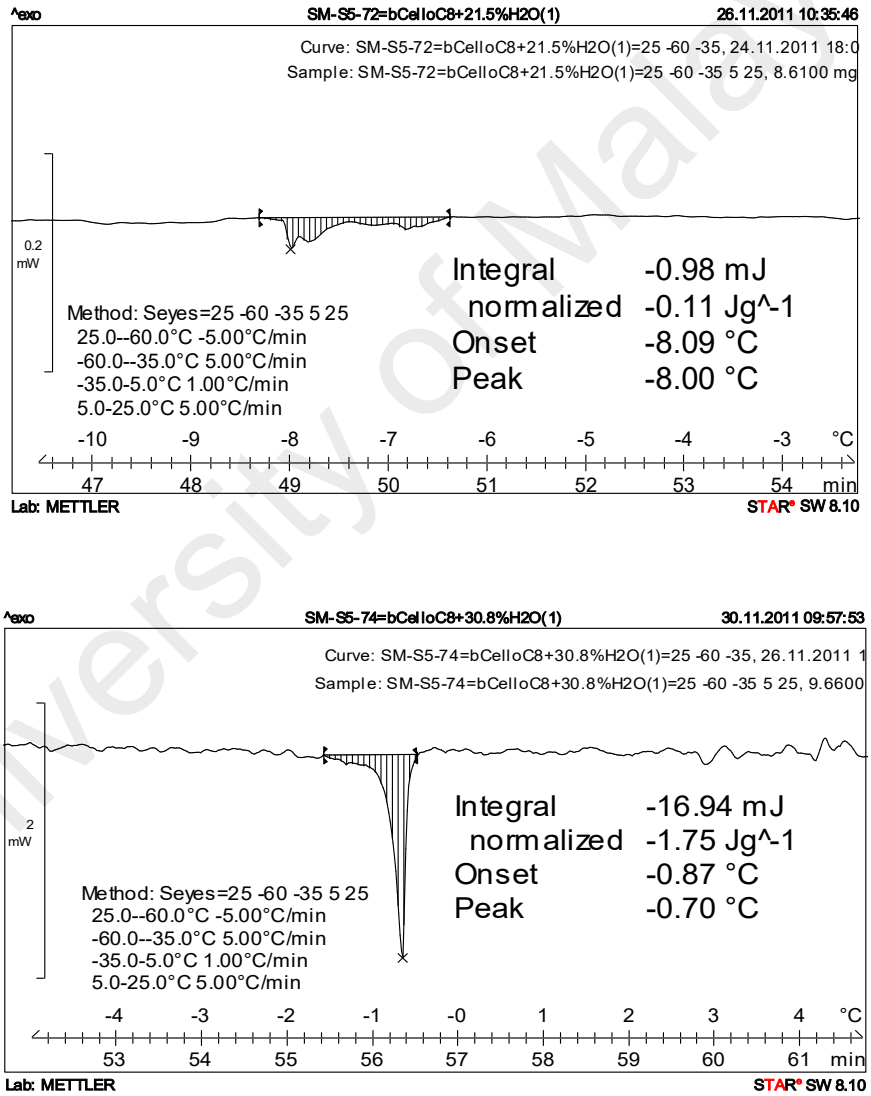

Figure 4-31 DSC thermograms for free water melting enthalpy.
For β-CelloC_8 +21.5 & 30.8 %H_2O.

It is observed that the melting point increases with increasing water content, which reflects decreasing contents of β-CelloC_8. This is normal, because the melting point decreases with increasing impurities (**Figure 4-31**).

(d) Dodecyl-β-lactoside (β-lactoC_{12})

The scope of the DSC investigation on the lamellar phase of β-LactoC_{12} is shown in **Table 4.26**.

Table 4.26 Sampling of β-LactoC_{12}+ %H_2O for DSC.

No.	Sample	% H_2O	Sample weight / mg
1	β-LactoC_{12}	5.0	7.02 , 8.85
2	β-LactoC_{12}	9.7	7.75 , 8.06
3	β-LactoC_{12}	16	8.27 , 9.31
4	β-LactoC_{12}	20	7.86 , 7.59
5	β-LactoC_{12}	40	7.14 , 7.22

The measurements and calculations are summarised in **Table 4.27**.

Table 4.27 DSC data analysis & calculation of bound water for β-LactoC_{12}.

No.	weight / mg	H_2O			βLactoC_{12}	n_{H2O} / $n_{\beta LactoC12}$	Enthalpy / J
		%	mg	μmol	μmol		
1	8.9	5.0	0.44	24	16	1.5	0.00
2	7.8	9.7	0.75	42	14	3.0	0.01
3	9.3	15	1.4	80	15	5.2	0.10
4	7.5	20	1.5	81	12	6.9	0.16
5	7.1	40	2.8	157	8.4	19	0.46

In this case, it was found that the bound water content can account for about 9% of the glycolipid. Therefore, the sample with only 5% water content did not contain free water. **Figure 4-32** indicates the bound water content to about 2 molecules per glycolipid. The reduction of bound water content with respect to the cellobioside analogue β-CelloC_{12} probably reflects the axial position of the hydroxyl group at C-4 of the lactose. This hydroxyl group is likely involved in intermolecular hydrogen bonding

between neighbouring glycolipid molecules and, hence, inactive for binding of water. However, the magnitude of the reduction of the bound water content remains surprising.

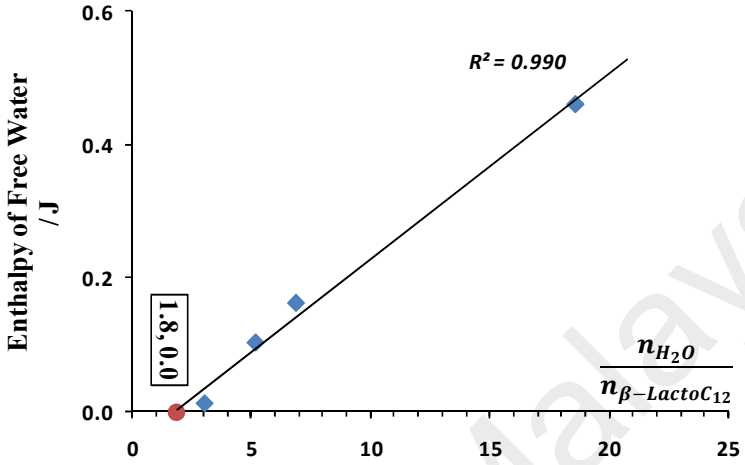

Figure 4-32 DSC data analysis: ice melting enthalpy .
In diferent water concentration for β-LactoC_{12}.

(e) Dodecyl-β-maltoside (β-maltoC_{12})

According to the previous molecules, numerous samples were prepared and investigated. The investigation scope is summarised in **Table 4.28**.

Table 4.28 Sampling of β-MaltoC_{12}+ %H_2O for DSC.

No.	Sample	% H_2O	Sample weight / mg
1	β-MaltoC_{12}	5.4	7.44 , 8.28 , 7.90
2	β-MaltoC_{12}	10	8.51 , 7.74 , 7.67
3	β-MaltoC_{12}	15	9.46 , 6.47 , 7.69
4	β-MaltoC_{12}	18	7.70 , 7.28 , 7.96
5	β-MaltoC_{12}	20	7.15 , 8.04 , 7.57
6	β-MaltoC_{12}	25	9.74 , 8.42 , 7.94
7	β-MaltoC_{12}	30	8.47 , 8.77 , 9.61
8	β-MaltoC_{12}	35	8.39 , 9.42 , 8.84
9	β-MaltoC_{12}	41	7.03 , 9.54 , 7.74

For a better comparison, the DSC peaks related to the melting points of free water in samples with different percentages of water in the β-MaltoC_{12} are shown in a graph (**Figure 4-33**).

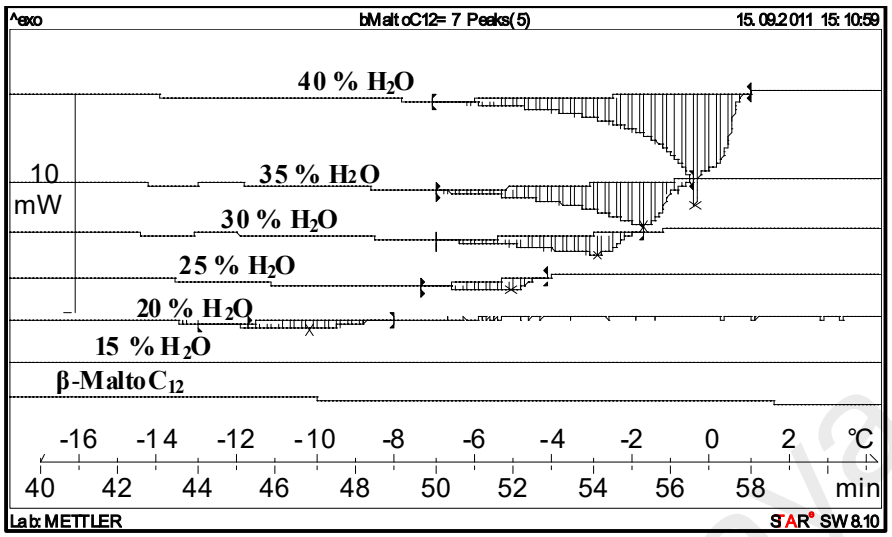

Figure 4-33 DSC thermograms for free water melting enthalpy of β-MaltoC_{12}.

Figure 4-33 revealed only bound-water up to a concentration of about 10% water, referring to a bound-water content of about 4 or 5 molecules water per surfactant .

In general for most of the concentration, scanning the sample three times at low temperature (about 0 ℃), with high and low scan rate, there was no phase change observed, see **Figure 4-26**. Furthermore even the process of freezing and melting were repeated three times, all three cases were similar and only one peak (due to the free water) was observed (see also **Figure 4-33**). However, in the system with 20% water, the melting peak is more shifted to the lower temperature. By increasing the percentage water in the system, the distance between the free water layer will also increase, which probably introduce two kind of water, the free water and water near layer. Consequently, there are two DSC peaks very close together observed for this concentration. Free water is more consistent with the behaviour of pure water. In systems where the amount of water is too low, the two lamellar layers are very close together, and in between there is little free water, so free water show slightly irregular behaviour. That is starting to melt at a lower temperature. In order to investigate this

detail behaviour require a further extensive research, which will be undertaken in the future.

The DSC measurements and calculations on samples of β-MaltoC_{12} are summarised in **Table 4.29**.

Table 4.29 DSC data analysis & calculation of bound water for β-MaltoC_{12}.

No.	weight / mg	H_2O			βMaltoC_{12}	n $_{H2O}$ / n $_{βMaltoC12}$	Enthalpy / J
		%	mg	µmol	µmol		
1	8.3	5.4	0.45	25	15.3	1.6	0.000
2	7.7	10	0.77	43	13.6	3.1	0.000
3	6.5	15	0.97	54	10.8	5.0	0.002
4	7.3	18	1.3	72	11.7	6.2	0.111
5	8.0	20	1.6	88	12.6	7.0	0.129
6	8.4	25	2.1	118	12.3	9.5	0.251
7	8.8	30	2.6	147	12.0	12	0.392
8	9.4	35	3.3	185	11.9	16	0.540
9	9.5	41	3.9	215	11.1	19	0.698

As seen in the above table, the sample of with 10% water content did not show any free water. In order to determine the bound water content more precisely, the melting enthalpy of ice in the glycolipid assemblies was plotted against the molar ratio of water and surfactant, as shown in which the number of moles drawing $\mathbf{n_{H_2O}}$ to the number of moles $\mathbf{n_{\beta MaltoC_{12}}}$ in terms of melting enthalpy of free water is indicated in **Figure 4-34**.

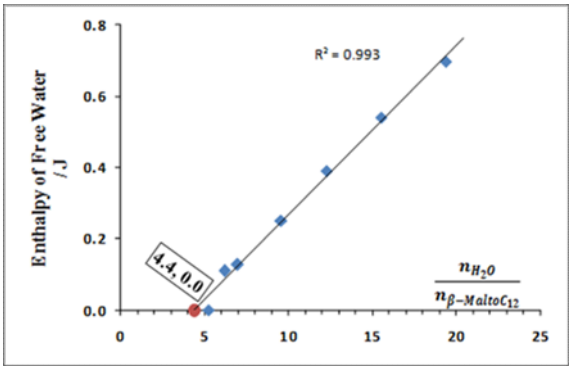

Figure 4-34 DSC data analysis: ice melting enthalpy.
In diferent water concentration for β-MaltoC_{12}.

Figure 4-34 indicates the number of bound water molecules for β-MaltoC_{12} as about 4 molecules, based on the extrapolated line to the x-axis, where the water melting enthalpy is zero.

4.1.3.2 Discussion

In estimating the bound water by the DSC technique the magnitude of the sample enthalpy at ca. 0 ℃ was compared to that of pure water. Frozen water is always assumed to be those from the free state. However, since there is an equilibrium between bound and free water, the remaining water contains both species, hence the DSC method to determine the bound water only represents an upper limit for the bound water, not the exact number. Furthermore, this number corresponds to the state at the 0 ℃ only. At higher temperatures the number is expected to be smaller. The melting enthalpy was calculated. The determined values (**Figure 4-27**) of 335 and 335 joules per gram (J/g) match closely the literature reported standard of enthalpy of pure water 334J/g with less than 1% error (Eggenhoffner, 1982; Lide, 2004). For the DSC investigation the melting enthalpy of H_2O, D_2O and free water in a lipid formulation was compared. As can be seen in **Figure 4-28** the melting peaks differ slightly. These shifts are due to the isotopic effect of deuterium, because heavy atoms require more energy to move causing an increase in melting temperature, on the one hand and melting point depression due to interaction with solutes (glycolipid molecules) on the other.

The measurement of the melting enthalpy of free water for β-CelloC_{12} was performed by using both, heavy (D_2O) and water (H_2O). The reason for the experiments with heavy water was the utilization of samples previously prepared for the ^{2}H-NMR

investigation. The tubes were broken after finishing the ^{2}H-NMR experiments and subsequently utilised for the DSC study. The DSC spectra surprisingly showed double peaks (**Figure 4-29**). This suggests that there are two types of bound water, hence in total three types of water including free water. The evaluation of the DSC results indicated a bound water content of 6-7 molecules water for β-CelloC_{12}. The bound water contents for the corresponding lactose and maltose analogues, β-LactoC_{12} and β-MaltoC_{12}, was with 2 and 4, respectively, significantly smaller. Although the sugar configuration largely affects the packing density of carbohydrates, and, hence, the potential interaction with water, this variation of the bound water content is surprising and raises doubts in the reliability of the method.

4.1.4 Comparison of the methods

Table 4.30 compares the results of the bound water content investigations described before. Besides, related literature-derived data from both experimental and computational simulation investigations are included as well. The entry for β-LactoC12, row number 4, indicate consistent results for the bound water content determination by DSC measurement of the ice-melting enthalpy, on the one hand, and the quadrupole splitting-based ^{2}H-NMR approach on the other. However, significant differences in the data are found for AOT in entry1. This mismatch of results obtained by various authors probably originates from differences of the investigated morphology. It is expected that a lamellar binary mixture exhibits a different interface compared to a water-in-oil emulsion, thus leading to inconsistent interactions of the surfactant head-group and water. Moreover, the size of droplets in an emulsion will affect the interface as well. This feature is reflected in the wide range of results from the computational study (Lemons et al., 2013). The determined bound water content for β-MaltoC_{12} is a good

agreement with a computational study (Manickam Achari et al., 2011 (unpublished)) and illustrate the potential value of bound water investigations for the understanding of lipid interactions. Overall the bound water content for the investigated disaccharide-based glycolipids, however, is quite heterogeneous. Although changes owing to packing constraints of the carbohydrate head-groups are expected, the variation range is unexpected. A more extensive investigation is required to either confirm the obtained results or identify limitations of the applied methods.

Table 4.30 Compare bound water in 3 metode.
^{2}H-NMR, DSC and hydrogen bonding in simolation method. Ref1 = (Hauser et al., 1989) & Ref2 = (Manickam Achari et al., 2011 (unpublished)) & Ref3 = (Lemons et al., 2013)

No.	Name	B.W. ^{2}H-NMR	B.W. DSC	H.B. Simlation
1	AOT	8.6 (8-9), $(11)_{Ref1}$	$(\sim \mathbf{6})_{Ref1}$	$(4\text{-}20)_{Ref3}$
2	β-CelloC_8	No Splitting	??	??
3	β-CelloC_{12}	No Splitting	6.5(6-7)	(3.4) (3-4) $_{Ref2}$
4	β-LactoC_{12}	1.9 (~ **2**)	1.8(~**2**)	??
5	β-MaltoC_8C_4	3.2 (~ **3**)	??	??
6	β-MaltoC_{12}	??	3.9(~**4**)	(3.3) (3-4) $_{Ref2}$

4.2 Stereochemistry investigation of monosaccharide glycolipids

This chapter is adopted from:

Hashim, R., Mirzadeh, S. M., Heidelberg, T., Minamikawa, H., Yoshiaki, T., & Sugimura, A. (2011). A reevaluation of the epimeric and anomeric relationship of glucosides and galactosides in thermotropic liquid crystal self-assemblies. Carbohydrate research, 346(18), 2948-2956.

Synthesised Monosaccharides, which their synthesis method is described in 3.1.2.5, are listed in Table **4.31**.

Table 4.31 Synthesised monosaccharide moleculs.

No.	Compounds	Yield(%)	Catalyst
1	β-Gluco$C_{12}C_8$	21	BF_3
2	α-GlucoC_6C_2	5	$SnCl_4$
3	α-Gluco$C_{10}C_6$	12	$SnCl_4$
4	α-Gluco$C_{14}C_{10}$	9	$SnCl_4$
5	β-GalactoC_6C_2	43	BF_3
6	α-GalactoC_8	7	BF_3

These materials went under study after being synthesised and purified using OPM and DSC techniques.

4.2.1 Thermotropic and lyotropic investigation (β-Gluco$C_{12}C_8$)

Here we describe the characterization of 2-octyl-1-dodecy-β-glucoside (β-Gluco$C_{12}C_8$) in terms of its thermotropic and lyotropic studies in particular its structure from the small angle x-ray crystallography. Octyl-dodecanyl-β-D-glucoside(β-Gluco$C_{12}C_8$) has a hydrophilic head-group containing glucoseand the chain is octyl-dodecanol from the Guerbet alcohol. This branched chain alcohol is one of the five Guerbet alcohols which can be purchased as shown in Table **4.32**.

Table 4.32 Guerbet alcohols.

No.	Compounds	Formula	Symbol
1	2-Ethyl-1-hexanol	$C_8H_{18}O$	-C_6C_2
2	2-Butyl-1-octanol	$C_{12}H_{26}O$	-C_8C_4
3	2-Hexyl-1-decanol	$C_{16}H_{34}O$	-$C_{10}C_6$
4	2-Octyl-1-dodecanol	$C_{20}H_{42}O$	-$C_{12}C_8$
5	2-Decyl-1-tetradecanol	$C_{24}H_{50}O$	-$C_{14}C_{10}$

The synthesised β-Gluco$C_{12}C_8$ was compared with four other molecules in the same series. These molecules are displayed in **Table 4.33** and their molecular structures are demonstrated in **Figure 4-35**.The octyl-dodecanyl-β-D-glucoside (highlighted) and

four other Guerbet glucosides which were made previously (Hairul Amani, 2010) are displayed in **Table 4.33** for comparison.

Table 4.33 Comparison 5 guerbet glucosides.

No.	Compounds	Yield/ %	Formula
1	β-GlucoC_6C_2	Not available	$C_{14}H_{28}O_6$
2	β-GlucoC_8C_4	Not available	$C_{18}H_{36}O_6$
3	β-Gluco$C_{10}C_6$	Not available	$C_{22}H_{44}O_6$
4	β-Gluco$C_{12}C_8$	20% (Current work)	$C_{26}H_{52}O_6$
6	β-Gluco$C_{14}C_{10}$	Not available	$C_{30}H_{60}O_6$

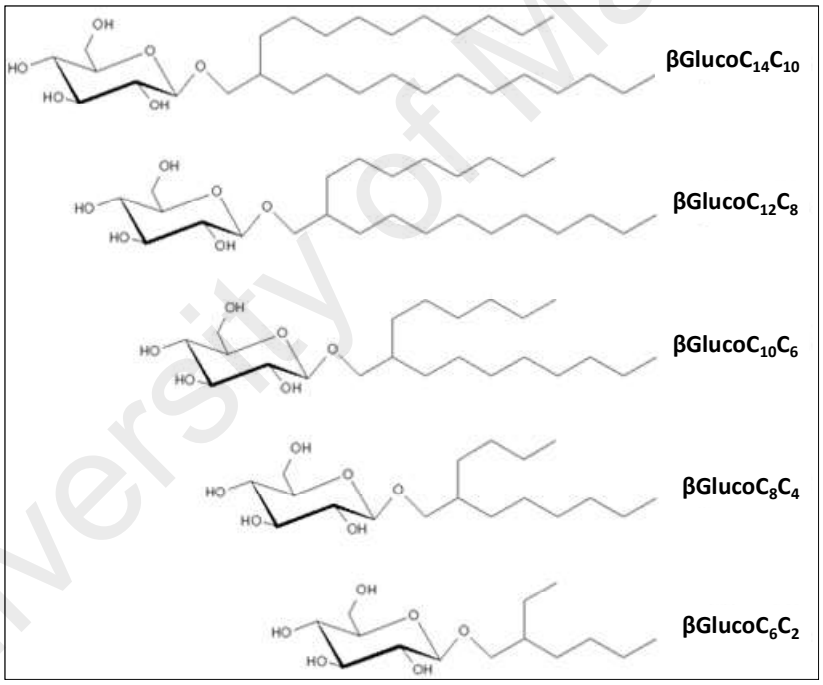

Figure 4-35 The chemical stracture of the branched chin β-glucosides.

The DSC spectrum of β-Gluco$C_{12}C_8$is shown in **Figure 4-36**. The transition temperature into the isotropic phase on heating is 113 ℃.

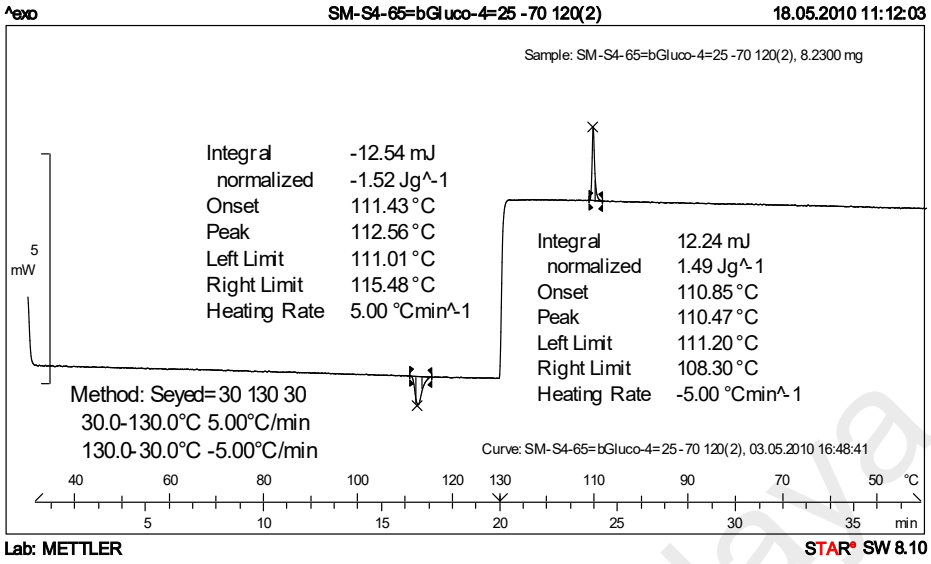

Figure 4-36 DSC of β-Gluco$C_{12}C_8$.

The longer chain compounds β-Gluco$C_{12}C_8$ form hexagonal H_{II} phases when dry and in excess water, with typical optical textures in dry and hydrated form are shown in **Figure 4-37**.

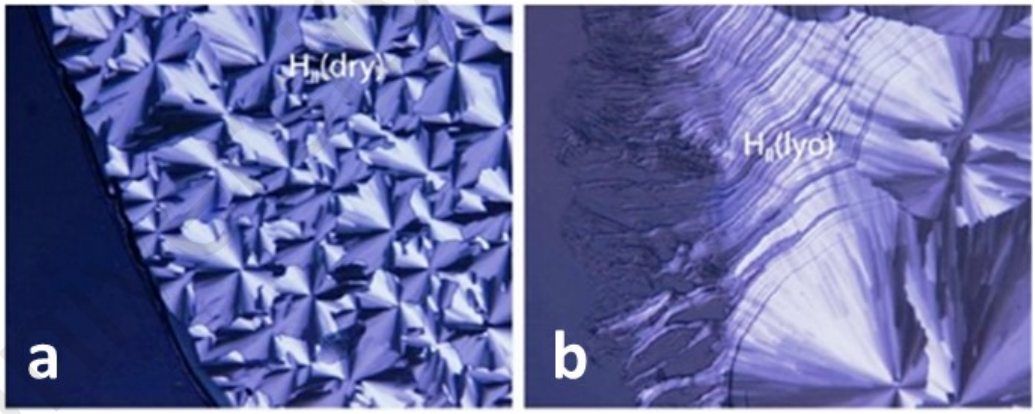

Figure 4-37 Thermotropic texture for β-Gluco$C_{12}C_8$.
(a) Thermotropic H_{II} texture at room temperature (b) lyotropic H_{II} texture after 7 h of contact penetration with water.

The thermotropic phase transition temperatures measured by OPM are summarised in Table **4.34** below along with the other four members of the Guerbet series glycosides as reported in (Brooks et al., 2011)

Table 4.34 Thermotropic phase transition.
Temperatures above 25℃ for the dry β-Glc samples determined by optical polarising microscopy these transition temperatures are measured after initial heating and cooling during sample preparation. The current material (β-Gluco$C_{12}C_8$) reported is highlighted.

Glycolipid	Phase transitions and transition temperatures
β-GlucoC_6C_2	L_C–L_2: 62 ℃ (heating)L_2–L_α: 59 ℃ (cooling)
β-GlucoC_8C_4	L_2 at all temperatures studied
β-Gluco$C_{10}C_6$	H_{II}–L_2: 55 ℃
β-Gluco$C_{12}C_8$	H_{II}–L_2: 113℃ (curent work yield=20%)
β-Gluco$C_{14}C_{10}$	H_{II}–L_2: 139 ℃

4.2.2 Epimeric and anomeric investigation

Stereochemistry of a glycolipid especially in the hydrophilic head-group is important. This aspect is known to affect the number of bound water that is connected to the head-group. For example a series of β-anomer glucosides have been investigated for their lyotropic phases. In addition the number of bound waters to these phases was also determined by deuterium NMR technique by using heavy water (D_2O) as probe (Misran et al., 2013). While this study focus on the β-anomers, the α-anomers (another isomer of sugar) have not been studied in the same manner. In addition, sugars stereochemistry also involves epimers, where the hydroxyl groups are either axially or equatorially oriented. We are interested with the C_4 epimers of both glucosides and galactosides. Here we present the study of epimers and anomers of glucosides and galactosides and determine the correlation between these stereoisomers. (Hashim et al., 2011)

A number of ten glycolipids were studied in the present research; five of them were synthesised in this study (**Table 4.35**) and the other five were already synthesised by other researchers.

Table 4.35 Synthesised monosaccharide moleculs.

No.	Compounds	Yield(%)	Catalyst
1	α-Glc-C_6C_2	5	$SnCl_4$
2	α-Glc-$C_{10}C_6$	12	$SnCl_4$
3	α-Glc-$C_{10}C_{10}$	9	$SnCl_4$
4	β-Gal-C_6C_2	43	BF_3
5	α-Gal-C_8	7	BF_3

4.2.2.1 Introduction

Glycolipids are amphiphiles with a hydrophilic sugar head-group and a hydrophobic alkyl chain. Some are amphitropic, that is, capable of forming liquid crystals in dry state and when solvated. They are usually associated with membranes and their functions are related to lyotropic and surfactant properties. The cell membrane is a fluid lamellar system, where the hydrophilic region is based on an extensive hydrogen bonding network. It is distinctly separated from the hydrophobic domain, which is dominated largely by repulsive, geometric driven interaction of the alkyl chains, often assumed to be randomly arranged and giving it a fluid nature. The simplistic concept of the glycolipid self-assembly requires a systematic examination of how the complex sugar structure relates to the properties and to uncover some of the driving forces responsible for its formation.

So far, investigation and interest in the possible thermotropic application of glycolipids is underexploited. For example, although glycolipids are chiral and ferroelectric, possible tilted structures (like SC) in the lipid organization have been reported only recently, even though ferroelectricity phenomena in cell membrane functions are known. The possible columnar structure, caused by the separation of the hydrophilic from the hydrophobic region, creates a polar order, from which a non-linear response to polarization is expected. However, such investigations are recent and

preliminary; some of these synthetic glycolipids have shown spontaneous macroscopic polarization along the columnar axis and may display a reversible signal of second harmonic generation (SHG) by heating.

Understanding the amphiphilic surfactant self-assembly phenomena, both in dry and hydrated forms, and the implications for bio- and material technology require basic experiments on pure materials, which are difficult to extract. A synthetic substitute is therefore, always desirable. From the early works of Jeffery (Jeffrey, 1986, 1990) and Vill (Vill, 1989), many synthetic glycolipids–mostly monoalkylated, have been prepared, but significantly few self-assembly related properties (especially thermotropic liquid crystals) have been reported. Previous studies on these, have demonstrated a direct correlation between molecular structure and liquid crystals behaviour, where common phases observed included smectic A (SA), columnar (Col) and bicontinuous cubic phases (Cub). See **Figure 4-38** for examples.

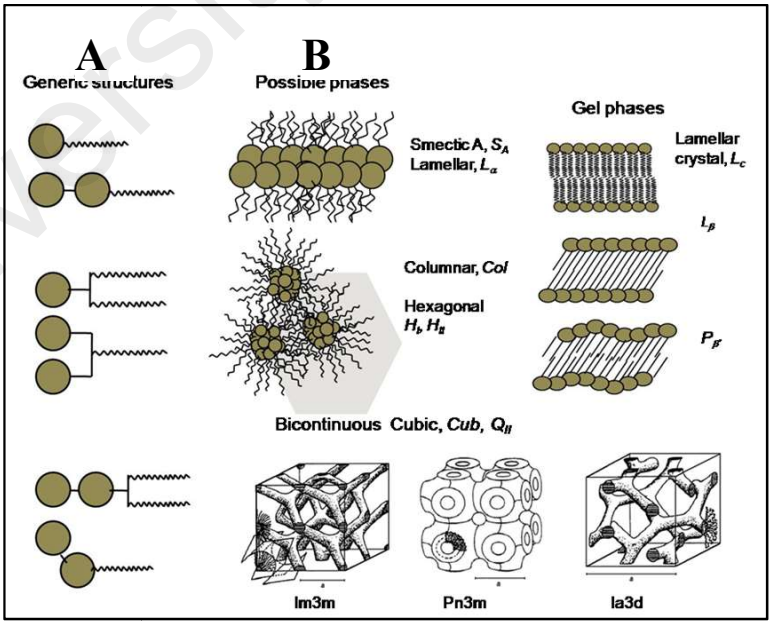

Figure 4-38 Generic structures of different glycolipids.
(simple and complex sugars, single and double lipid chains) are shown in (a). The possible thermotropic phases for these as reported previously are shown in (b).
Figur from(Hashim et al., 2011)

Moreover, molecular amphiphilic nature is the driving force for the thermotropic phase formation, due to the microscopic phase separation of a dichotomy, such as hydrophilic / lipophilic. Minimum molecular size is important; the dichotomic balance can be tuned to obtain an optimum lipid chain length for a given polar head-group. Sugar stereochemistry (epimers and anomers) influences the thermotropic behaviours; hydroxyl groups (OHs) increase the melting transition from hydrated solid to the liquid crystal phase and widen the range of the ordered phase before clearing into the isotropic phase. Different behaviours are observed for the sugar head-group of various oligosaccharides, even though the difference between them is very subtle. Malto-oligosaccharides with a $(1 \rightarrow 4\alpha)$ link for example, form a tertiary structure of flexible helix, while the corresponding cello-oligosaccharides with a $(1 \rightarrow 4\beta)$ link exhibit extended ribbon structure. Due to the non-linear alignment of the glucose units in maltose ($1 \rightarrow 4\alpha$-linkage) the corresponding lipids have lower melting transitions and are more soluble than the cellobiose β-isomers, which are expected to pack more compactly, hence exhibiting a higher melting temperature. Flexibility of the alkyl chain is important and there is a simple dependency of the transition temperatures on the chain length. For monoalkylated glycolipids, a minimum of about seven carbons chain is required to exhibit a liquid crystal phase. The transition temperature into the isotropic phase usually increases with increasing chain length until a maximum is reached, beyond which increasing chain length depresses the phase transition due to the ease of chain randomization. Although monoalkylated glycolipids are interesting, membrane lipids (both phospholipids and glycolipids) are usually double tailed, often involving two non-equivalent chains. Hence chain branching plays an important role in membrane stability, and many synthetic branched chain glycolipids were developed by various groups, for example 1,2-dialkyl/diacyl-glycerol-based, 1,3-glyco-glycero-lipids and Guerbet glycosides. Unlike monoalkylated glycosides, Guerbet glycosides have a

simple asymmetric branched chain. They also exhibit a variety of ordered phases (S_A, Col and Cubic) from below the room-temperature, except in the case of lactosides, whose anomalous behaviour is due to the presence of an end-galactose sugar unit. A few of these glycosides even show thermotropic polymorphism. Therefore, the Guerbet chain, which has high hydrophobicity, generally lowers the melting point from the crystalline state of these glycosides into their ordered phases-α behaviour similar to their precursor alcohols, which are all liquids at room-temperature. Guerbet glycosides show the same thermotropic clearing transition tendency in homologous series as monoalkylated analogues, that is, the transition temperature into the isotropic phase increases initially with increasing chain length until a maximum is reached. Beyond this maximum, increasing the chain length will decrease the transition temperature and promote non-lamellar or curved phases, such as cubic and columnar phases.

An interesting phenomenon observed from these studies suggests a possible structural connection between α-galactosides and β-glucosides. It was found that the behaviour of a series of pure α-galactosides is similar to recently reported behaviour of pure β-glucosides. This has led to the speculation that the epimeric/anomeric pairs may have similar structural arrangements within their hydrophilic region. It has been attributed to the relative configuration of the anomeric linkage and the hydroxyl group at C-4, which are Trans to each other (see **Figure 4-39**).

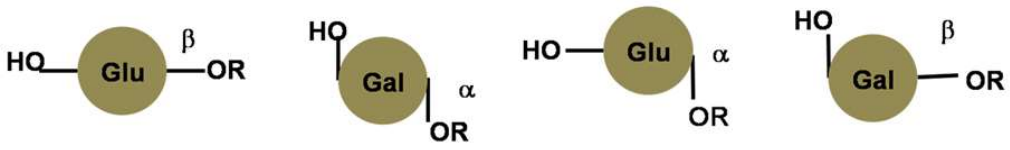

Figure 4-39 Correlation between axial/equatorial bond. At 4th carbon position to the α/β-glycosidic 1–4 bond may influence intralayer hydrogen bonding.

In the present report, we try to confirm this phenomenon by comparing three new α-Guerbet glucosides, namely 2-ethyl-hexyl α-D-glucopyranoside (α-GlcC_6C_2), 2-hexyl-decyl α-D-glucopyranoside (α-Glc$C_{10}C_6$) and 2-decyl-tetradecyl α-D-glucopyranoside (α-Glc$C_{14}C_{10}$), with previously reported β-galactosides. This epimeric/anomeric pair has a cis-configuration of the 4-OH and the anomeric bond. In addition, we have also determined the thermotropic phase behaviour of octyl α-D-galactopyranoside to complete the epimer/anomer quartet. Although the latter has been previously synthesised, its liquid crystal behaviour, to the best of our knowledge, has not been reported.

4.2.2.2 Discussions

The OPM textures and DSC thermograms for α-GlcC_6C_2, α-Glc$C_{10}C_6$, α-Glc$C_{14}C_{10}$, α-GlcC_8 and α-GalC_8 are given in **Figure 4-40**, while **Table 4.36** summarises and compares the transition temperatures of these glycosides with previously reported results for the corresponding β-4-epimers.

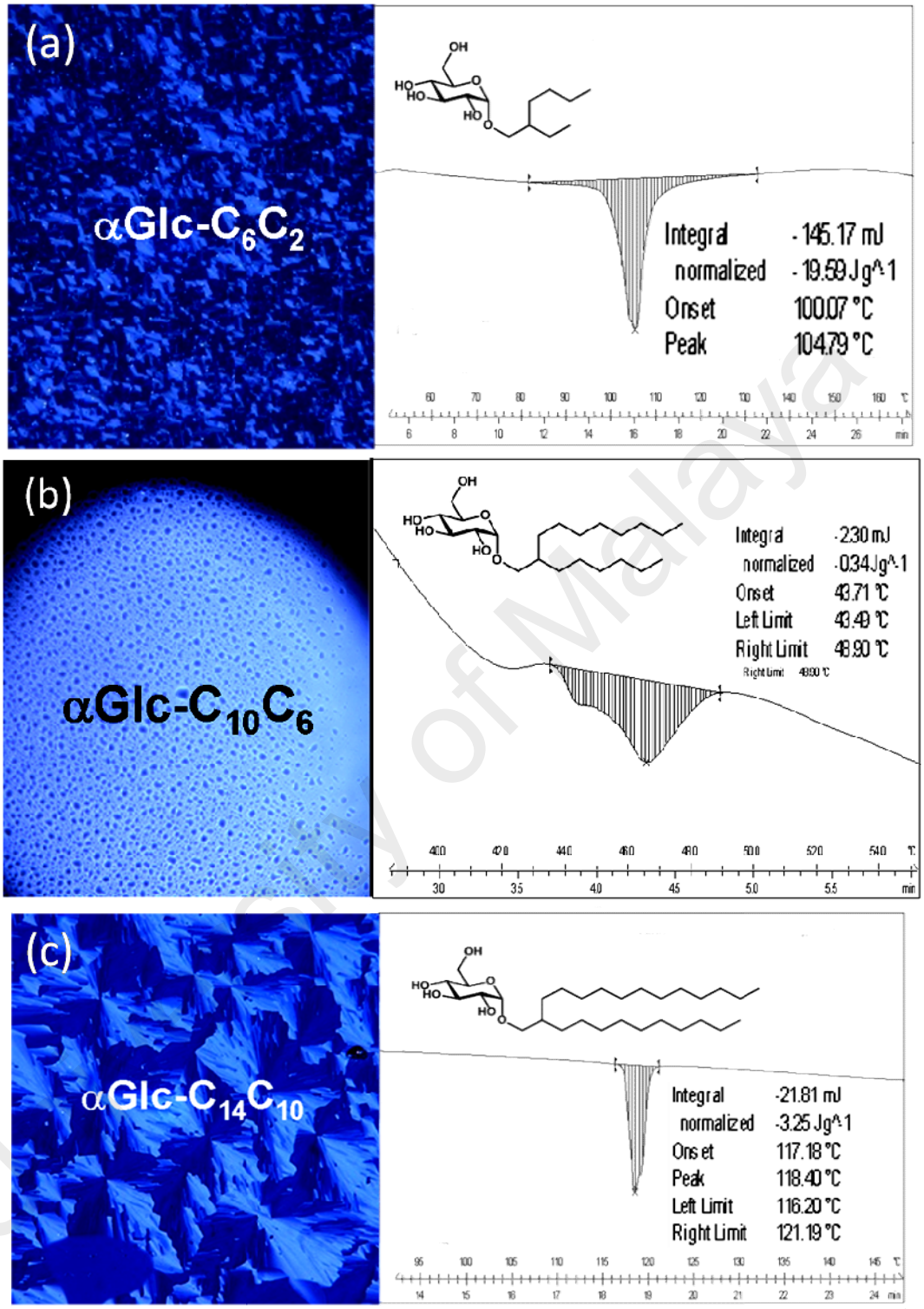
(a)
αGlc-C6C2
Integral -145.17 mJ
normalized -19.59 Jg^-1
Onset 100.07 °C
Peak 104.79 °C
(b)
αGlc-C10C6
Integral -2.30 mJ
normalized -0.34 Jg^-1
Onset 43.71 °C
Left Limit 43.49 °C
Right Limit 48.90 °C
(c)
αGlc-C14C10
Integral -21.81 mJ
normalized -3.25 Jg^-1
Onset 117.18 °C
Peak 118.40 °C
Left Limit 116.20 °C
Right Limit 121.19 °C

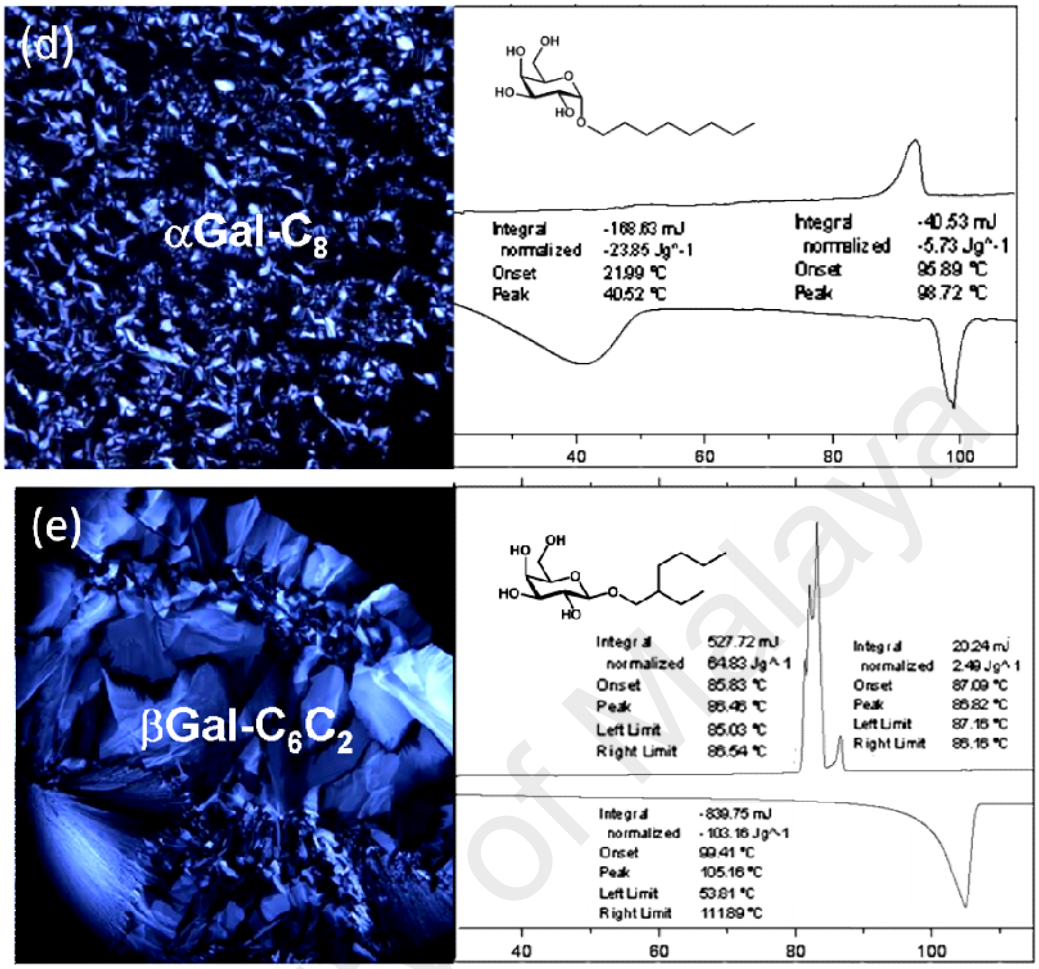

Figure 4-40 Thermotropic phase behaviours of the three α-glucosides. Characterised by OPM textures and the corresponding DSC thermograms.

The α-GlcC_6C_2 and β-GalC_6C_2 show almost the same transition temperature for the clearing into the isotropic liquid, as shown in **Table 4.36**. However, the previously reported transition enthalpy for β-GalC_6C_2 of about 24.2 kJ mol^{-1}, exceeds the range of typical liquid crystal transitions. We have therefore repeated this measurement with an initial heating scan rate of 10 °C per min and a slower rate (0.5 °C min^{-1}) for cooling and reheating. The present result identifies the phase transition at 105 °C upon heating and reheating as a melting process from a crystal to the isotropic phase. The OPM texture in **Figure 4-39** confirms this assignment.

The liquid crystal phase transition is only observed on cooling at 87 ℃, indicating that this compound displays a monotropic transition behaviour. Like the lower homolog, α-Glc$C_{14}C_{10}$ and β-Gal$C_{14}C_{10}$ also gave similar transition temperatures and enthalpies, but in this case the transformation was between the columnar and the isotropic phase (Col-Iso). In the case of the previously reported β-Gal$C_{14}C_{10}$ however, no crystal to columnar transition was observed for α-Glc$C_{14}C_{10}$. This may be due to strong hydrogen-bonding interactions for non-reducing galactose units, as previously indicated for lactosides.

The transition enthalpy quantifies the energy change due to the structural changes within the self-assembly, when a phase transition occurs. For a crystal to a liquid crystalline phase transformation, the latent heat change is greater than that of a liquid crystal to an isotropic phase. For example, the transition of a crystal into a columnar phase requires ΔH of more than 63 kcal/mol (~263 kJ/mol) for a galactopyranosyl-glycerol, while only less than 2 kJ mol^{-1} is needed for the corresponding liquid crystal to isotropic transition. Thus, the observed data **Table 4.36** reasonably accounts for the liquid crystalline phase transitions of both S_A to Iso and Col to Iso. We should expect the former to be slightly higher than the latter, as packing within the smectic layer is more than within a columnar structure, hence greater hydrogen bonding applies to the former.

Table 4.36 Thermotropic phases, transitions temperatures and enthalpies.
For α/β-gluco/galactoside pairs; present results are bold. Refrences (Hashim et al., 2011).Ref: 1=(Nilsson et al., 1998) & 2=(Rodzi, 2006) & 3=(Sakya &Seddon, 1997) & 4=(Goodby, 1984) & 5=(Dorset & Rosenbusch, 1981).

α-glycosides (currentwork)	**Phases (transition T in ℃)**	**ΔH_M (kJ mol^{-1})**	**Epimeric β-glycosides**	**Phases (transition T in ℃)**	**ΔH_M (kJ mol^{-1})**
αGlc-C_6C_2 [1]	*Cr* ? S_A (105 ± 4) *Iso*	5.7	βGal-C_6C_2	(S_A87) *Cr* 111 *Iso*	(1.3) 24.2 [2]
αGlc-$C_{10}C_6$	*Cr* ? *Micellar* (45 ± 4) *Iso*	0.14	βGal-$C_{10}C_6$	*Cr* 52 *Col* 69 *Iso* [2]	0.8 [2]
αGlc-$C_{14}C_{10}$	*Cr* ? *Col* (118 ± 4) *Iso*	1.7	βGal-$C_{14}C_{10}$	*Cr* 80 *Col* 123 *Iso* [2]	1.2 [2]
αGal-C_8	*Cr* ~40 S_A (95 ± 4) *Iso*	1.4	βGlc-C_8	*Cr* 69 S_A 107 *Iso* [3]	0.40 [4]
αGlc-C_8	*Cr* 69 S_A116 *Iso*[3]	0.49 [5]	βGal-C_8	*Cr* 96 S_{Ad}127 *Iso* [3]	

Unlike in previously described examples, the compounds with a total chain length of 16 carbon atoms, that is, α-Glc$C_{10}C_6$ and β-Gal$C_{10}C_6$ exhibit neither similar phases nor transition temperatures. As these glycosides are of different purity (anomeric impurities) and within a region (of chain length), where the hydrophilic and lipophilic balance is highly sensitive, these two results are not comparable. Moreover, in a recent study, βGlc-$C_{10}C_6$ gave an inverse micellar phase (no birefringence was observed), which was not a liquid crystal, below the isotropic phase transition. Due to this inconsistent phase behaviour, an extensive investigation was conducted, which revealed the presence of very minor amounts of hydration water transformed the hexagonal assembly into the micellar phase (details will be reported elsewhere). This phase sensitivity has not been observed for any other chain length and is believed to be due to a critical balance of the oppositely directing effects of the head-group and the chain. It was argued that, due to packing frustration, the Guerbet derived β-glucosides and a galactoside shaving chain lengths above 12 carbons in total, prefer to curve and form a non-lamellar phase. However, a chain length of 12, which can be extended to 16 upon addition of hydration water, is insufficiently long to stabilise the columnar phase. This results in an inverse aggregated micellar phase instead, whose structure maybe confirmed by X-ray diffraction.

Computer simulations of monoalkylated α/β-octyl glucosides and galactosides in the thermotropic S_A phase were conducted and these simple bilayer models were investigated to understand the nature of bonding within the hydrophilic region and the effect of sugar stereochemistry. Although numerous computer simulations on lipid bilayers have been reported before, this investigation is the only example of the thermotropic system devoid of any solvent interaction. Also, a fixed lipid chain was

used throughout the investigation, enabling a systematic comparison of sugar configurations. Hydrogen bonding was grouped into inter and intralayer interactions, of which the latter dominated the clearing temperature. Some of the results are quoted here in **Table 4.37**. It was noted that a cis-configuration of the 4-OH and the glycosidic linkage correlated with higher intralayer hydrogen bonding compared to the trans-pair. This observation matches our present results, as indicated in **Table 4.37**. It is even possible to use the H-bonding strength for a relative prediction of clearing temperatures.

Table 4.37 Correlation of simulation results for hydrogen bonding. And clearing temperature of thermotropic glycolipid assemblies. Ref: 1=(Chong et al., 2007) & 2=(Sakya &Seddon, 1997) & *=for α-GalC_8 is determined from the present work.

Lipid	Exp. clearing transition (℃)	H-Bonding from simulation[1]		Calc. clearing transition (℃) (intralayer H-bond)		Calc. clearing transition (℃) (total H-bond)	
		Intralayer	Total	α-GlcC_8	β-GlcC_8	α-GlcC_8	β-GlcC_8
β-GlcC_8[2]	107	2.7	3.5	106	-	85	-
α-GalC_8*	95	2.4	3.9	68	69	121	145
α-GlcC_8[2]	116	2.8	3.8	-	117	-	140
β-GalC_8[2]	127	2.9	3.5	134	135	85	106

Table 4.37 indicates a reasonably good correlation of intralayer H-bonding and clearing temperature, whereas the total H-bonding cannot explain the relative clearing temperatures. An exception to this apparently good correlation is that for the αGal-C_8. The experimental clearing transition (98 ℃) exceeds the prediction (68 ℃) quite considerably. The discrepancy is probably due to some uncertainty in the measurement of intralayer H-bond in the simulation. Intermolecular H-bonding effects have been previously applied to explain the different behaviour of sugar isomers. In a study reported by (Kikuchi et al., 1993). The binding of alkyl glycosides to a cyclic resorcinol tetramer was found to be largely influenced by the intra-complex guest–guest (alkyl glycosides) H-bonding. This implies that the alkyl glycosides form a network of

hydrogen-bonds within the host system. Hydrogen bonding affects solvophobicity/ solvophilicity due to the geometry, stereo selectivity and cooperativity, hence indirectly supporting the simulation findings. Apparently this concept also applies to the columnar phase; although self-assembly structure differs from the lamellar system. Therefore, the epimeric/anomeric pair may be grouped even for the longer chained decyl-tetradecyl α/β-gluco/galactoside pairs, see **Table 4.38**.

Table 4.38 Transition into the isotropic phase from computer simulation.
Predicted based on intra-layer hydrogen bonding of octyl-glucosides and galactosides are given.

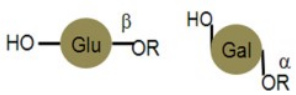 Trans-configuration of 4-OH/aglycon			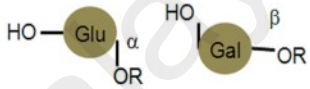 Cis- configuration of 4-OH/aglycon		
Simulation	**T(S_A- Iso)/ ℃ Intra-layer H-bond**		**Simulation**	**T(S_A- Iso)/ ℃ Intra-layer H-bond**	
Ref.	α-GlcC_8	β-GlcC_8	Ref.	α-GlcC_8	β-GlcC_8
β-GlcC_8	106	ref (107)	αGlc-C_8	ref. (116)	117
α-GalC_8	68	69	βGal-C_8	134	135
Experimental (straight chain)	**T(S_A- Iso) (℃)**	**Ref**	**Experimental (straight chain)**	**T(S_A- Iso) (℃)**	**Ref**
β-GlcC_8	107	(Sakya &Seddon, 1997)	α-GlcC_8	116	(Sakya &Seddon, 1997)
α-GalC_8	98 ± 2	present work	β-GalC_8	127	(Sakya &Seddon, 1997)
β-GlcC_{18}	146	(Hori & Ikegami, 1959)	α-GlcC_{18}	150	(Hori & Ikegami, 1959)
α-GalC_{18}	145.9	(Hori & Ikegami, 1959)	β-GalC_{18}	164	(Hori & Ikegami, 1959)
Experimental (Guerbet chain)	**T(S_A/Col- Iso) (℃)**	**Ref**	**Experimental (Guerbet chain)**	**T(S_A/Col- Iso) (℃)**	**Ref**
β-GlcC_6C_2	55	(Hashim et al., 2006)	α-GlcC_6C_2	105 ± 3	present work
α-GalC_6C_2	67	(Rodzi, 2006 (M.Sc))	β-GalC_6C_2	87± 2 , 111 ± 2 (*Cr-Iso*)	present work
β-Glc$C_{14}C_{10}$	95	(Hashim et al., 2006)	α-Glc$C_{14}C_{10}$	118 ± 3	present work
α-Gal$C_{14}C_{10}$	104	(Rodzi, 2006 (M.Sc))	β-Gal$C_{14}C_{10}$	123	(Rodzi, 2006 (M.Sc))

To our knowledge, data for α-galactopyranosides are scarce in the literature, probably due to the more challenging preparation of the α-anomers. For monoalkylated compounds only one complete set of anomer–epimers, that is, octadecyl α/β-D-gluco-/galactopyranoside, has been prepared and investigated by (Hori & Ikegami, 1959). The clearing phase transition temperatures are given in **Table 4.38**. Again the data confirms our suggestion regarding the similar behaviour of the epimeric/anomeric trans-pair and higher clearing temperatures of the corresponding cis-pair.

4.2.2.3 Outlook

The present work aims to demonstrate a possible epimeric-anomeric relationship in pyranoside lipids, namely α-gluco/β-galactoside and α-galacto/β-glucoside. Both single and double chain glycolipids were investigated to confirm the hypothesis; thus the behaviour applies to lamellar as well as to columnar assemblies. However, due to the formation of a micellar phase in between these two assembly types, the correlation does not match for a limited chain range of branched glycosides, that is, the Guerbet C16 ($C_{10}C_6$). This may be because the micellar phase is not liquid crystalline with a definite structural arrangement, or it could simply be due to a purity issue of the samples (anomeric impurities as well as traces of water). Relative clearing temperatures of lamellar systems can be explained by intralayer hydrogen bonding, which is highly affected by the relative orientation of the 4-OH functional group and the anomerically bonded a glycon.

CHAPTER 5:CONCLUSIONS ANDOUTLOOK

5.1 Conclusions

The application of ^{2}H-NMR for the determination of bound water content is limited. Although consistent results applying different probes were obtained for AOT, which were in reasonable agreement to previously reported results (Hauser et al., 1989), the method failed for most of the investigated glycolipids, owing to the absence of an observable quadrupole splitting. Moreover, in other cases very high temperatures, exceeding the boiling point of water significantly, were required in order to obtain a quadrupole splitting. In view of the experienced failure rate, instrumental limitations, required NMR time (particularly due to extensive heating and cooling periods) and potential hazards based on the development of pressure, particularly in lower concentrated samples, the technique has proven ineffective for the bound water content determination of glycolipids.

Bound water content in glycolipids can be determined by DSC. Although bound water, as non-freezing water, should be accessible in both cooling and heating mode, only the latter provided reasonable results. The reason for the failure of the cooling mode may be kinetic constraints, leading to an incomplete freezing of non-bound water within the time constraints of a DSC scan. In order to achieve reliable results a longer exposure of the sample to a temperature of -60 ℃ is crucial prior to the melting scan. Despite this constraint the method is both easy to perform and economic, and, therefore, is recommended to future investigations of bound water contents.

Comparison of the results of the bound water content obtained from ^{2}H-NMR and DSC revealed reasonable consistence of the results. The DSC determined bound water content may, however, slightly exceed the one determined by NMR, but overall the difference can be considered minor.

The bound water content the investigated glycolipids is significantly lower than the number of hydroxyl groups on the surfactant molecules. This suggests that even at higher water content glycolipid bilayers exhibit significant hydrogen bonding between the sugar head-groups and, hence, contribute to the stability of the bilayer assembly. Alternatively, a multidentate binding of water involving more than one hydroxyl group is possible. However, assuming that multiple water binding at least partially involves two or more glycolipid molecules, this leads to water mediated inter-head-group hydrogen binding, which also contribute to the bilayer stability.

The stereochemistry at the inter glycosidic linkage has significant impact on the bond water content of glycolipids. The α-configurated maltosides exhibit significantly higher bound water contents than β-configurated cellobioside analogues. This finding, suggesting more hydrogen bonding between sugars inβ-(1,4)-linked glucosides compared to α-analogues, is in agreement with higher packing density and stronger intermolecular binding of cellulose-fibres compared to amylase.

The comparison of the behaviour of glucosides and galactosides revealed an anomeric/epimeric relation of compounds. This refers to the relative orientation of the hydroxyl group at C-4. While the latter is facing out of the lamellar assembly for the β-glucoside and the α-galactoside, the corresponding hydroxyl groups in the α-glucoside and the β-galactoside are directed into the bilayer. This difference significantly affects

the molecular assembly stability of the lamellar phase, reflected in the clearing temperature of the lamellar liquid crystalline phase.

5.2 Outlook

An extension of the DSC-based bound water content investigations, probably linked to computational studies, is suggested to investigate remaining effects of structural diversity of glycolipids on the bilayer stability. While the stereochemical effect of the inter glycosidic linkage for 1,4-linked glucosides has been investigated, similar investigations for alternative 1,6-linked disaccharides remain to be investigated. In view of the remarkable effect of the direction of the 4-OH group in glucose and galactose a comparison of cellobiosides and lactosides is highly recommended. Finally, the current investigations have focussed exclusively on lamellar bulk phases. In view of the curvature of vesicles, the results for a lamellar bulk phase and a vesicle is expected to differ. While ^{2}H-NMR cannot investigate vesicles owing to the absence of a macroscopic liquid crystalline phase, micro-DSC might enable the investigation of vesicles as well. This way, even the effect of the size of a vesicle on its stability may be investigated.

APPENDIX A: DSC SPECTRA

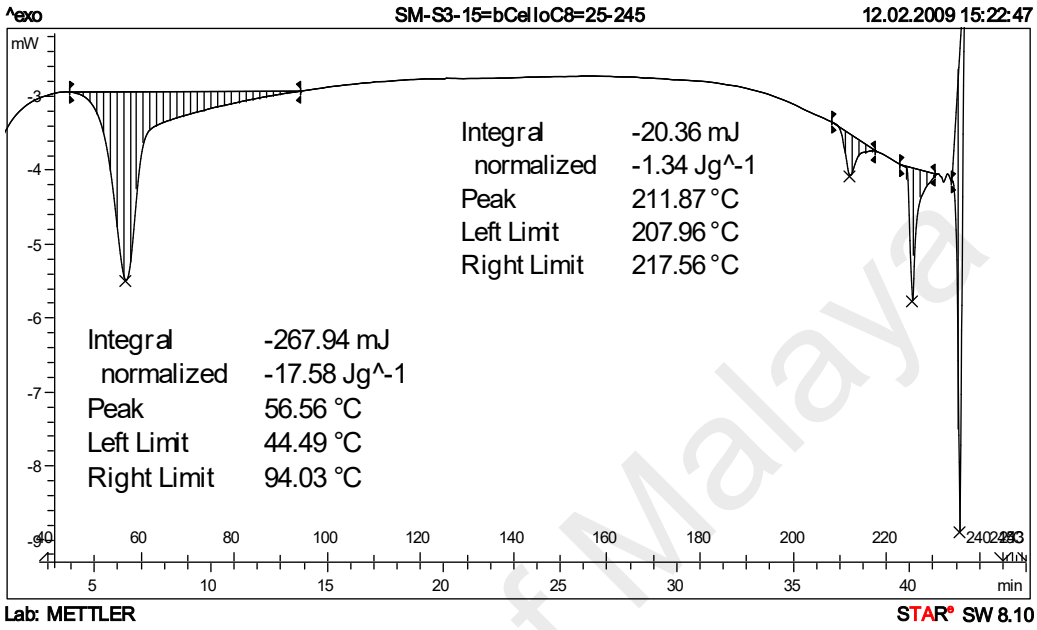

Figure 5-1 DSC scans for β-CelloC_8 at heating of 5 ℃/min.

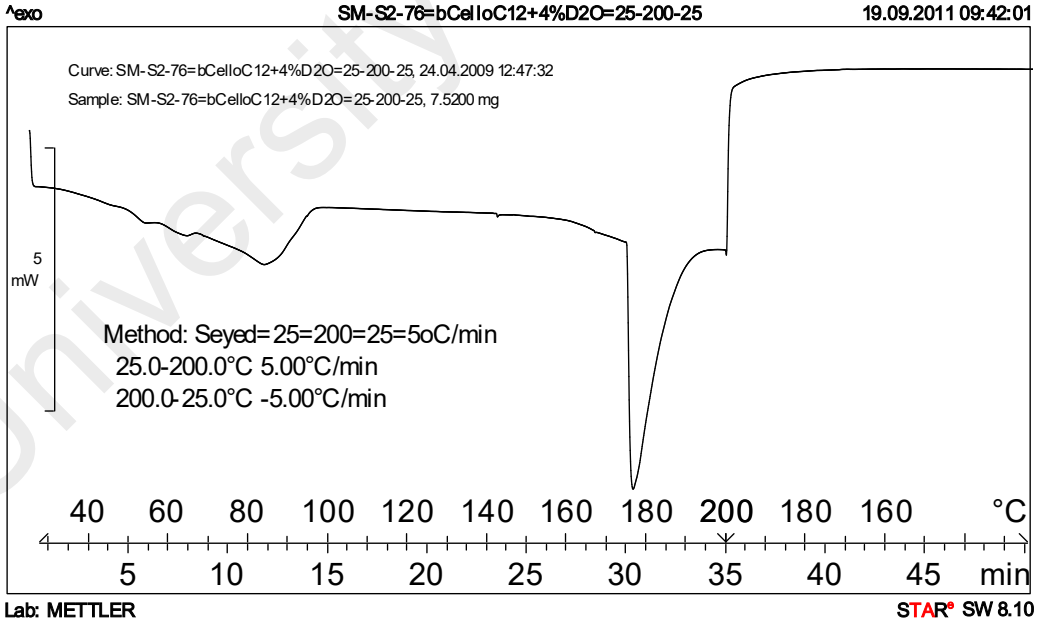

Figure 5-2 DSC scans for β-CelloC_{12} at heating of 5 ℃/min.

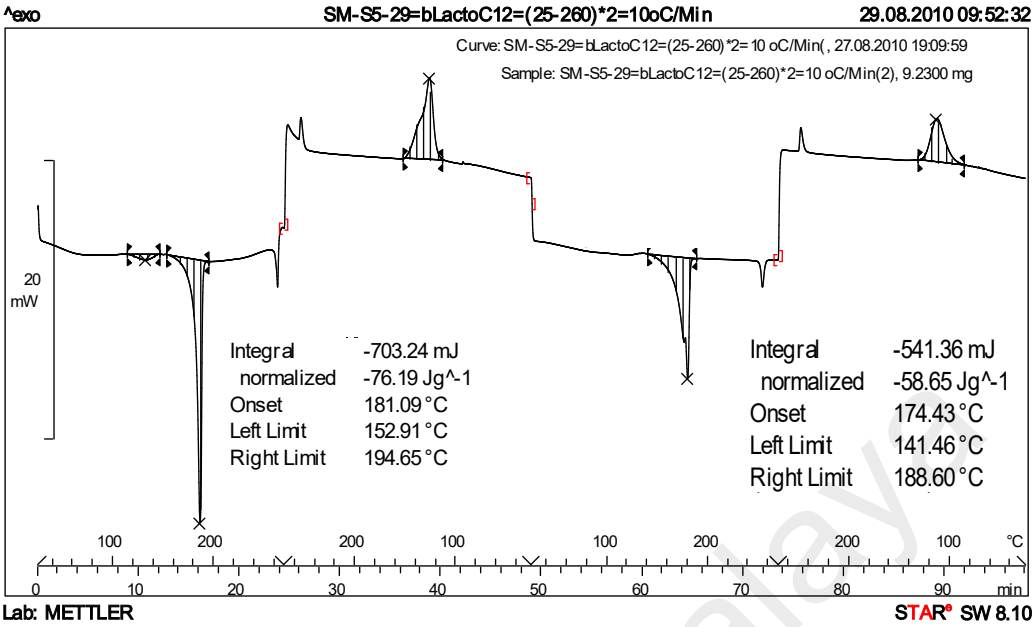

Figure 5-3 DSC scans for β-LactoC_{12} at heating of 10 °C/min.

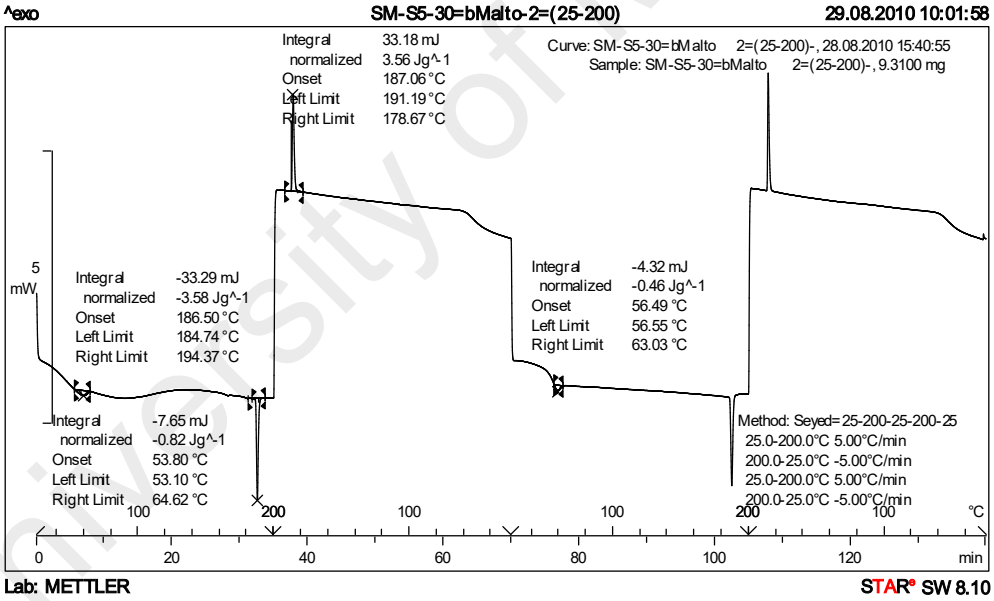

Figure 5-4 DSC scans for β-MaltoC_8C_4 at heating of 5 °C/min.

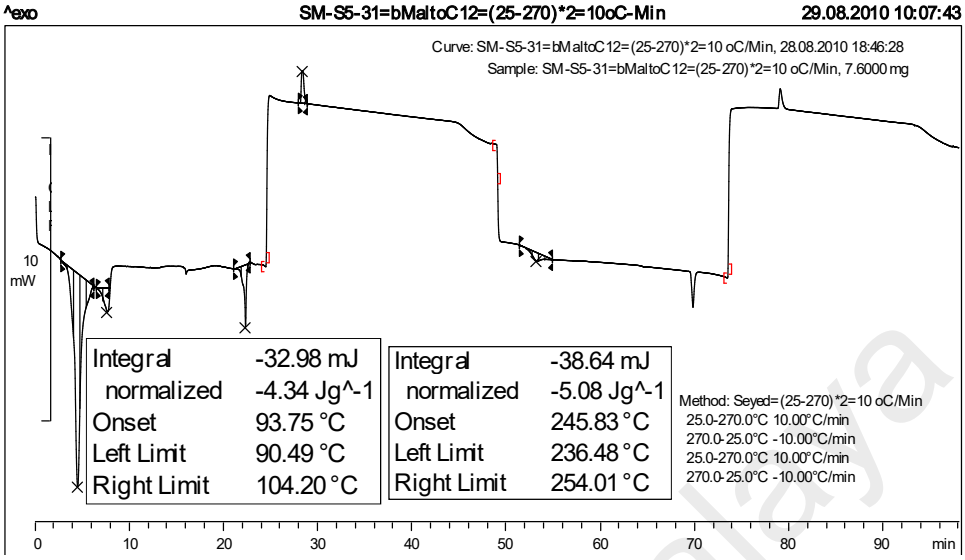

Figure 5-5 DSC scans for β-MaltoC_{12} at heating of 10 ℃/min.

APPENDIX B: OPM TEXTURES DRY/THERMOTROPIC

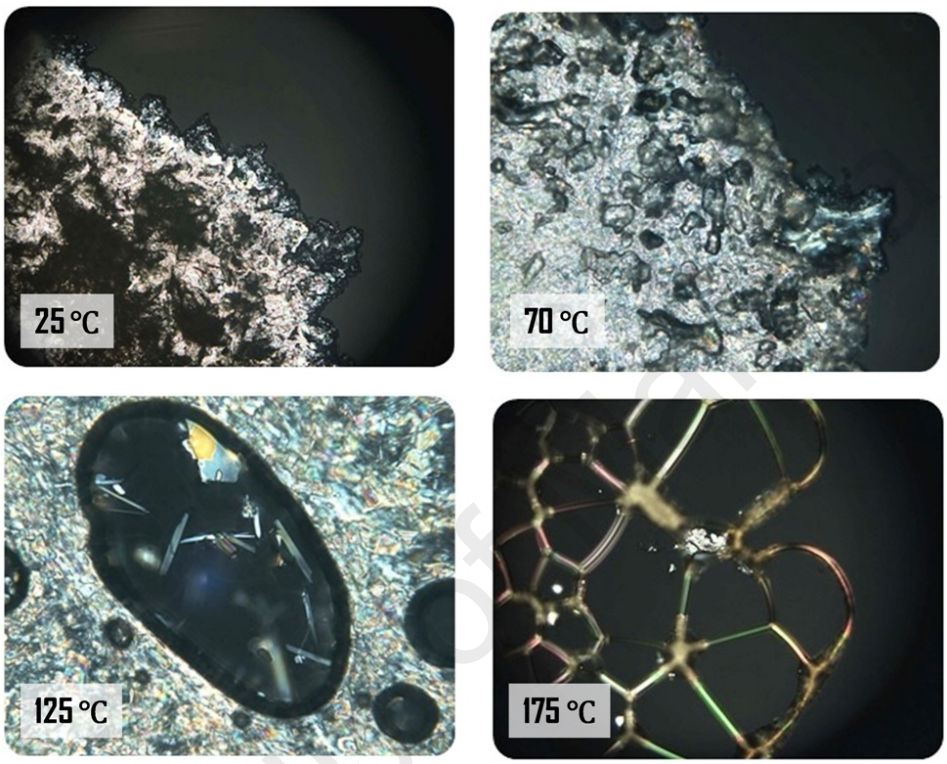

Figure 5.6 OPM textures dry/thermotropic sample of β-CelloC_8.

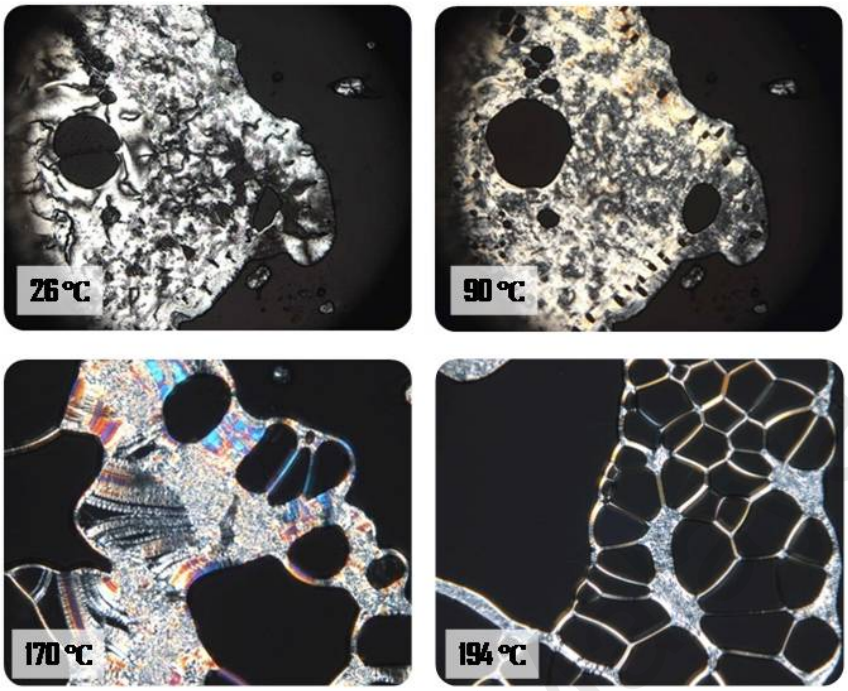

Figure 5.7 OPM textures dry/thermotropic sample of β-CelloC_{12}.

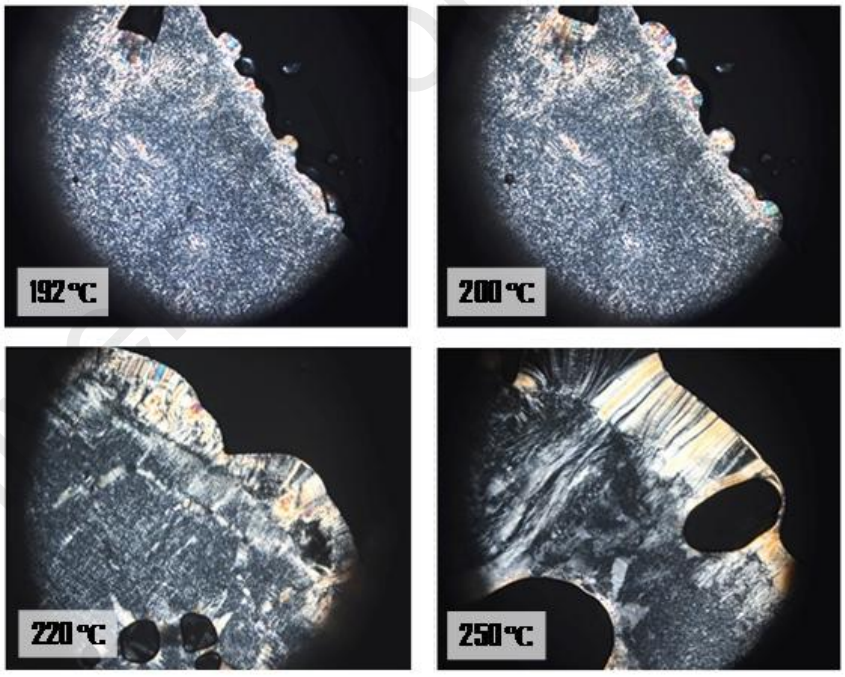

Figure 5.8 OPM textures dry/thermotropic sample of β-LactoC_{12}.

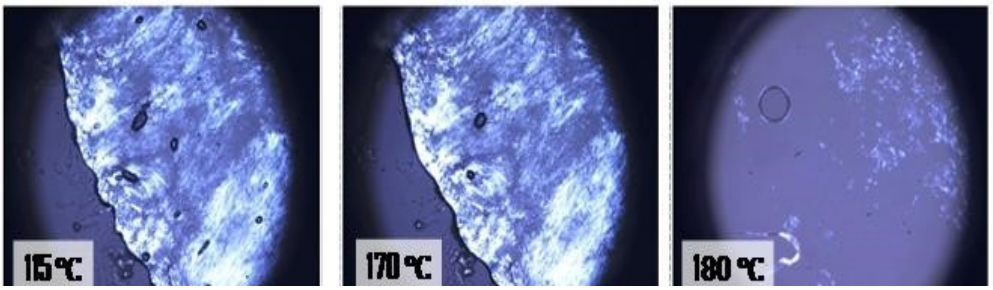

Figure 5.9 OPM textures dry/thermotropic sample of β-MaltoC_8C_4.

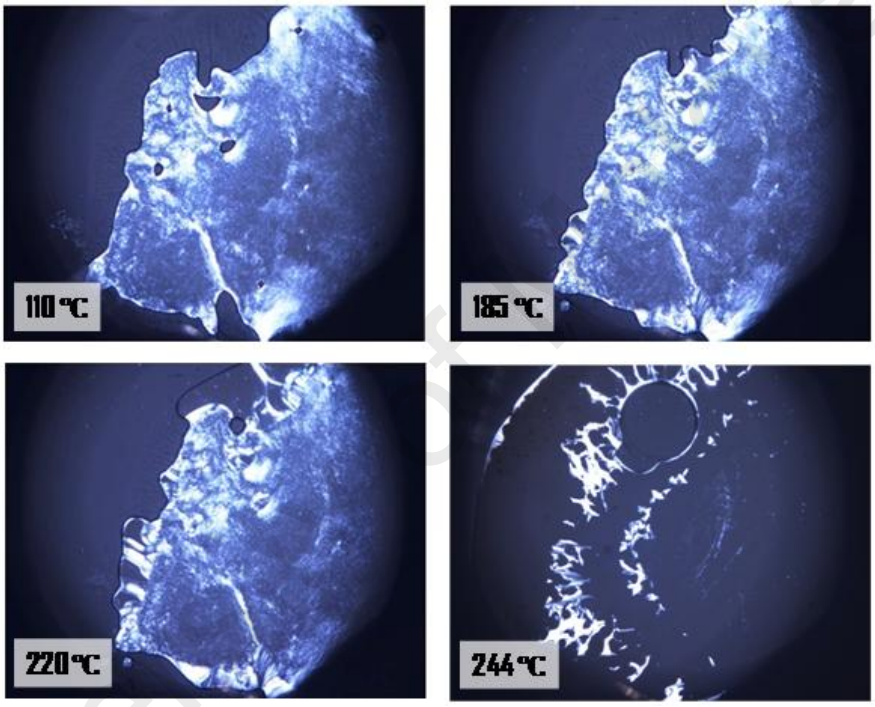

Figure 5.10 OPM textures dry/thermotropic sample of β-MaltoC_{12}.

APPENDIX C: OPM TEXTURES OF WATER PENETRATION

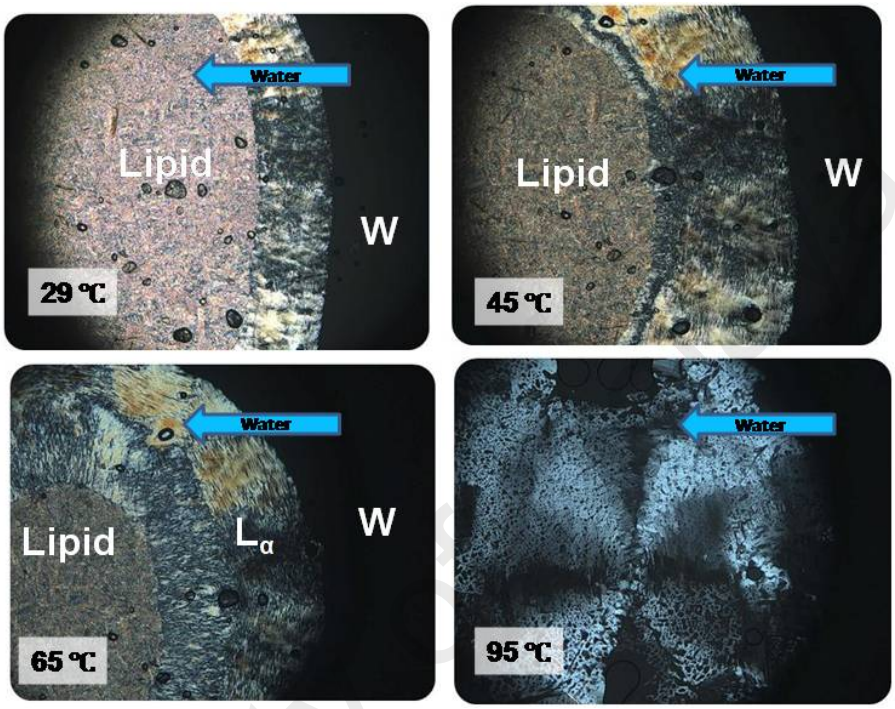

Figure 5.11 DSC scans for β-CelloC_8 at heating of 5 ℃/min.

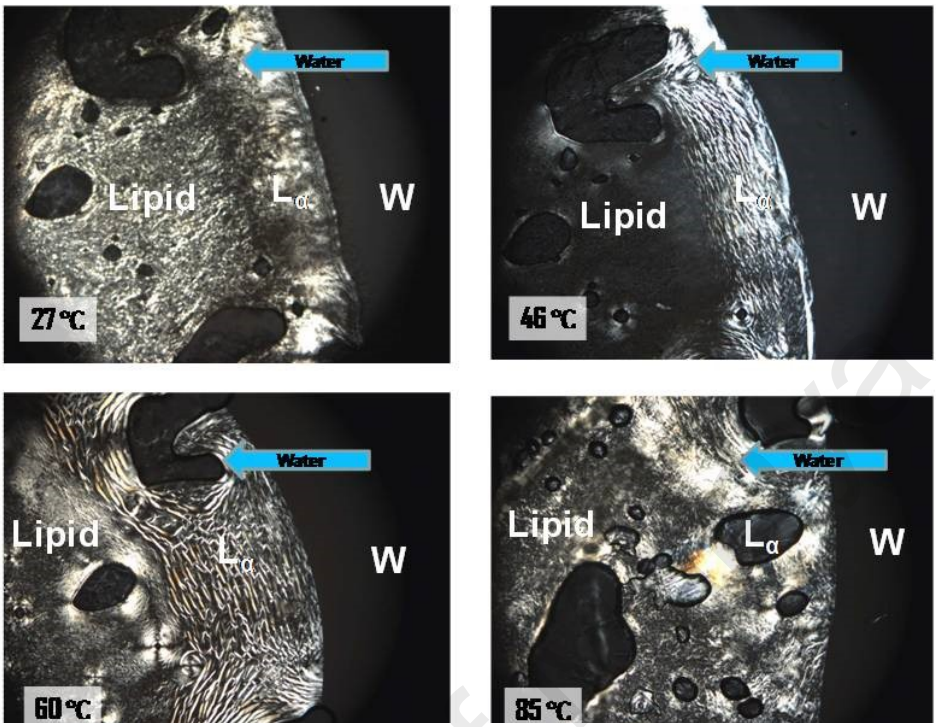

Figure 5.12 OPM textures of β-CelloC_{12} contact penetration with water.

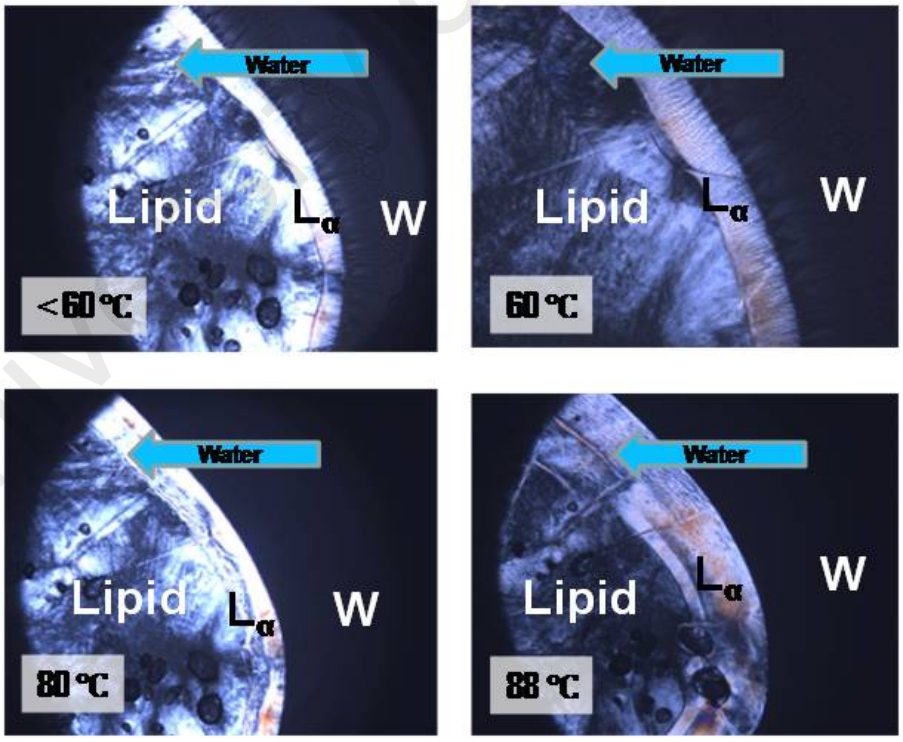

Figure 5.13 OPM textures of β-LactoC_{12} contact penetration with water.

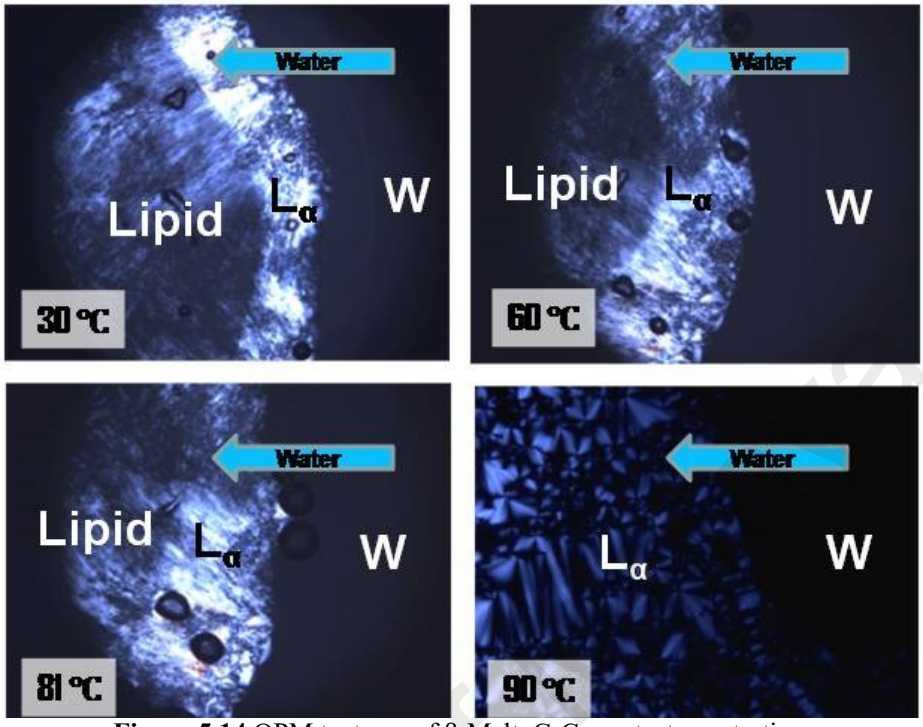

Figure 5.14 OPM textures of β-MaltoC_8C_4 contact penetration

REFERENCES

Achari, V. M., Nguan, H. S., Heidelberg, T., Bryce, R. A., & Hashim, R. (2012). Molecular Dynamics Study of Anhydrous Lamellar Structures of Synthetic Glycolipids: Effects of Chain Branching and Disaccharide Headgroup. *Journal of Physical Chemistry B, 116*(38), 11626-11634. doi: Doi 10.1021/Jp302292s

Ahmadi, S. (2014). *Modelling and Computer Simulation Studies of Sugar Based Amphiphilic Systems.* University of Malaya. Retrieved from http://studentsrepo.um.edu.my/4853/

Ahmadi, S., Achari, V. M., Nguan, H., & Hashim, R. (2014). Atomistic Simulation Studies of the A/B-Glucoside and Galactoside in Anhydrous Bilayers: Effect of the Anomeric and Epimeric Configurations. *Journal of Molecular Modeling, 20*(3), 1-12.

Al-Hamdani, U. J. (2011). Mesomorphic Properties of an Homologous Series of Thioalkyl-Terminated Azomesogens. *International Journal of Molecular Sciences, 12*(5), 3182-3190.

Alberts, B., Bray, D., Lewis, J., Raff, M., Roberts, K., & Watson, J. Molecular Biology of the Cell. 1994, New York and London: Garland Publishing, Inc.

Alkeskjold, T. T., Scolari, L., Noordegraaf, D., Lægsgaard, J., Weirich, J., Wei, L., Tartarini, G., Bassi, P., Gauza, S., & Wu, S.-T. (2007). Integrating Liquid Crystal Based Optical Devices in Photonic Crystal Fibers. *Optical and Quantum Electronics, 39*(12-13), 1009-1019.

Allen, H. J., & Kisailus, E. C. (1992). *Glycoconjugates: Composition: Structure, and Function*: CRC Press.

Andersen, O. S., & Koeppe, R. E., II. (2007). Bilayer Thickness and Membrane Protein Function: An Energetic Perspective *Annual Review of Biophysics and Biomolecular Structure* (Vol. 36, pp. 107-130).

Andronikashvili, E., Mrevlishvili, G., Sokhadze, V., & Kvavadze, K. (1976). Thermal Properties of Collagen in Helical and Random Coiled States in the Temperature Range from 4° to 300° K. *Biopolymers, 15*(10), 1991-2004.

Auvray, X., Petipas, C., Anthore, R., Ricolattes, I., & Lattes, A. (1995). X-Ray-Diffraction Study of the Ordered Lyotropic Phases Formed by Sugar-Based Surfactants. *Langmuir, 11*(2), 433-439. doi: 10.1021/la00002a012

Auvray, X., Petipas, C., Dupuy, C., Louvet, S., Anthore, R., Rico-Lattes, I., & Lattes, A. (2001). Small-Angle X-Ray Diffraction Study of the Thermotropic and Lyotropic Phases of Five Alkyl Cyclic and Acyclic Disaccharides: Influence of the Linkage between the Hydrophilic and Hydrophobic Moieties. *The European Physical Journal E, 4*(4), 489-504.

Barón, M. (2001). Definitions of Basic Terms Relating to Low-Molar-Mass and Polymer Liquid Crystals (Iupac Recommendations 2001). *Pure and Applied Chemistry, 73*(5), 845-895.

Baus, M., & Colot, J.-L. (1989). Ferroelectric Nematic Liquid-Crystal Phases of Dipolar Hard Ellipsoids. *Physical Review A, 40*(9), 5444.

Bertozzi, C. R., & Rabuka, D. (2009). Structural Basis of Glycan Diversity.

Blackmore, E. S., & Tiddy, G. J. T. (1990). Optical Microscopy, Multinuclear Nmr (H-2,N-14, and Cl-35) and X-Ray Studies of Dodecyl-Trimethylammonium and Hexadecyl-Trimethylammonium Chloride Water Mesophases. *Liquid Crystals, 8*(1), 131-151.

Bonicelli, M. G., Ceccaroni, G. F., & La Mesa, C. (1998). Lyotropic and Thermotropic Behaviour of Alkylglucosides and Related Compounds. *Colloid and Polymer Science, 276*(2), 109-116.

Brooks, N. J., Hamid, H. A., Hashim, R., Heidelberg, T., Seddon, J. M., Conn, C. E., Mirzadeh Hosseini, S. M., Zahid, N. I., & Hussen, R. S. D. (2011). Thermotropic and Lyotropic Liquid Crystalline Phases of Guerbet Branched-Chain-D-Glucosides. *Liquid Crystals, 38*(11-12), 1725-1734.

Brown, G. (2012). *Liquid Crystals and Biological Structures*: Elsevier.

Burgoyne, J., Holmes, M. C., & Tiddy, G. J. (1995). An Extensive Mesh Phase Liquid Crystal in Aqueous Mixtures of a Long Chain Nonionic Surfactant. *The Journal of Physical Chemistry, 99*(16), 6054-6063.

Burnell, E., & de Lange, C. (2005). Nmr as a Tool in the Investigation of Fundamental Problems in Ordered Liquids. *Solid State Nuclear Magnetic Resonance, 28*(2), 73-90.

Cabuil, V., Schwarz, J., Contescu, C., & Putyera, K. (2004). Dekker Encyclopedia of Nanoscience and Nanotechnology: Taylor & Francis.

Carvell, M., Hall, D. G., Lyle, I. G., & Tiddy, G. J. (1986). Surfactant–Water Interactions in Lamellar Phases. An Equilibrium Binding Description of Interbilayer Forces. *Faraday discussions of the Chemical Society, 81*, 223-237.

Castellano, J. A. (2005). The Story of Liquid Crystal Displays and the Creation of an Industry. *World Scientific Publishing*.

Chandrasekhar, S. (1992). Liquid Crystals 2nd Ed.,(1992) (2nd ed.): Cambridge University Press.

Chapman, D., Williams, R. M., & Ladbrooke, B. D. (1967). Physical Studies of Phospholipids. Vi. Thermotropic and Lyotropic Mesomorphism of Some 1, 2-Diacyl-Phosphatidylcholines (Lecithins). *Chemistry and Physics of Lipids, 1*(5), 445-475.

Chen, R. H. (2011). *Liquid Crystal Displays: Fundamental Physics and Technology*: John Wiley & Sons.

Chong, T. T., Heidelberg, T., Hashim, R., & Gary, S. (2007). Computer Modelling and Simulation of Thermotropic and Lyotropic Alkyl Glycoside Bilayers. *Liquid Crystals, 34*(2), 267-281. doi: Doi 10.1080/02678290601130192

Curatolo, W. (1987a). Glycolipid Function. *Biochimica et biophysica acta, 906*(2), 137.

Curatolo, W. (1987). Glycolipid Function. *Biochimica et Biophysica Acta (BBA)-Reviews on Biomembranes, 906*(2), 137-160.

Curatolo, W. (1987b). The Physical-Properties of Glycolipids. *Biochimica et biophysica acta, 906*(2), 111-136. doi: 10.1016/0304-4157(87)90008-6

Date, R. W., Iglesias, E. F., Rowe, K. E., Elliott, J. M., & Bruce, D. W. (2003). Metallomesogens by Ligand Design. *Dalton Transactions*(10), 1914-1931.

Davey, R., Allen, K., Blagden, N., Cross, W., Lieberman, H., Quayle, M., Righini, S., Seton, L., & Tiddy, G. (2002). Crystal Engineering–Nucleation, the Key Step. *CrystEngComm, 4*(47), 257-264.

Demus, D., Goodby, J. W., Gray, G. W., Spiess, H. W., & Vill, V. (2011). *Handbook of Liquid Crystals, Low Molecular Weight Liquid Crystals I: Calamitic Liquid Crystals*: John Wiley & Sons.

Dierking, I. (2006). *Textures of Liquid Crystals*: John Wiley & Sons.

Dolgaleva, K., Wei, S. K., Lukishova, S. G., Chen, S. H., Schwertz, K., & Boyd, R. W. (2008). Enhanced Laser Performance of Cholesteric Liquid Crystals Doped with Oligofluorene Dye. *JOSA B, 25*(9), 1496-1504.

Domenici, V., Geppi, M., & Veracini, C. A. (2007). Nmr in Chiral and Achiral Smectic Phases: Structure, Orientational Order and Dynamics. *Progress in Nuclear Magnetic Resonance Spectroscopy, 50*(1), 1-50. doi: 10.1016/j.pnmrs.2006.10.001

Dorset, D. L., & Rosenbusch, J. P. (1981). Solid State Properties of Anomeric 1-O-N-Octyl-D-Glucopyranosides. *Chemistry and Physics of Lipids, 29*(4), 299-307.

Eggenhoffner, R. (1982). Landolt-Bornstein - Numerical Data and Functional-Relationships in Science and Technology, New Series, Group 3, Crystal and Solid-State Physics, Vol 7, Pt D2, Key Elements, B, Al, Ga, in, Tl, Be - Allmann,R, Pies,W, Weiss,A. *Scientia, 117*(9-12), 684-685.

Eggens, I., Fenderson, B., Toyokuni, T., Dean, B., Stroud, M., & Hakomori, S. (1989). Specific Interaction between Lex and Lex Determinants - a Possible Basis for Cell Recognition in Preimplantation Embryos and in Embryonal Carcinoma-Cells. *Journal of Biological Chemistry, 264*(16), 9476-9484.

Finer, E. G. (1973). Interpretation of Deuteron Magnetic Resonance Spectroscopic Studies of the Hydration of Macromolecules. *Journal of the Chemical Society, Faraday Transactions 2: Molecular and Chemical Physics, 69*, 1590-1600.

Froix, M. F., & Nelson, R. (1975). The Interaction of Water with Cellulose from Nuclear Magnetic Resonance Relaxation Times. *Macromolecules, 8*(6), 726-730.

Funari, S. S., Holmes, M. C., & Tiddy, G. J. (1994). Intermediate Lyotropic Liquid Crystal Phases in the C16eo6/Water System. *The Journal of Physical Chemistry, 98*(11), 3015-3023.

Garstecki, P., & Holyst, R. (2002). Scattering Patterns of Self-Assembled Cubic Phases. 1. The Model. *Langmuir, 18*(7), 2519-2528.

Garstecki, P., & Hołyst, R. (2001). Scattering Patterns of Self-Assembled Gyroid Cubic Phases in Amphiphilic Systems. *The Journal of chemical physics, 115*(2), 1095-1099.

Garti, N., Aserin, A., Tiunova, I., & Fanun, M. (2000). A Dsc Study of Water Behaviour in Water-in-Oil Microemulsions Stabilised by Sucrose Esters and

Butanol. *Colloids and Surfaces A: Physicochemical and Engineering Aspects, 170*(1), 1-18.

Gawrisch, K., Arnold, K., Gottwald, T., Klose, G., & Volke, F. (1978). 2d Nmr Studies of the Phosphate-Water Interaction in Dipalmitoylphosphatidylcholine-Water System. *Stud. Biophys, 74*, 13-14.

Giammona, G., Goffredi, F., Turco Liveri, V., & Vassallo, G. (1992). Water Structure in Water/Aot/< I> N</I>-Heptane Microemulsions by Ft-Ir Spectroscopy. *Journal of Colloid and Interface Science, 154*(2), 411-415.

Goodby, J. (1984). Liquid Crystal Phases Exhibited by Some Monosaccharides. *Molecular Crystals and Liquid Crystals, 110*(1-4), 205-219.

Grossmann, G., Opekarova, M., Malinsky, J., Weig-Meckl, I., & Tanner, W. (2007). Membrane Potential Governs Lateral Segregation of Plasma Membrane Proteins and Lipids in Yeast. *The EMBO journal, 26*(1), 1-8.

Hairul Amani, A. H. (2010). Transfer Thesis. *Imperial College London*.

Halle, B., & Wennerstrom, H. (1981). Interpretation of Magnetic-Resonance Data from Water Nuclei in Heterogeneous Systems. *Journal of Chemical Physics, 75*(4), 1928-1943.

Halls, J. E., Bourne, R. W., Wright, K. J., Partington, L. I., Tamba, M. G., Zhou, Y., Ramakrishnappa, T., Mehl, G. H., Kelly, S. M., & Wadhawan, J. D. (2012). Electrochemistry of Organometallic Lyotropic Chromonic Liquid Crystals. *Electrochemistry Communications, 19*, 50-54. doi: 10.1016/j.elecom.2012.02.032

Hamasuna, D., Luckhurst, G. R., Sugimura, A., Timimi, B. A., Usami, K., & Zimmermann, H. (2008). Deuterium Nmr Spectra of a Monodomain Nematic: Angular Dependence of the Linewidths. *Thin Solid Films, 517*(4), 1394-1401. doi: 10.1016/j.tsf.2008.09.053

Hamasuna, D., Luckhurst, G. R., Sugimura, A., Timimi, B. A., & Zimmermann, H. (2011). Director Alignment by Crossed Electric and Magnetic Fields: A Deuterium Nmr Study. *Physical Review E, 84*(1). doi: 10.1103/PhysRevE.84.011705

Hashim, H. H. A. (2004). *Syntyesis and Liquid Crystal Phase Behaviour of Branched Chain Alkylglycosides.*

Hashim, R., Hashim, H. H. A., Rodzi, N. Z. M., Hussen, R. S. D., & Heidelberg, T. (2006). Branched Chain Glycosides: Enhanced Diversity for Phase Behaviour of Easily Accessible Synthetic Glycolipids. *Thin Solid Films, 509*(1), 27-35.

Hashim, R., Hashim, H. H. A., Rodzi, N. Z. M., Hussen, R. S. D., & Heidelberg, T. (2006). Branched Chain Glycosides: Enhanced Diversity for Phase Behaviour of Easily Accessible Synthetic Glycolipids. *Thin Solid Films, 509*(1-2), 27-35. doi: 10.1016/j.tsf.2005.09.009

Hashim, R., Mirzadeh, S. M., Heidelberg, T., Minamikawa, H., Yoshiaki, T., & Sugimura, A. (2011). A Reevaluation of the Epimeric and Anomeric Relationship of Glucosides and Galactosides in Thermotropic Liquid Crystal Self-Assemblies. *Carbohydrate Research, 346*(18), 2948-2956.

Hatakeyama, H., Nakamura, K., & Hatakeyama, T. (1980). Studies on Factors Affecting the Molecular Motion of Lignin and Lignin-Related Polystyrene Derivatives. *Trans Pulp Pap Canada, 81*, 105-110.

Hatakeyama, T., Nakamura, K., & Hatakeyama, H. (1988). Determination of Bound Water-Content in Polymers by Dta, Dsc and Tg. *Thermochimica Acta, 123*, 153-161. doi: 10.1016/0040-6031(88)80018-2

Hauser, H., Haering, G., Pande, A., & Luisi, P. L. (1989). Interaction of Water with Sodium Bis (2-Ethyl-1-Hexyl) Sulfosuccinate in Reversed Micelles. *The Journal of Physical Chemistry, 93*(23), 7869-7876.

Ho, C., Slater, S. J., & Stubbs, C. D. (1995). Hydration and Order in Lipid Bilayers. *Biochemistry, 34*(18), 6188-6195. doi: 10.1021/bi00018a023

Holte, L. L., & Gawrisch, K. (1996). Influence of Lipid Hydration on Hydrocarbon Chain Order - a H-2 Nmr Study. *Biophysical journal, 70*(2), WP228-WP228.

Hori, R., & Ikegami, Y. (1959). *Yakugaku Zasshi (J. Pharm. Soc. Japan)*, 79, 80.

Hsieh, C.-H., & Wu, W.-g. (1995). Three Distinct Types of Unfrozen Water in Fully Hydrated Phospholipid Bilayers: A Combined 2 H-and 31 P-Nmr Study. *Chemistry and Physics of Lipids, 78*(1), 37-45.

Ishizuka, I., & Yamakawa, T. (1985). Glycoglycerolipids. *New Comprehensive Biochemistry, 10*, 101-197.

Israelachvili, J. (1991). Intermolecular and Surface Forces 2nd Edn (London: Academic).

Ito, T., Shirakawa, H., & Ikeda, S. (1974). Simultaneous Polymerization and Formation of Polyacetylene Film on the Surface of Concentrated Soluble Ziegler-Type Catalyst Solution. *Journal of polymer science: polymer chemistry edition, 12*(1), 11-20.

Jákli, A., & Saupe, A. (2006). *One-and Two-Dimensional Fluids: Properties of Smectic, Lamellar and Columnar Liquid Crystals*: CRC Press.

Jeffrey, G. A. (1986). Carbohydrate Liquid Crystals. *Accounts of Chemical Research, 19*(6), 168-173.

Jeffrey, G. A. (1990). Crystallographic Studies of Carbohydrates. *Acta Crystallographica Section B: Structural Science, 46*(2), 89-103.

Jeffrey, G. A., & Bhattacharjee, S. (1983). Carbohydrate Liquid-Crystals. *Carbohydrate Research, 115*, 53-58.

Kaasgaard, T., & Drummond, C. J. (2006). Ordered 2-D and 3-D Nanostructured Amphiphile Self-Assembly Materials Stable in Excess Solvent. *Physical Chemistry Chemical Physics, 8*(43), 4957-4975.

Kates, M. (1990). *Glycolipids, Phosphoglycolipids, and Sulfoglycolipids*: Plenum Press.

Kerch, G., Glonin, A., Zicans, J., & Meri, R. M. (2012a). A Dsc Study of the Effect of Ascorbic Acid on Bound Water Content and Distribution in Chitosan-Enriched Bread Rolls During Storage. *Journal of Thermal Analysis and Calorimetry, 108*(1), 73-78. doi: 10.1007/s10973-011-1485-x

Kerch, G., Glonin, A., Zicans, J., & Meri, R. M. (2012b). A Dsc Study of the Effect of Bread Making Methods on Bound Water Content and Redistribution in Chitosan Enriched Bread. *Journal of Thermal Analysis and Calorimetry, 108*(1), 185-189. doi: 10.1007/s10973-011-2029-0

Kikuchi, Y., Toi, H., & Aoyama, Y. (1993). Complexation of Alkyl Glycosides with Cyclic Resorcinol Tetramer in Apolar Organic Media: Geometrical Requirement for the Intracomplex Sugar-Sugar Interactioin. *Bulletin of the Chemical Society of Japan, 66*(6), 1856-1858.

Kodama, M., Abe, M., Kawasaki, Y., Hayashi, K., Ohira, S., Nozaki, H., Katagiri, C., Inoue, K., & Takahashi, H. (2004). Estimation of Interlamellar Water Molecules in Sphingomyelin Bilayer Systems Studied by Dsc and X-Ray Diffraction. *Thermochimica Acta, 416*(1-2), 105-111. doi: 10.1016/j.tca.2003.01.003

Koeltzow, D. E., & Urfer, A. D. (1984). Preparation and Properties of Pure Alkyl Glucosides, Maltosides and Maltotriosides. *Journal of the American Oil Chemists Society, 61*(10), 1651-1655. doi: 10.1007/bf02541651

Koenigs, W., & Knorr, E. (1901). Ueber Einige Derivate Des Traubenzuckers Und Der Galactose. *Berichte der deutschen chemischen Gesellschaft, 34*(1), 957-981.

Konig, S., Sackmann, E., Richter, D., Zorn, R., Carlile, C., & Bayerl, T. M. (1994). Molecular-Dynamics Ct Water in Oriented Dppc Multilayers Studied by Quasi-Elastic Neutron-Scattering and Deuterium-Nuclear Magnetic-Resonance Relaxation. *Journal of Chemical Physics, 100*(4), 3307-3316.

Kopp, V., Fan, B., Vithana, H., & Genack, A. (1998). Low-Threshold Lasing at the Edge of a Photonic Stop Band in Cholesteric Liquid Crystals. *Optics letters, 23*(21), 1707-1709.

Koynova, R., & Tenchov, B. (2013). Transitions between Lamellar and Non-Lamellar Phases in Membrane Lipids and Their Physiological Roles. *OA Biochemistry, 1*, 1-9.

Kuhnau, U., Madler, B., Wurlitzer, S., Rapp, G., & Schmiedel, H. (1997). Incorporation of Thermotropic Liquid Crystals in Phospholipid Monolayers: Necessary Condition of Homeotropic Anchoring. *Molecular Crystals and Liquid Crystals Science and Technology Section a-Molecular Crystals and Liquid Crystals, 304*, 171-178. doi: 10.1080/10587259708046958

Kulkarni, C. V. (2011). Nanostructural Studies on Monoelaidin–Water Systems at Low Temperatures. *Langmuir, 27*(19), 11790-11800.

Kumar, S. (2001). *Liquid Crystals: Experimental Study of Physical Properties and Phase Transitions*: Cambridge University Press.

Kwong, W. L., Gan, W. C., Majid, W. H. A., Hashim, R., & Heidelberg, T. (2010). Pyroelectric Detection in Glycolipid Thin Film. *Thin Solid Films, 518*(15), 4412-4416. doi: DOI 10.1016/j.tsf.2010.01.022

Lang, S. (2002). Biological Amphiphiles (Microbial Biosurfactants). *Current Opinion in Colloid & Interface Science, 7*(1), 12-20.

Lasic, D. D. (1993). *Liposomes: From Physics to Applications*: Elsevier Science Ltd.

Laughlin, R. G. (1992). The Role of Swelling Methods in Surfactant Phase Science: Past, Present, and Future. *Advances in Colloid and Interface Science, 41*, 57-79.

Lee, D.-J., Su, A., & Mujumdar, A. S. (2013). Bound Water Content in Wet Materials. *Drying Technology, 31*(2), 202-206. doi: 10.1080/07373937.2012.694946

Lemons, B. G., Richens, D. T., Anderson, A., Sedgwick, M., Crans, D. C., & Johnson, M. D. (2013). Stabilization of a Vanadium (V)–Catechol Complex by Compartmentalization and Reduced Solvation inside Reverse Micelles. *New Journal of Chemistry, 37*(1), 75-81.

Lewis, B. A., & Engelman, D. M. (1983). Lipid Bilayer Thickness Varies Linearly with Acyl Chain-Length in Fluid Phosphatidylcholine Vesicles. *Journal of Molecular Biology, 166*(2), 211-217. doi: 10.1016/s0022-2836(83)80007-2

Liang, Q., Liu, P., Liu, C., Jian, X., Hong, D., & Li, Y. (2005). Synthesis and Properties of Lyotropic Liquid Crystalline Copolyamides Containing Phthalazinone Moiety and Ether Linkages. *Polymer, 46*(16), 6258-6265.

Lide, D. R. (2004). *Crc Handbook of Chemistry and Physics*: CRC press.

Lindhorst, T. K. (2000). *Essentials of Carbohydrate Chemistry and Biochemistry*: Wiley-VCH Weinheim, Germany.

Lockhoff, O. (1991). Glycolipids as Immunomodulators - Syntheses and Properties. *Angewandte Chemie-International Edition in English, 30*(12), 1611-1620. doi: 10.1002/anie.199116111

Loewenstein, A., & Igner, D. (1993). Deuterium Nmr-Studies of N-Octyl-D-Glucopyranoside, N-Nonyl-D-Glucopyranoside, N-Decyl-D-Glucopyranoside Liquid-Crystalline Systems. *Liquid Crystals, 13*(4), 531-539.

Luckhurst, G. R. (1988). Pretransitional Behaviour in Liquid-Crystals - the Roles of Nuclear Magnetic-Resonance Spectroscopy and Molecular-Field Theory. *Journal of the Chemical Society-Faraday Transactions Ii, 84*, 961-986. doi: 10.1039/f29888400961

Luckhurst, G. R., Miyamoto, T., Sugimura, A., Takashiro, T., & Timimi, B. A. (2001). The Surface-Induced Static Director Distribution in Thin Nematic Liquid Crystal Films: A Deuterium Nuclear Magnetic Resonance Spectroscopy Study. *Journal of Chemical Physics, 114*(23), 10493-10503.

Luckhurst, G. R., Miyamoto, T., Sugimura, A., & Timimi, B. A. (2002). Field-Induced Director Dynamics in a Nematic Liquid Crystal: A Molecular Site Dependence? *Journal of Chemical Physics, 116*(12), 5099-5106. doi: 10.1063/1.1452106

Luzzati, V., Mustacchi, H., & Skoulios, A. (1957). Structure of the Liquid-Crystal Phases of the Soap-Water System: Middle Soap and Neat Soap. *Nature*(180), 600-601.

Magne, F. C., Portas, H., & Wakeham, H. (1947). A Calorimetric Investigation of Moisture in Textile Fibers1a. *Journal of the American Chemical Society, 69*(8), 1896-1902.

Magne, F. C., & Skau, E. L. (1952). Nonfreezing Water and Nonfreezing Benzene Capacities of Cottons and Modified Cottons. *Textile Research Journal, 22*(11), 748-756.

Manickam Achari, V., Nguan, H. S., Heidelberg, T., Bryce, R. A., & Hashim, R. (2011 (unpublished)). *Molecular Dynamic Study Lyotropic Lamellar Phases of Straight and Branched Chin Alkyl Maltosides*

Manickam Achari, V., Nguan, H. S., Heidelberg, T., Bryce, R. A., & Hashim, R. (2012). Molecular Dynamics Study of Anhydrous Lamellar Structures of Synthetic Glycolipids: Effects of Chain Branching and Disaccharide Headgroup. *The Journal of Physical Chemistry B, 116*(38), 11626-11634.

ManickamAchari, V., Bryce, R. A., & Hashim, R. (2014). Conformational Dynamics of Dry Lamellar Crystals of Sugar Based Lipids: An Atomistic Simulation Study.

Marsh, D. (2001). Polarity and Permeation Profiles in Lipid Membranes. *Proceedings of the National Academy of Sciences of the United States of America, 98*(14), 7777-7782. doi: 10.1073/pnas.131023798

Marsh, D. (2002). Membrane Water-Penetration Profiles from Spin Labels. *European Biophysics Journal with Biophysics Letters, 31*(7), 559-562. doi: 10.1007/s00249-002-0245-z

Martin, J. D., Keary, C. L., Thornton, T. A., Novotnak, M. P., Knutson, J. W., & Folmer, J. C. W. (2006). Metallotropic Liquid Crystals Formed by Surfactant Templating of Molten Metal Halides. *Nature Materials, 5*(4), 271-275. doi: 10.1038/nmat1610

Mashaghi, A., Partovi-Azar, P., Jadidi, T., Nafari, N., Maass, P., Tabar, M. R. R., Bonn, M., & Bakker, H. J. (2012). Hydration Strongly Affects the Molecular and Electronic Structure of Membrane Phospholipids. *Journal of Chemical Physics, 136*(11). doi: 10.1063/1.3694280

Matsumoto, Y., Fujino, N., & Nasu, S. (1986). The Influence of Bound Water and Fe(Ii) on the Determination of T.Fe Content in X-Ray-Fluorescence Analysis of Iron-

Ore. *Tetsu to Hagane-Journal of the Iron and Steel Institute of Japan, 72*(9), 1271-1278.

Matsunaga, D., Tamaki, T., & Ichimura, K. (2003). Azo-Pendant Polyamides Which Have the Potential to Photoalign Chromonic Lyotropic Liquid Crystals. *Journal of Materials Chemistry, 13*(7), 1558-1564. doi: 10.1039/b300254c

McNaught, A. D. (1996). Nomenclature of Carbohydrates (Iupac Recommendations 1996). *Pure and Applied Chemistry, 68*(10), 1919-2008.

Meier, M., & Seelig, J. (2010). Lipid and Peptide Dynamics in Membranes Upon Insertion of N-Alkyl-B-D-Glucopyranosides. *Biophysical journal, 98*(8), 1529-1538.

Memmer, R. (2001). Determination of Equilibrium Pitch of Cholesteric Phases by Isobaric–Isothermal Monte Carlo Simulation. *The Journal of chemical physics, 114*(18), 8210-8222.

Memmer, R. (2002). Liquid Crystal Phases of Achiral Banana-Shaped Molecules: A Computer Simulation Study. *Liquid Crystals, 29*(4), 483-496.

Michael, T. M., John, M. M., & Jack, P. (2003). Brock Biology of Microorganisms. *International Edition*.

Michel, J., Tirado-Rives, J., & Jorgensen, W. L. (2009). Prediction of the Water Content in Protein Binding Sites. *Journal of Physical Chemistry B, 113*(40), 13337-13346. doi: 10.1021/jp9047456

Mirzadeh Hosseini, S., Hashim, R., Heidelberg, T., & Timimi, B. A. (2012). Bound Water Investigations on Disaccharide Based Glycolipids *Nanoformulation* (pp. 205-211): The Royal Society of Chemistry.

Misran, O., Timimi, B. A., Heidelberg, T., Sugimura, A., & Hashim, R. (2013). Deuterium Nmr Investigation of the Lyotropic Phases of Alkyl Beta-Glycoside/D2o Systems. *Journal of Physical Chemistry B, 117*(24), 7335-7344. doi: 10.1021/jp401787b

Morley, W. G., & Tiddy, G. J. T. (1993). Phase-Behaviour of Monoglyceride Water-Systems. *Journal of the Chemical Society-Faraday Transactions, 89*(15), 2823-2831. doi: 10.1039/ft9938902823

Nagarajan, R. (2002). Molecular Packing Parameter and Surfactant Self-Assembly: The Neglected Role of the Surfactant Tail. *Langmuir, 18*(1), 31-38.

Nagle, J. F., & Tristram-Nagle, S. (2000). Structure of Lipid Bilayers. *Biochimica Et Biophysica Acta-Reviews on Biomembranes, 1469*(3), 159-195. doi: 10.1016/s0304-4157(00)00016-2

Nakamura, K., Hatakeyama, T., & Hatakeyama, H. (1981). Studies on Bound Water of Cellulose by Differential Scanning Calorimetry. *Textile Research Journal, 51*(9), 607-613.

Nees, D., & Wolff, T. (1996). Interactions of Aot Lyotropic Liquid Crystals and Photochemical Reactions of Hydroxystilbazolium Bromides: Steering Reactions and Switching Phases. *Langmuir, 12*(20), 4960-4965. doi: 10.1021/la960406i

Neto, A. M. F., & Salinas, S. R. (2005). *The Physics of Lyotropic Liquid Crystals: Phase Transitions and Structural Properties* (Vol. 62): OUP Oxford.

Nguan, H. S., Heidelberg, T., Hashim, R., & Tiddy, G. J. T. (2010). Quantitative Analysis of the Packing of Alkyl Glycosides: A Comparison of Linear and Branched Alkyl Chains. *Liquid Crystals, 37*(9), 1205-1213. doi: Doi 10.1080/02678292.2010.492245

Nilsson, F., Söderman, O., & Johansson, I. (1998). Four Different C 8 G 1 Alkylglucosides. Anomeric Effects and the Influence of Straight Vs Branched Hydrocarbon Chains. *Journal of Colloid and Interface Science, 203*(1), 131-139.

Nomura, S., Hiltner, A., Lando, J., & Baer, E. (1977). Interaction of Water with Native Collagen. *Biopolymers, 16*(2), 231-246.

Onori, G., & Santucci, A. (1993). Ir Investigations of Water Structure in Aerosol Ot Reverse Micellar Aggregates. *The Journal of Physical Chemistry, 97*(20), 5430-5434.

Plimpton, R. G. (1988). Pool Thermometer: Google Patents.

Pope, J., & Cornell, B. (1979). A Pulsed Nmr Study of Lipids, Bound Water and Sodium Ions in Macroscopically-Oriented Lecithin/Water Lyotropic Liquid Crystal Model Membrane Systems. *Chemistry and Physics of Lipids, 24*(1), 27-43.

Preston, J., & Tawde, G. (1956). 10—Freezing Point Depression in Assemblages of Moist Fibres. *Journal of the Textile Institute Transactions, 47*(3), T154-T165.

Prost, J. (1995). *The Physics of Liquid Crystals*: Oxford university press.

Ramamoorthy, A. (2007). *Thermotropic Liquid Crystals: Recent Advances*: Springer Science & Business Media.

Rawicz, W., Olbrich, K. C., McIntosh, T., Needham, D., & Evans, E. (2000). Effect of Chain Length and Unsaturation on Elasticity of Lipid Bilayers. *Biophysical journal, 79*(1), 328-339.

Raynes, P. (1993). Liquid Crystals—Second Edition, by S Chandrasekhar, Cambridge University Press,(1992), Isbn 0-521-41747-3 (Hb), Isbn 0-521-42741-X (Pb).

Rendall, K., & Tiddy, G. J. T. (1984). Interaction of Water and Oxyethylene Groups in Lyotropic Liquid-Crystalline Phases of Poly(Oxyethylene) N-Dodecyl Ether Surfactants Studied by H-2 Nuclear Magnetic-Resonance Spectroscopy. *Journal of the Chemical Society-Faraday Transactions I, 80*, 3339-3357.

Rendall, K., Tiddy, G. J. T., & Trevethan, M. A. (1983). Optical Microscopy and Nuclear Magnetic-Resonance Studies of Mesophases Formed at Compositions between Hexagonal and Lamellar Phases in Sodium N-Alkanoate+Water Mixtures and Related Surfactant Systems. *Journal of the Chemical Society-Faraday Transactions I, 79*, 637-&.

Rodzi, N. (2006). *Branched Chain Galactosides and Melibiosides: Synthesis and Mesomorphic Properties.*

Rodzi, N. B. M. (2006 (M.Sc)). *Branched Chain Galactosides and Melibiosides: Synthesis and Mesomorphic Properties (M.S. Thesis).* (M.Sc.), University of Malaya, Kuala Lumpur.

Rosano, H. L., Nixon, A. L., & Cavallo, J. L. (1989). Interfacial Stoichiometry of a Microemulsion System. *The Journal of Physical Chemistry, 93*(11), 4536-4539.

Ruckenstein, E., & Nagarajan, R. (1975). Critical Micelle Concentration. Transition Point for Micellar Size Distribution. *The Journal of Physical Chemistry, 79*(24), 2622-2626.

Sakya, P., & Seddon, J. (1997). Thermotropic and Lyotropic Phase Behaviour of Monoalkyl Glycosides. *Liquid Crystals, 23*(3), 409-424.

Sakya, P., & Seddon, J. M. (1997). Thermotropic and Lyotropic Phase Behaviour of Monoalkyl Glycosides. *Liquid Crystals, 23*(3), 409-424. doi: 10.1080/026782997208334

Sandström, D., Stenutz, R., Widmalm, G., & Maliniak, A. (1996). Deuterium Nmr Study of a Probe Molecule Dissolved in a Carbohydrate Liquid Crystal. *Journal of the Chemical Society, Faraday Transactions, 92*(1), 111-115.

Sciortino, F., Geiger, A., & Stanley, H. E. (1992). Network Defects and Molecular Mobility in Liquid Water. *The Journal of chemical physics, 96*(5), 3857-3865.

Seddon, J., & Templer, R. (1995). Structure and Dynamics of Membranes. *Elsevier, Amsterdam*, 97-160.

Seddon, J. M. (1996). Lyotropic Phase Behaviour of Biological Amphiphiles. *Berichte Der Bunsen-Gesellschaft-Physical Chemistry Chemical Physics, 100*(3), 380-393.

Senatra, D., Guarini, G. G. T., Gabrielli, G., & Zoppi, M. (1984). Low Temperature Study of W/O Microemulsions by Differential Scanning Calorimetry and Dielectric Measurements. *Journal De Physique, 45*(7), 1159-1174.

Senatra, D., Lendinara, L., & Giri, M. (1991). W/O Microemulsions as Model Systems for the Study of Water Confined in Microenvironments: Low Resolution 1 H Magnetic Resonance Relaxation Analysis. *Trends in Colloid and Interface Science V*, 122-128.

Shinoda, K., Carlsson, A., & Lindman, B. (1996). On the Importance of Hydroxyl Groups in the Polar Head-Group of Nonionic Surfactants and Membrane Lipids. *Advances in Colloid and Interface Science, 64*, 253-271. doi: 10.1016/0001-8686(95)00287-1

Simionescu, C. I., Percec, V., & Dumitrescu, S. (1977). Polymerization of Acetylenic Derivatives. Xxx. Isomers of Polyphenylacetylene. *Journal of polymer science: polymer chemistry edition, 15*(10), 2497-2509.

Singh, S. (2000). Phase Transitions in Liquid Crystals. *Physics Reports, 324*(2), 107-269.

Singh, S., & Dunmur, D. A. (2002). *Liquid Crystals: Fundamentals*: World Scientific.

Sluckin, T. J., Dunmur, D. A., & Stegemeyer, H. (2004). Crystals That Flow. *Liquid Crystals Series Taylor & Francis: London*.

Sluckin, T. J., Dunmur, D. A., & Stegemeyer, H. (2004). *Crystals That Flow: Classic Papers from the History of Liquid Crystals*: Taylor & Francis London.

Smirnova, I., Suttiruengwong, S., & Arlt, W. (2004). Feasibility Study of Hydrophilic and Hydrophobic Silica Aerogels as Drug Delivery Systems. *Journal of Non-Crystalline Solids, 350*, 54-60.

Soderberg, I., Drummond, C. J., Furlong, D. N., Godkin, S., & Matthews, B. (1995). Nonionic Sugar-Based Surfactants - Self-Assembly and Air/Water Interfacial Activity. *Colloids and Surfaces a-Physicochemical and Engineering Aspects, 102*, 91-97. doi: 10.1016/0927-7757(95)03250-h

Squires, A. M., Templer, R., Seddon, J., Woenkhaus, J., Winter, R., Narayanan, T., & Finet, S. (2005). Kinetics and Mechanism of the Interconversion of Inverse Bicontinuous Cubic Mesophases. *Physical Review E, 72*(1), 011502.

Starkulla, G. F., Kapatsina, E., Baro, A., Giesselmann, F., Tussetschläger, S., Kaller, M., & Laschat, S. (2009). Influence of Spacer Chain Lengths and Polar Terminal Groups on the Mesomorphic Properties of Tethered 5-Phenylpyrimidines. *Beilstein journal of organic chemistry, 5*(1), 63.

Tantrawong, S. (2014). Liquid Crystals: Rediscovered Materials. *Materials Today, 17*(3), 147-148.

Tenchov, B. (1991). On the Reversibility of the Phase Transitions in Lipid-Water Systems. *Chemistry and Physics of Lipids, 57*(2), 165-177.

Tiddy, G. J. (1980). Surfactant-Water Liquid Crystal Phases. *Physics Reports, 57*(1), 1-46.

Träuble, H., & Haynes, D. H. (1971). The Volume Change in Lipid Bilayer Lamellae at the Crystalline-Liquid Crystalline Phase Transition. *Chemistry and Physics of Lipids, 7*(4), 324-335.

Tresset, G. (2009). The Multiple Faces of Self-Assembled Lipidic Systems. *BMC Biophysics, 2*(1), 3.

Uehara, H., & Hatano, J. (2002). Pressure-Temperature Phase Diagrams of Ferroelectric Liquid Crystals. *Journal of the Physical Society of Japan, 71*(2), 509-512.

Ulrich, A. S., & Watts, A. (1994). Molecular Response of the Lipid Headgroup to Bilayer Hydration Monitored by H-2-Nmr. *Biophysical journal, 66*(5), 1441-1449.

Vicari, L. (2003). *Optical Applications of Liquid Crystals*: Taylor & Francis.

Vill, V., Bokcher, T., Thiem, J., Fischer, F. (1989). Studies on Liquid-Crystalline Glycosides. *Liq.Cryst., 6*(3), 349-356.

Virchow, R. L. K. (1860). *Cellular Pathology: As Based Upon Physiological and Pathological Histology. Twenty Lectures Delivered in the Pathological Institute of Berlin During the Months of February, March and April, 1858*: RM De Witt.

Von Minden, H., Brandenburg, K., Seydel, U., Koch, M., Garamus, V., Willumeit, R., & Vill, V. (2000). Thermotropic and Lyotropic Properties of Long Chain Alkyl Glycopyranosides. Part Ii. Disaccharide Headgroups. *Chemistry and Physics of Lipids, 106*(2), 157-179.

von Rybinski, W. (1996). Alkyl Glycosides and Polyglycosides. *Current Opinion in Colloid & Interface Science, 1*(5), 587-597.

Vorländer, D., & Apel, A. (1932). Die Richtung Der Kohlenstoff-Valenzen in Benzolabkömmlingen (Ii.). *Berichte der deutschen chemischen Gesellschaft (A and B Series), 65*(7), 1101-1109.

Wassall, S. R. (1996). Pulsed Field-Gradient-Spin Echo Nmr Studies of Water Diffusion in a Phospholipid Model Membrane. *Biophysical journal, 71*(5), 2724-2732.

Witonsky, R. J., & Scarantino, J. W. (2001). Liquid Crystal Thermometer: Google Patents.

Zaccai, G., Blasie, J., & Schoenborn, B. (1975). Neutron Diffraction Studies on the Location of Water in Lecithin Bilayer Model Membranes. *Proceedings of the National Academy of Sciences, 72*(1), 376-380.

Zahid, N. I., Conn, C. E., Brooks, N. J., Ahmad, N., Seddon, J. M., & Hashim, R. (2013). Investigation of the Effect of Sugar Stereochemistry on Biologically Relevant Lyotropic Phases from Branched-Chain Synthetic Glycolipids by Small-Angle X-Ray Scattering. *Langmuir, 29*(51), 15794-15804.

Zheliaskova, A., Marinov, R., & Derzhanski, A. (1999). Phase Stability of Three Component Lyotropic Liquid Crystals. *Journal of Molecular Structure, 513*(1-3), 9-14. doi: 10.1016/s0022-2860(99)00110-6

LIST OF SCIENTIFIC CONTRIBUTIONS

Published:

Hashim, R. , Mirzadeh, S. M., Heidelberg, T., Minamikawa, H., Yoshiaki, T., & Sugimura, A. (2011). A reevaluation of the epimeric and anomeric relationship of glucosides and galactosides in thermotropic liquid crystal self-assemblies. Carbohydrate research, 346(18), 2948-2956.

Nicholas J. Brooks, H. A. A. H., Rauzah Hashim*, Thorsten Heidelberg, John M. Seddon*, & Charlotte E. Conn, Seyed M. Mirzadeh Hosseini, N. Idayu Zahid and Rusnah Syahila Duali Hussen (2011). Thermotropic and lyotropic liquid crystalline phases of Guerbet branched -chain β-D-glucosides. [Jurnal]. Liquid Crystals, 38(11-12), 1725-1734.

Mohammad, S., Hosseini, M., Hashim, R., Heidelberg, T., & Timimi, B. A. (2012). Bound Water Investigations on Disaccharide Based Glycolipids. Nanoformulation (336), 205-211.

Presentations:

Oral:

Candidature Defence (11 July 2009)

PhD Seminar (13 September 2013)

Poster:

Seyed Mohammad Mirzadeh Hosseini, Rauzah Hashim, Thorsten Heidelberg; Investigations of Bound Water in Lyotropic Glycolipids by D-NMR and DSC; Liquid Crystal and Self-Assembly Workshop (LCSA) @ PECIPTA; 10 October 2009; Convention Centre (KLCC) , Kuala Lumpur, Malaysia.

Seyed Mohammad Mirzadeh Hosseini, Rauzah Hashim, Thorsten Heidelberg; Water Content Investigation on Disaccharide Surfactants; InForm Connect Seminar; 13-15 January 2010; Rimba Ilmu University of Malaya; Kuala Lumpur, Malaysis

Seyed Mohammad Mirzadeh Hosseini, Rauzah Hashim, Thorsten Heidelberg;; Evaluation of Simulation by Bound Water Investigation Base on Deuterium NMR & DSC Spectroscopy; 3rd International Symposium on the Manipulation of Advanced Smart Materials; 31 August – 3 September 2010; I & I Land Shijonawate Osaka, Japan.

Seyed Mohammad Mirzadeh Hosseini, Rauzah Hashim, Thorsten Heidelberg; Evaluation of Simulation by Bound Water Investigation; Emerging Trends in Chemistry; 26th– 28rd October 2010; Department of Chemistry University of Malaya; Kuala Lumpur, Malaysia

Seyed Mohammad Mirzadeh Hosseini, Rauzah Hashim, Thorsten Heidelberg; Bound Water Investigation Based on ^{2}H-NMR Spectroscopy & Differential Scanning Calorimetry; International Conference on Materials for Advanced Technologies (ICMAT2011); 26 June – 1 July 2011; Suntec, Suntec City, Singapore

Attendance:

NanoFormulation, 26 June – 1 July 2011

Optimal Solvent Recovery &Thermostatic Efficiency (30 Sept 2011)